ABSTRACT

XIAO, GUANXI. The Role of Epidermal Growth Factor Receptor (EGFR) in Neurogenesis and Gliogenesis. (Under the direction of Dr. Troy Ghashghaei).

The stem cell population that gives rise to the central nervous system (CNS) includes both neurogenic and gliogenic progeny. The timing of neurogenesis and gliogenesis is exquisitely controlled through the interaction of extra- and intracellular mechanisms that control both the proliferation and fate specification in siblings that are derived from individual cell divisions throughout the developing CNS. Remarkably, neurogenesis occurs primarily during embryonic development, while gliogenesis is at later stages of embryogenesis and peaks during early postnatal life. The programmed balance between neurogenesis and gliogenesis is critical for functional maturation of the CNS and its disruption can lead to numerous diseases including multiple sclerosis, epilepsies, and various forms of gliomas. A fundamental current question in developmental neurobiology concerns lineal mechanisms involved in specification and emergence of neuronal and glial cells types throughout the brain. Importantly, a gliogenic switch has been well documented in the division of brain progenitors during perinatal development and a number of mechanisms regulate this developmental process. Using neural stem cells (NSCs) as a platform together with genetic and cellular approaches, I demonstrate that the epidermal growth factor receptor (EGFR) is an essential regulator in NSC fate specification. Conditional genetic loss-of-function approach was utilized to delete EGFR expression in neural stem/progenitor cells, illustrating reduction of glial cells during early postnatal brain development. Deletion of EGFR also comprised the proliferation capacity of neural stem/progenitor cells. I also found that EGFR regulates expression and function selectively in an Olig2+ domain of the rostral

forebrain during perinatal stage. *In vivo*, using Mosaic Analysis with Double Markers on chromosome 11 (MADM), we revealed that EGFR is required in a cell autonomous fashion for gray matter astrocyte generation and induction of Olig2 expression to generate oligodendrocytes. Non EGFR expressing progenitors promote the glial cell fate acquisition of their clonally-associated EGFR expressing sister cells in the forebrain through clonal cell-cell interactions.

The Role of Epidermal Growth Factor Receptor (EGFR) in Neurogenesis and Gliogenesis

by
Guanxi Xiao

A dissertation submitted to the Graduate Faculty of
North Carolina State University
in partial fulfillment of the
requirements for the degree of
Doctor of Philosophy

Physiology

Raleigh, North Carolina

2014

APPROVED BY:

_____	_____
Dr. Troy Ghashghaei Committee Chair	Dr. David Threadgill
_____	_____
Dr. Jun Ninomiya-Tsuji	Dr. Nanette Nascone-Yoder
_____	
Dr. Philip Sannes	

BIOGRAPHY

Guanxi Xiao was born in Zhongshan, China in 1984. In 2008, he got his bachelor's degree in Traditional Chinese Medicine of Hunan University in China. He continued his medical study in Florida College of Integrated Medicine in Orlando and Florida and got the master degree in 2009. He then joined the graduate program in Molecular Biomedical Sciences, College of Veterinary Medicine at North Carolina State University to pursue a doctoral degree. His thesis dissertation was under the direction of Dr. Troy Ghashghaei.

ACKNOWLEDGMENTS

I would like to give a millions thanks to my advisor Dr. Ghashghaei for his guidance and continuous supports. This work would not have been possible without the generous gift of genetic mice generated by my committee member Dr. David Threadgill. I also would like to thank my other committee members Dr. Nanette Nascone-Yoder, Dr. Jun Ninomiya-Tsuji, Dr. Philip Sannes for their insightful suggestions to my projects. Finally I am very grateful to my family and friends for having given me support and encouragement.

TABLE OF CONTENTS

LIST OF FIGURES

LIST OF ABBREVIATIONS

NSC: neural stem cell

CNS: central nervous system

IPC: intermediate progenitor cell

NE: neuroepithelial cell

RG: radial glial cell

VZ: ventricular zone

SVZ: subventricular zone

MZ: marginal zone

PPL: preplate layer

SEZ: subependymal zone

RMS: rostral migratory stream

OB: olfactory bulb

BrdU: Bromodeoxyuridine

MADM: mosaic analysis with double markers

KD: kilo Dalton

bp: base pair

LGE: lateral ganglionic eminence

CC: corpus callosum

BACKGROUND

Two major types of cells allow the mammalian central nervous system (CNS) to function: neurons and glia. Neurons receive and process external or internal stimuli through electrical or chemical signals. Glial cells include astrocyte, oligodendrocyte, microglia and ependymal cell, which regulate and maintain neuronal functions through structural support, water and ion balance, nutrient and oxygen supply, and more. Thus, homeostasis in the CNS is critically dependent on the precise coordination of neuronal and glial interactions.

The balance in neuronal-glial interactions is in part regulated through precise control over production of appropriate numbers of each cell type, and their correct positioning in the various circuits of the brain during embryonic and perinatal development. This control is a function of intracellular and extracellular signals that regulates neural stem cell (NSC) divisions during various stages of development. Abnormal production of neurons or glia is in fact a hallmark of various neurodevelopmental diseases such as multiple sclerosis, autism, brain tumors, and many other conditions (Compston et al., 2008; Ligon et al., 2006; Wegiel et al., 2010). Therefore, improving our understanding of neuronal/glial cell fate specification in NSCs in distinct CNS regions offers hope not only for better understanding mechanisms involved in neurodevelopmental disorders, but also for potential utilization of NSCs and cellular reprogramming for treatment of brain disorders, and even for application of regenerative approaches to the injured CNS. The primary goal of the research conducted for this dissertation was to determine the role of Epidermal Growth Factor Receptor (EGFR) in neuronal/glial cell fate specification in NSCs during mammalian brain development and

defining novel cellular mechanisms that regulate the balance between neurogenesis and gliogenesis.

Neurogenesis during embryonic brain development

Neurons are the primary functional units of the nervous system, which communicate with each other via synapses. The production of neurons, known as neurogenesis, occurs mostly during embryonic development in the mammalian CNS. The CNS (including the brain and spinal cord) is derived from the neural tube, a structure formed by closure of a neuroectodermal tissue (neural plate) in the early vertebrate embryo (Sadler 2005) (Fig.1). Neural tube originates as a single layer of neuroepithelial cells (NEs), the first generation of NSCs in the CNS. NEs are polarized with their apical membrane anchored to the inner face of the neural tube. This surface of the neural tube is in contact with the fluid within the ventricular system and later becomes the ventricular zone (VZ), in which the cell bodies of NEs are retained. Simultaneously, NEs extend their basal processes outward to contact the basal lamina along the pial surface of the developing brain (Götz & Huttner 2005) (Figure 1).

After the formation of a pseudostratified neural tube, NEs divide rapidly to create additional layers and eventually form the basic structures of the CNS including the forebrain, midbrain, hindbrain and spinal cord (Figure 1). This expansion is highly dependent on the ability of NEs to temporally lock themselves into a period of controlled rounds of symmetric divisions during early embryonic CNS development. Indeed, it has been shown that early NEs of the cerebral cortices in the telencephalon undergo a restricted period of symmetric

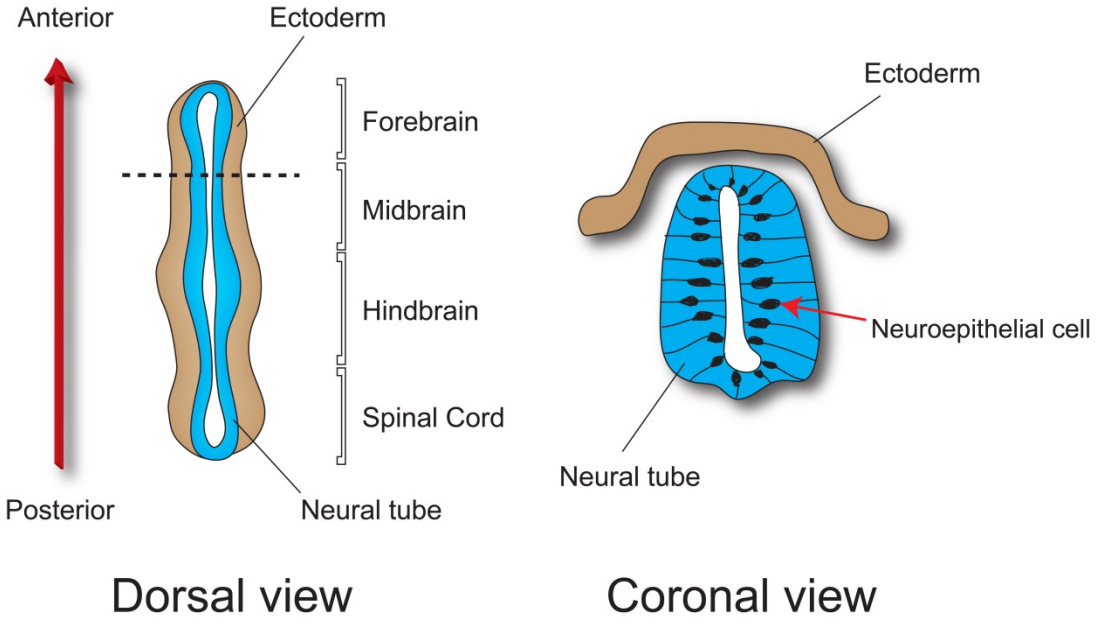

Figure 1. Neural tube structure. Dorsal view of a neurulating embryo (left) and coronal view of the neural tube (right). The position of the coronal view is indicated by dash line in the dorsal view. Neural tube begins as a layer of pseudostratified neuroepithelial cells. Neural tube subdivides to eventually develop into four distinct regions of the CNS: forebrain, midbrain, hindbrain and spinal cord.

divisions when they expand in number and likely contribute to growth and expansion of primary vesicle of the brain.

Following their expansion, NEs begin their differentiating divisions through asymmetric mitoses to generate limited numbers of radial glial cells (RGs) and neurons (Götz & Huttner 2005). Importantly, NEs transform into RGs and continue to divide asymmetrically driving the neurogenic period of tissue development in the brain (reviewed by Rowitch & Kriegstein, 2010) (Figure 2). RGs constitute the NSCs that will give rise to most, if not all, neurons in the embryonic CNS (Noctor et al. 2004).

RGs lose some features of NEs such as exhibition of tight junctions and begin to express astrocyte-associated genes such as those encoding the brain lipid-binding protein (Blbp) and the glutamate transporter (Glast). These genes are generally not expressed in early NEs (Feng et al. 1994; Hartfuss et al. 2001). However, NEs and RGs share many similar characteristics, such as both undergoing mitosis in the VZ while maintain physical contact with the pial surface with their basal radial processes. In addition, Both NEs and RGs express the intermediate filament protein Nestin, which is widely expressed in many progenitor cells throughout the developing CNS (Anthony et al. 2004; Lendahl et al. 1990).

Based on the morphology of RGs (radial processes anchoring the apical and basal surfaces of developing cortex), they were originally considered as scaffold cells that support guidance cues for neuronal migration decades ago (Rakic 1971; Rakic 1972). The neurogenic and gliogenic potential of RGs, functioning as NSCs, were only recently recognized. The multipotency of RG is found not only in embryonic period, but also in postnatal development. In Sally Temple's study, the dividing cells were isolated from E14

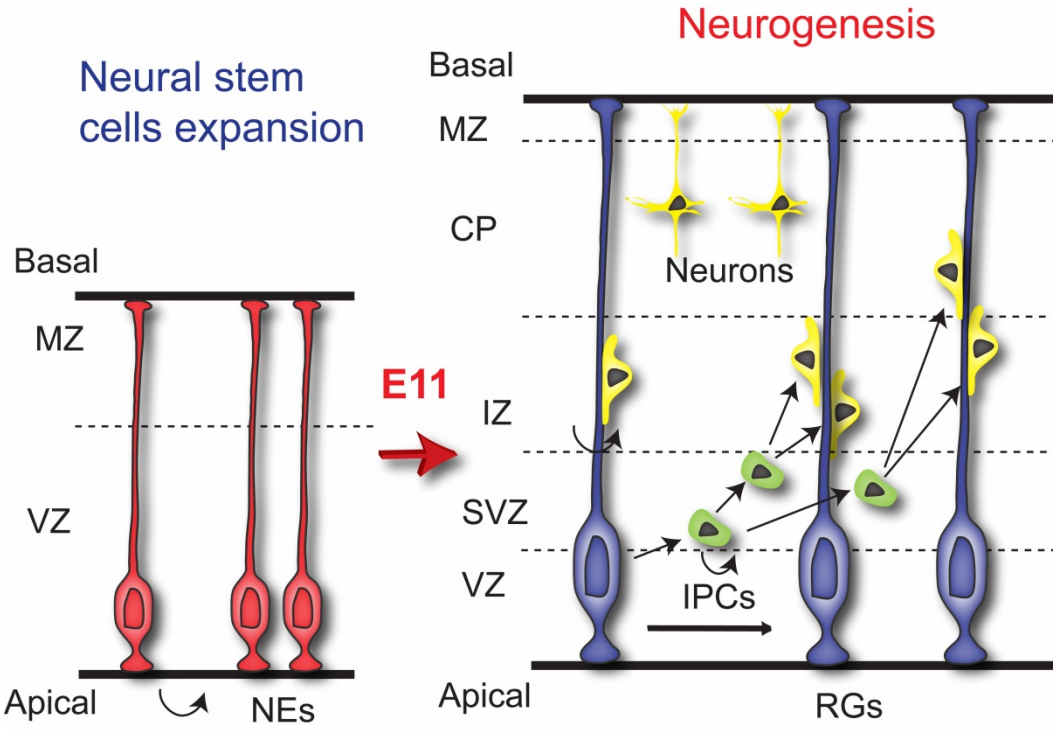

Figure 2. Divisions of NEs and RGs during cortical development. NEs undergo symmetric division to generate two NEs to expand the NSCs pool for neurogenesis (left panel). During the onset of neurogenesis, NEs transform into RGs, which begin asymmetric divisions to generate neurons (right panel). RGs can undergo asymmetric division to generate one RG and one neuron or IPC. Majority of IPCs undergo symmetric division to generate two neurons. NEs: neuroepithelial cells; RGs: radial glial cells; IPCs: intermediate progenitors; VZ: ventricular zone; SVZ: subventricular zone; IZ: intermediate zone; CP: cortical plate; MZ: marginal zone

embryonic forebrain ventricular zone, where RGs were located. Single cells were then cultured *in vitro*. She found that a variety of cell types containing neurons and glial cells was able to generate from a single dividing RG (Temple 1989). Later, studies built on Temple's findings by using green fluorescent protein (GFP) to label RGs in combination with cell sorting technologies that emerged around the turn of the millennium (Malatesta et al. 2000). In their findings, sorting progenitors labeled with GFP or dye Dil were cultured to assess their differentiation potential. Most of the isolated progenitors expressed the RG markers Glast and Blbp and were able to generate neurons and glial cells *in vitro*. Similar evidence was provided by Arturo Alvarez-Buylla et al, using the Cre/loxP based lineage tracing method (Merkle et al. 2004). Cre is a 38 kilo Dalton (KD) recombinase enzyme, which is encoded by bacteriophage P1but not mammalian cells (Abremski & Hoess 1984). Loxp is a 34 base pair (bp) DNA sequence again exclusive to bacteria, which consists of two 13bp inverted repeats and an 8bp asymmetric core sequence which provides directionality. Cre recognizes and binds to loxP sites to mediate recombination, including excision/integration, inversion and translocation depending on the alignment and direction of two loxP sites (Figure 3) (Nagy 2000). Alvarez-Buylla's group cloned the cre coding sequence into an adenovirus and infected neonatal RGs through direct injections into the lateral cerebral ventricles of mice which had a cre-responsive reporter so they could track their targeted cells. The reporter gene was expressed after Cre mediated-recombination by removing the stop codon flanked by two loxp sites. This type of 'lineage tracing' has become a gold standard in developmental biology. What they found was that reporter-positive RGs and their progeny gave rise to multiple lineages of neurons and glia in the developing brain *in vivo*, including

neurons, astrocytes, oligodendrocytes and ependymal cells. In addition, the isolated RGs differentiated into various cell types when cultured *in vitro* (Merkle et al. 2004).

Around the same period, a number of laboratories experimented with ex-vivo preparations of the embryonic brain to time-lapse image labeled RGs and their dynamic behaviors during critical neurogenic and gliogenic periods of development in their *in vivo* environment. These studies provided critical dynamic and direct time-lapse evidence that unequivocally indicated the neurogenic potential of RGs. In early embryonic brain slices, RGs targeted by retrovirus carrying GFP generated neurons either directly, or indirectly through formation of intermediate progenitor cells (IPCs) (Noctor et al. 2004; Haubensak et al. 2004). During the entire process of cell division, it became clear that RGs remain in contact with the ventricular surface through their apical end-feet, while also maintaining their polarity through basal processes that extend to the pial surface in contact with the meninges (Figure 2).

The culmination of not only the aforementioned studies, but numerous other studies from multiple laboratories have painted a more clear picture of NEs, RGs, neurogenesis, and gliogenesis in the developing rodent brain, where most of the stages in CNS development have been well characterized. It is now clear that the onset of neurogenesis begins around embryonic day (E) 10-11(Altman & Bayer 1991; Haubensak et al. 2004) (Figure 2). At this mid-gestation stage (rodent embryos are generally born around 20 days post-fertilization), NEs in the VZ undergo a differentiation process whereby they switch from dividing symmetrically (expansive division: NE→NE+NE) to asymmetric divisions (neurogenic divisions) to generate neurons and RGs. Through asymmetric division, each RG is able

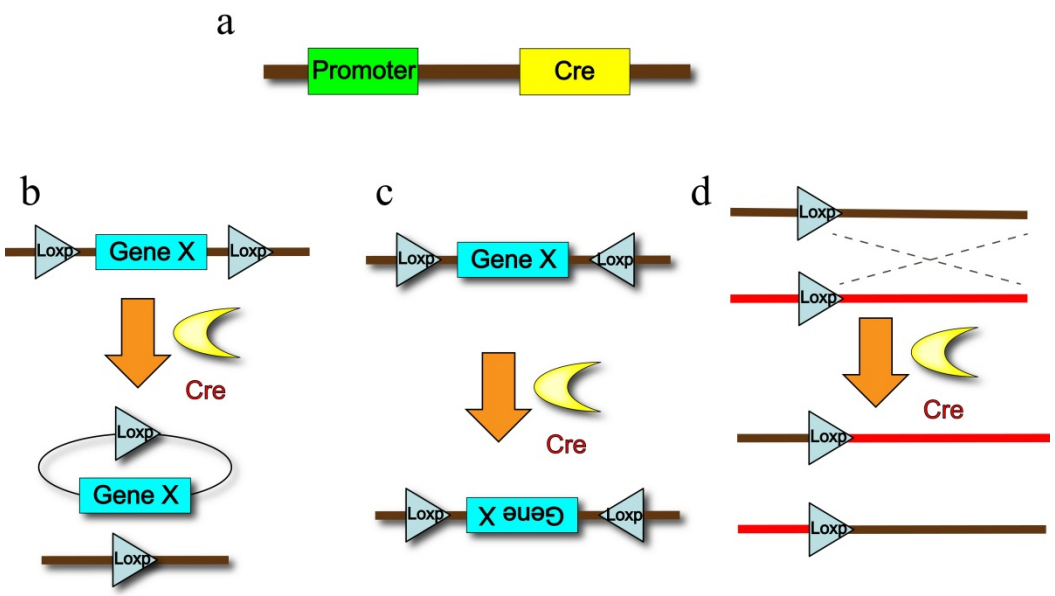

Figure 3. Cre/loxp recombination system. (a). The expression of Cre enzyme is driven by specific promoter to mediate tissue or cell type specific recombination. The results of Cre-mediate recombination depend on the location and orientation of two loxp sites. **(b).** If the loxP sites locate on the same chromosome with the same direction, Cre recombinase mediates the gene deletion**. (c).** The opposite direction of two loxp sites on the same chromosome results in gene inversion. **(d).** If the loxP sites are located on different chromosomes recombinase mediates a chromosomal translocation.

to generate two daughter cells with distinct cell fates: RG and neuron or neurogenic IPC (Noctor et al. 2004; Miyata et al. 2001; Miyata et al. 2004). Therefore, asymmetric divisions result in generation of neurons, while at the same time help maintain the pool of NSCs in developing brain. Newborn neurons that are generated from asymmetric RG divisions exhibit migratory properties. The migrating neurons move toward the cortical plate along the radial glial fibers of RGs to occupy different layers of the cerebral cortex (Rakic 1972; Nadarajah et al. 2003). Positioning of these migrating neurons is well organized according to their birthdate (Figure 4). The early-born neurons occupy lower layers while late-born neurons reside in the upper layers, composing an inside-out organization (Angevine & Sidman 1961; Rakic 1974). During migration, newborn neurons display dynamic morphological alterations with a leading edge toward the pial surface and trailing tail facing the VZ. Once the migrating neurons reach the upper layer on top of the older neurons, they move away from the radial processes towards their destined laminar position (Kriegstein & Noctor 2004).

As mentioned, an important aspect of neurogenesis is through the divisions of IPCs. Unlike NEs and RGs, the divisions of IPCs occur predominantly in the embryonic subventricular zone (SVZ), away from the VZ. In this context, IPCs are also referred to as "basal progenitors" (Smart 1973; Miyata et al. 2004). In addition to their location, IPCs are distinct from RGs in that they display multipolar processes in the SVZ and do not form adherent contacts with the ventricular or pial surfaces (Figure 2). IPCs take on distinct molecular characteristics such as the expression of transcription factors Svet1, Cux1/Cux2 and Tbr1/Tbr2, which are important for neuron differentiation, but not Blbp or Glast

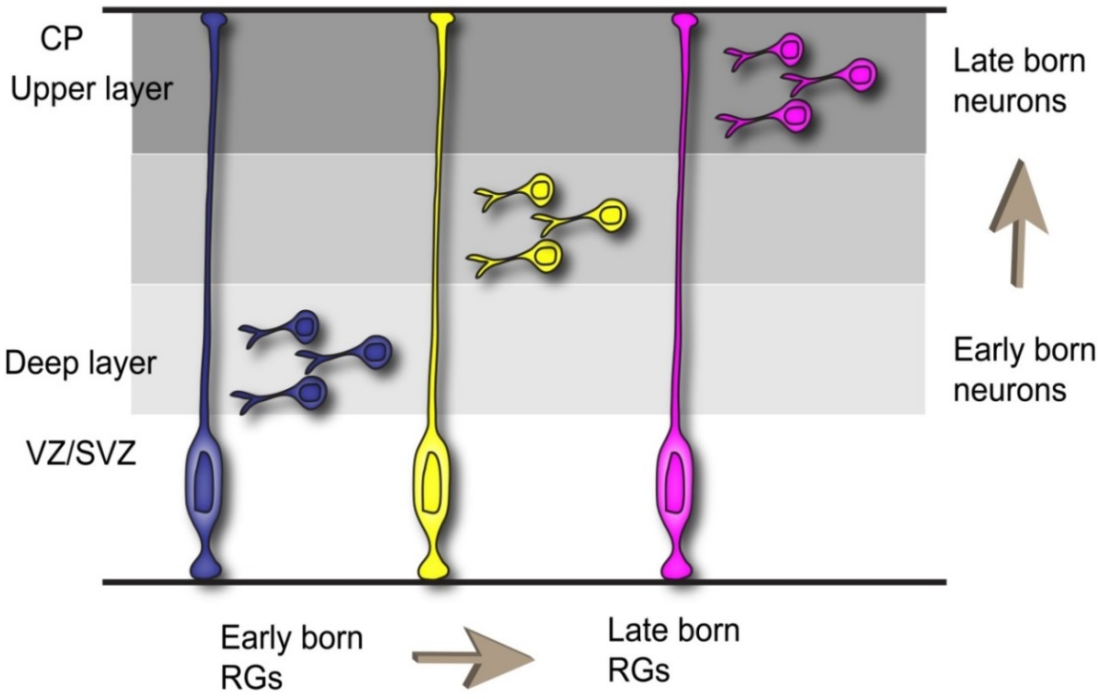

Figure 4: Laminar development of the cerebral cortex. Early-born neurons generated from RGs target deeper layers of the CP, and late-born neurons migrate past early-born neurons to settle in the upper layers. RGs: radial glial cells; VZ: ventricular zone; SVZ: subventricular zone; CP: cortical plate

(Tarabykin et al. 2001; Zimmer et al. 2004; Englund et al. 2005; Hartfuss et al. 2001). More importantly, these progenitors almost exclusively undergo symmetric divisions for at least one round of cell cycle and give rise to neurons during embryonic brain development. For example, more than 90% of Tbr2 expressing mitotic progenitors give rise to neurons during neurogenesis (Englund et al. 2005). Several lines of evidence demonstrated that IPCs help rapidly generate large pools of neurons in appropriate corridors of the developing brain (reviewed by Kriegstein et al. 2006). During early stage of neurogenesis (E11.5-E12.5), IPCs account for more than 50% of lower layer neurons production (Haubensak et al. 2004). At mid-stage of neurogenesis, the numbers of neurons that are generated from IPCs range from 30% (E14) to almost 100% (E13) (Miyata et al. 2004). Even when neurogenesis declines at its later stages (E16-E18), 30-55% of IPCs maintain their neurogenic divisions to generate upper-layer neurons (Tarabykin et al. 2001; Kowalczyk et al. 2009). Therefore, the generation of neurons from NEs/RGs is largely amplified through expansion of IPCs, which ultimately determine the size of distinct neuronal populations and impact the size of the cerebral cortices in various species (reviewed by Kriegstein et al. 2006).

After the massive production of neurons, neurogenesis declines as the proliferation of IPCs decreases during late embryonic cortical development and it is nearly completed before birth (Kowalczyk et al. 2009; Englund et al. 2005).

Gliogenesis during perinatal brain development

Following the decline in neurogenesis, gliogenesis or production of glial cells, accelerates around birth and dramatically increases during the first few weeks of postnatal brain development (reviewed by Kriegstein & Alvarez-Buylla 2009). Glial cells, also known as neuroglia, were first proposed to be different functional elements than neurons in the nervous system around the middle of the 19th century, a discovery generally attributed to Virchow (Virchow 1854; reviewed by Kettenmann & Verkhratsky 2008). Glial cells are divided into four distinct subtypes based on their function, morphology and origin: macroglia (astrocytes, oligodendrocytes, ependymal cells) and microglia. While macroglia are derived from RGs and IPCs in the brain (ectodermal origin), microglia are derived from the blood (mesodermal origin) during midgestation (Figure 5) (reviewed by Ginhoux et al. 2013). Astrocytes and oligodendrocytes are distributed throughout the white (axonal tracts) and gray (neuropil) matters of the mature CNS, where they function as supporting cells for various neural networks in the mature nervous system.

Astrocytes provide multiple functions to support the CNS, such as structural support, water and ions balance and the maintenance of blood brain barrier (reviewed by Wang & Bordey 2008). Astrocytes display heterogeneity both regionally and morphologically. Detailed morphological studies reveal that at least two main categories of astrocytes are localized in the white and gray matter. Fibrous astrocytes display long unbranched cellular processes in the white matter, yielding a classic “star-like” appearance. These astrocytes can be histologically distinguished from other glia by their expression of the intermediate

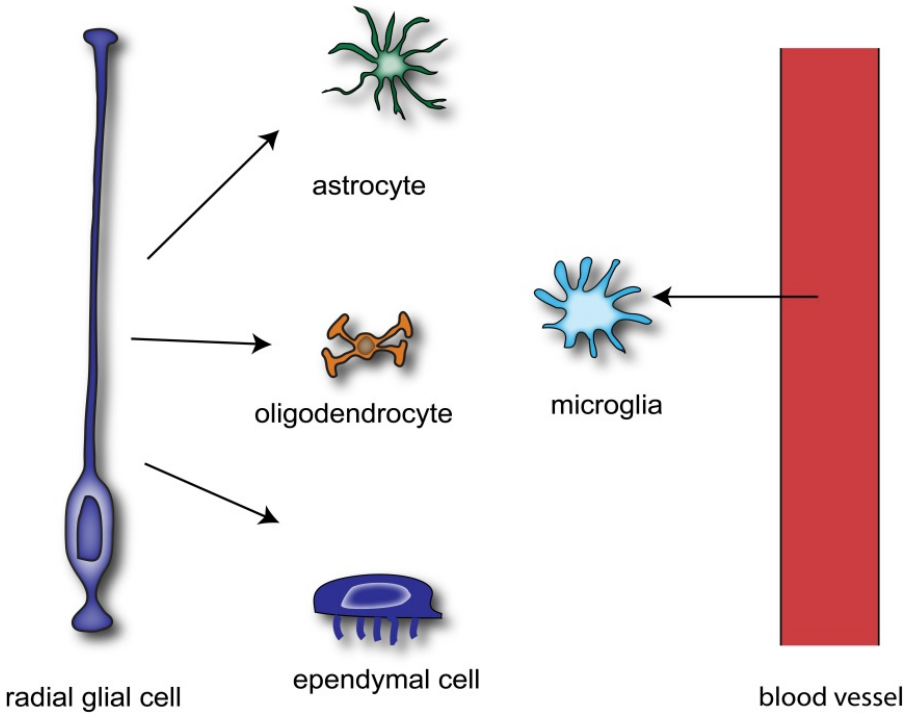

Figure 5. Subtypes of glial cells. There are four types of glial cells in the brain. Astrocyte, oligodendrocyte and ependymal cell are derived from radial glial cells, while microglia moves into the brain from blood vessel.

filament Glial Fibrillary Acid Protein (GFAP). Another set are protoplasmic astrocytes, which are located in the gray matter where they exhibit numerous short processes, but are poorly labeled with GFAP. In addition, protoplasmic astrocytes establish anatomical domains that limits their overlapping with neighboring astrocytes (Bushong et al. 2004). These structural, molecular and regional diversities suggest that there is likely functional heterogeneity among astrocytes in the CNS (review by Zhang & Barres 2010). For example, a subset of astrocyte, known as reactive astrocyte, is well characterized to response to brain injury. These reactive astrocytes form scars to prevent further damage and they are largely labeled by GFAP (Tatsumi et al. 2008). In addition, time-lapse live imaging revealed that white matter astrocytes are more sensitive to injury than gray matter astrocytes (Shannon et al. 2007). Interestingly, another subset of GFAP+ astrocytes located in the SVZ are NSCs, which are important for neuron and glial cell generation during development (Doetsch 2003).

The primary function of oligodendrocytes is to form the myelin sheath that wraps around axons, especially in major fiber tracts of the CNS. Myelin sheath increases the speed of saltatory conduction of electrical impulses (action potentials) in axonal fibers allowing rapid and efficient electrical propagation across neural networks. In addition to myelination, oligodendrocyte progenitors are able to form synapses with neurons, indicating an interaction between oligodendrocytes and neurons (Maldonado & Angulo 2014), although the nature and significance of this communication remains unknown. Unlike astrocytes, mature oligodendrocytes do not express GFAP. Instead, they express various oligodendrocyte lineage markers, including myelin basic protein (MBP) and basic helix loop helix transcription factor Olig1.

In the developing brain of rodents, astrocytes are generated around E18, followed by a peak in their production during the first few weeks of postnatal development. The differentiated oligodendrocytes are not produced until birth (Altman & Bayer 1991). Glial cells can be generated directly through transformation of RGs or from the differentiation of gliogenic IPCs (Merkle et al. 2004; Parnavelas 1999). During embryonic development, RG cell bodies are located in the apical surface of VZ. At the end of neurogenesis, when RGs gradually lose their neurogenic properties, they detach from the VZ and migrate into the SVZ and into the maturing neuropil where they transform into multipolar and fibrous astrocytes. Time-lapse imaging provided direct evidence that the transformation occurs in late embryonic SVZ (Noctor et al. 2008). Noctor et al (Noctor et al. 2008) labeled RGs by retrovirus carrying GFP reporter gene at E15-16 rat embryos. The GFP labeled RGs underwent several rounds of division to generate daughter cells. Some of the daughter cells displayed typical RGs morphology with radial fiber contacting the pial surface, which eventually translocated to the SVZ and transformed into astrocytes (Noctor et al. 2008). Other RGs that remain in the VZ transform into ependymal cells to form a thin ependymal layer (Jacquet et al. 2009). Embryonic SVZ is then transformed into the postnatal subependymal zone (SEZ) with the differentiation of ependymal cells after birth (Figure 6). In addition, some RGs are thought to maintain their stem cell properties but contain astrocyte-like characteristics, which are important for early postnatal gliogenesis. A small population of postnatal NSCs remain quiescent in the SEZ (Doetsch et al. 1999; Merkle et al. 2004).

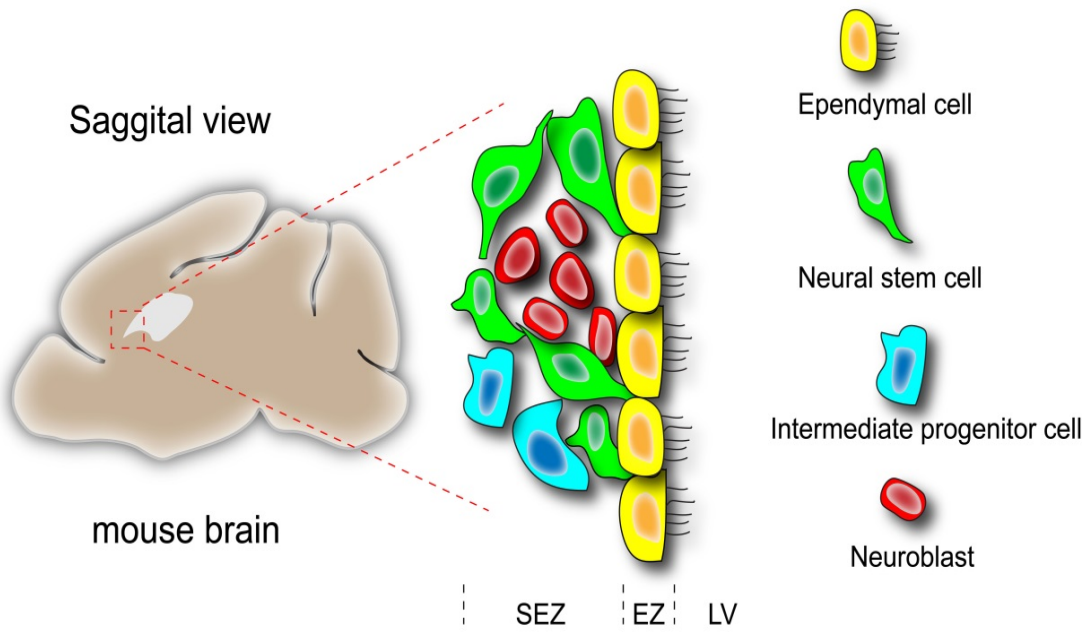

Figure 6. Schematic structure of postnatal subependymal zone (SEZ).

Sagittal view of mouse brain is shown in left panel. SEZ and ependymal zone (EZ: a layer of ependymal cells) are lining the lateral ventricle (LV). NSCs are located in the SEZ, which will give rise to neurogenic or gliogenic IPCs and neuroblast during postnatal brain development.

In addition to transformation of RGs, glial cells can be produced from asymmetric division of RGs, which generates gliogenic IPCs during gliogenesis. Instead of generating neurons, these progenitor cells possess gliogenic potential and give rise to glial cells (Figure 7). Retroviral fate-mapping approaches have been utilized to study the potential glial cell fate specification of RGs and their progeny IPCs *in vivo*. The retrovirus carrying lacZ reporter gene, which encodes beta-galactosidase, was injected into the lateral ventricles. The targeted RGs and their progeny were identified by X-gal staining. When the infected cells were closely distributed (less than 500μm in diameter), they were considered belonging to a clone, which were derived from the same RG (Parnavelas 1999). During neurogenic period, early embryonic retrovirus labeled RGs revealed that very few clones of astrocytes or oligodendrocyte progenitors were derived from RGs at E14 in SVZ. However, the number of clones that consists of astrocytes or oligodendrocytes was highly increased around birth when neurogenesis is almost completed (Parnavelas 1999). In addition, gliogenic IPCs have the capacity to migrate through gray and white matter. They proliferate to expand the populations of astrocytes or oligodendrocytes depending on the developmental period and homeostatic status of the brain region to where they migrate (reviewed by Suzuki & Goldman 2003).

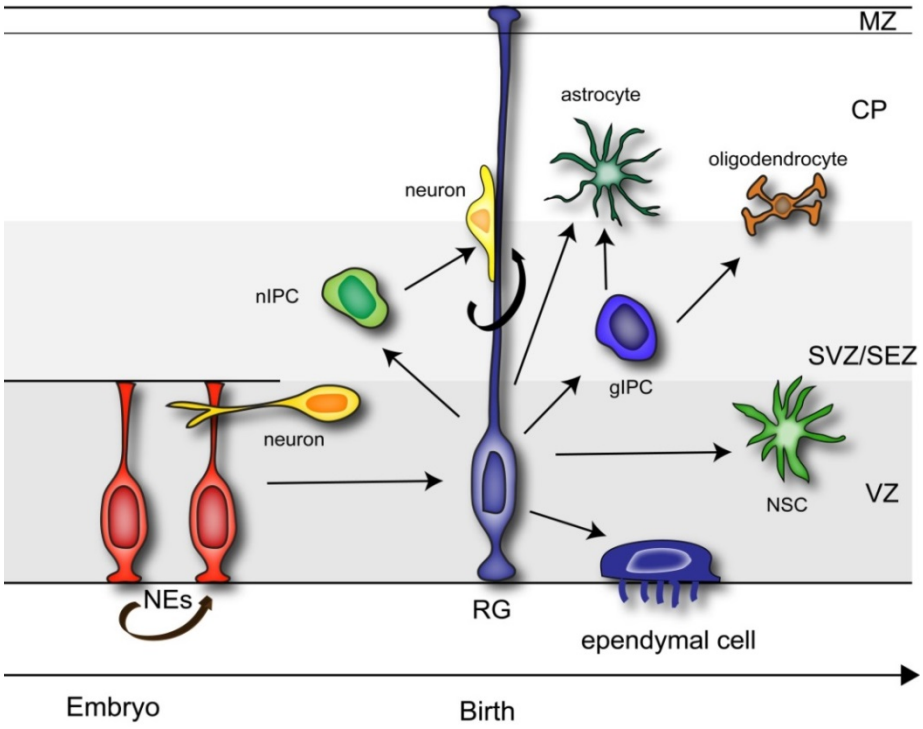

Figure 7. Model of neurogenesis and gliogenesis during cortical development. Before neurogenesis, NEs divide symmetrically to expand NSCs pool. When neurogenesis begins, NEs give rise to RGs, which then divide asymmetrically to generate neurons or neurogenic IPCs. Gliogenesis occurs during perinatal development. RGs transform into glial cells or generate gliogenic IPCs, which then give rise to glial cells. NEs: Neuroepithelial cells; RG: Radial glial cell; nIPC: neurogenic intermediate progenitor cell; gIPC: gliogenic intermediate progenitor cell; VZ: Ventricular zone; SVZ: Subventricular zone; SEZ: Subependymal zone; CP: Cortical plate; MZ: Marginal zone

The switch between neurogenesis and gliogenesis: neural stem cell fate specification during development

NSCs possess both neurogenic and gliogenic potentials during development, but neurogenesis begins earlier than gliogenesis. This temporal segregation in generation of neurons, astrocytes and oligodendrocytes is precisely controlled throughout neural development. The most important and fundamental question here is how cell fate is determined and specified temporally during neural development? Temporally defined fate specification is largely regulated by cell-intrinsic mechanisms such as those driven by distinct transcription factors. Evidence exists demonstrating that the sequential generation of neural and glial cells also occurs in culture, as isolated cortical progenitors generate neurons prior to glial cells (Qian et al. 2000; Shen et al. 2006). In addition, previous studies demonstrated that subtypes of neurons in different layers of the cerebral cortices are specified through a progressive restriction in neurogenic potentials of NSCs/IPCs. For example, isolated cortical progenitors transplanted from older into to younger embryonic brains fail to generate early-born neurons, indicating that NSCs/IPCs are intrinsically fate-restricted during development (Frantz & McConnell 1996). *In vitro* clonal analyses provided additional evidence which demonstrates the intrinsic regulation of temporal cell fate in NSCs. For example, NSCs derived from embryonic stem cells are able to generate neurons in a temporal and laminar order without any morphogens, with older neurons positioning themselves into deeper layers and younger neurons in superficial layers (Gaspard et al. 2008; Eiraku et al. 2008).

The mechanisms of intrinsic transcriptional regulation controlling neurogenesis and gliogenesis have been studied extensively in the developing cerebral cortex. At the initial stages of neurogenesis, asymmetric division of NSCs (RGs) generates one cell with multipotency to maintain the stem cell pool and the other is fate-restricted to differentiate into neurons. Several lines of evidence suggest that high levels of proneural basic helix-loop-helix (bHLH) genes are expressed during this period, which are essential to promote neurogenesis. These proneural genes include the Neurogenins (Ngn1 and Ngn2) and the mammalian achaete-scute homolog-1 (Mash1), both of which are primarily expressed by NSCs and IPCs in the VZ of the mammalian telencephalon, but not in the cortical plate (Guillemot & Joyner 1993; Lo et al. 1991; Sommer et al. 1996). Loss-of-function studies have revealed the important functions of proneural genes in neurogenesis. For example, in the absence of Mash1, progenitors in the ventral forebrain dramatically decrease, which leads to a severe loss of neuronal production in the cerebral cortex and basal ganglia (Casarosa et al. 1999). In Mash1 and Ngn2 double mutants, the neurogenesis defect was even more prominent. Both ventral and dorsal NSCs and IPC specification was disrupted, resulting in a significant reduction of cortical neurons (Fode et al. 2000). The important functions of these proneural genes are not only to initiate and promote neurogenesis, but also to inhibit gliogenesis. In addition to the decrease of neuronal production, a phenotype of enhanced and premature astrogliosis was exhibited in Mash1and Ngn2 mutants (Nieto et al. 2001). In contrast, overexpression of proneural bHLH genes using retroviral injection blocks gliogenesis in the cerebral cortex during the period of gliogenesis (Cai et al. 2000). *In vitro* clonal analysis demonstrated that overexpression of Ngn1 in NSCs/IPCs inhibits the

generation of astrocytes (Sun et al. 2001), while NSCs/IPCs largely differentiated into astrocytes rather than neurons in the absence of Ngn2 and Mash1 in culture (Nieto et al. 2001). In addition to proneural gene regulation, cortical neurons are also specified in a non-Ngn dependent manner. For example, Paired homeobox gene 6 (Pax6) is a transcription factor that is expressed in RGs (Englund et al. 2005). The specification of early born cortical neurons requires down-regulation of Pax6 in NSCs and IPCs, which sequentially express the T-box transcription factors Tbr1 and Tbr2 (Englund et al. 2005). Interestingly, the late born cortical neurons are specified in a Pax6 dependent manner with interactions with another transcription factor, Tlx (Schuurmans et al. 2004).

Once neurogenesis is completed and neurons migrate to the destined location, the production of oligodendrocyte occurs for axon myelination. The bHLH Oligodendrocyte transcription factors (Olig1 and Olig2) have been indicated in glial cell specification of NSCs (Takebayashi & Yoshida 2000; Zhou & Anderson 2002; Marshall et al. 2005). Olig1 and Olig2 are expressed in oligodendrocyte progenitors and mature oligodendrocytes in the ventral telencephalon and spinal cord (Lu et al. 2000; Zhou et al. 2000; Tekki-Kessaris et al. 2001). Loss-of-function studies demonstrated that oligodendrocytes were completely lost throughout the CNS in Olig1/Olig2 double mutants (Zhou & Anderson 2002; Lu et al. 2002). Conversely, ectopic expression of Olig1 or Olig2 promotes gliogenesis (Lu et al. 2001; Lu et al. 2000; Marshall et al. 2005). Olig genes are not only important for oligodendrocyte fate specification, but also for astrogliosis. In the early postnatal forebrain, overexpression of Olig2 in SEZ progenitors resulted in an increase in generation of both astrocytes and oligodendrocytes (Marshall et al. 2005).

In addition to intrinsic mechanism, the developmental program of temporal fate specification is also regulated by extrinsic signals from the local CNS environment. For example, Morrow et al (Morrow et al. 2001) has demonstrated that embryonic NSCs/IPCs give rise to distinct cell lineages when cultured on top of cortical slices at different ages. When NSCs were grafted onto embryonic cortical slices, they primarily generated neurons. In contrast, grafting of the same age NSCs onto postnatal cortices resulted in differentiation into glial cells. In addition, cell fate decisions of these NSCs were regulated by modifying the concentration of fibroblast growth factor (FGF) and ciliary neurotrophic factor (CNTF) (Morrow et al. 2001), indicating that signaling by cell membrane receptors modulates temporal cell fate specification of NSCs in response to local environmental changes.

At the onset of gliogenesis, the expression of proneural genes decreases, resulting in the decline of neuronal production (Ma et al. 1997). Notch receptor signaling has been implicated in this switch from neurogenesis to gliogenesis by regulating proneural genes expression. The well-established roles of Notch signaling are in the maintenance of NSC properties and inhibition of neurogenesis during CNS development (reviewed by Yoon & Gaiano 2005). During the neurogenic period, the Notch pathway inhibits neurogenesis through the expression of downstream effector Hes proteins, which function to repress the proneural genes expression and degradation (Sriuranpong & Borges 2002; Sakamoto et al. 2003). Thus, NSCs remain in an undifferentiated state when notch signaling is active. Another important function of Notch is to promote glial cell fate specification in NSCs. The Notch intracellular domain forms a transcription complex with the DNA binding protein CSL, which then binds to the GFAP promoter region to activate its transcription. Therefore, NSCs

begin to express GFAP protein, a typical astrocytic marker, and eventually differentiate into astrocytes (Ge et al. 2002). Moreover, various studies have indicated that overexpression of the Notch effector Hes promotes progenitors differentiate into astrocytes (Tanigaki et al. 2001; Wu et al. 2003).

In addition to Notch, fibroblast growth factor receptor (FGFR) signaling also has a functional role in NSC fate specification. NSCs have been successfully cultured and differentiated into various cell types by modifying the concentrations of FGF-2, a binding ligand of FGFR (Qian et al. 1997). The important role of FGFR signaling in generation of glial cells has been illustrated by Gain-of-function studies. FGF promotes the production of oligodendrocyte lineage cells in a sonic hedgehog independent manner (Nery et al. 2001; Kessaris et al. 2004). In addition, clonal analysis of cultured cortical progenitors indicated that FGF induces glial cell fate of NSCs/progenitors and differentiates them into astrocytes by interacting with cytokine signaling pathways (Morrow et al. 2001). These studies indicated that the neurogenic-to-gliogenic switch depends upon the precise coordination between intrinsic regulation (e.g., expression and function of transcription factors) and extracellular signals. However, the developmental requirement of extracellular signals in the switch from neurogenesis to gliogenesis is still not fully understood. For example, although FGF signaling has an important role in NSC fate specification, the expression of FGFR1 occurs as early as E8 in rodent telencephalon (Wanaka et al. 1991), which is much earlier than gliogenesis, suggesting that FGF maybe not required to induce the switch from neurogenesis to gliogenesis during brain development.

Epidermal growth factor receptor (EGFR) in neurogenesis and gliogenesis

Another important signal during forebrain development emerges from the activity of the epidermal growth factor receptor (EGFR). EGFR is a cell membrane spanning receptor from the ErbB family, with homology to closely associated members ErbB2, ErbB3 and ErbB4. EGFR is a glycoprotein with a molecular weight of 170 KD. The full length EGFR is encoded by a 1210 amino acids precursor polypeptide, which is cleaved to a final fragment of 1186 amino acids (Jorissen 2003). The molecular structure of EGFR is characterized by four domains: an extracellular domain, a transmembrane domain, a juxtamembrane domain and an intracellular domain within its carboxyl-terminus (Figure 7). EGFR signaling is activated by ligand binding and dimerization. The well characterized ligands for EGFR are the epidermal growth factor (EGF), heparin-binding EGF-like growth factor (HB-EGF), β-cellulin, transforming growth factor alpha, amphiregulin, epiregulin, epigen and the neuregulins (Harris 2003). While two EGFR monomers can dimerize to form a functional homodimer, EGFR can also form heterodimers with other ErbB members. After binding of extrinsic ligands such as EGF, dimerization of EGFR initiates autophosphorylation of its intracellular C-terminal tail (Figure 8), which then triggers a number of intracellular kinase cascades including the PI3K/Akt (phosphoinositide 3-kinase/ v-akt murine thymoma), MAPK (the mitogen-activated protein kinases) and STAT pathways. This complex signaling network functions to regulate cell survival, proliferation, migration and differentiation (Chandra et al. 2013; Caric et al. 2001; Ayuso-Sacido et al. 2010).

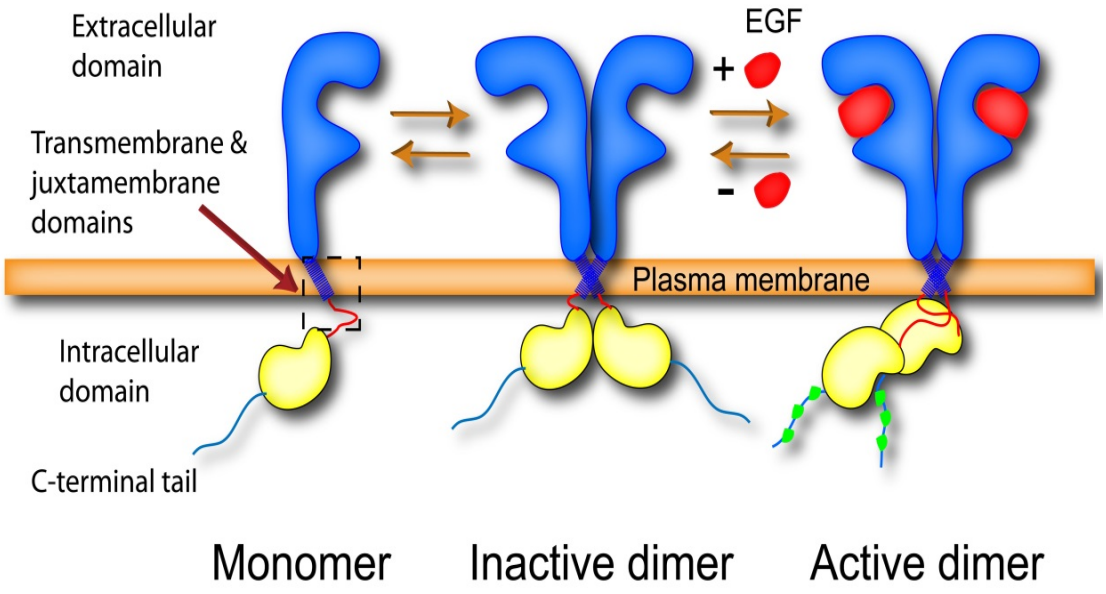

Figure 8. EGFR structure before and after dimerization and ligand binding. EGFR consists of four distinct domains. EGFR is able to form inactive dimer before ligand binding. EGFR signaling is activated after ligand binding and dimerization. Autophosphorylation occurs in C-terminal tail of the intracellular domain, when then initiates a complex signaling pathway.

EGFR is expressed by NSCs and progenitor cells in developing brain and its expression is highly dynamic during CNS development (Doetsch et al. 2002; Ivkovic et al. 2008; Cesetti et al. 2009). EGFR has been reported to be detectable around E13 in the mouse forebrain at very low levels (Caric et al. 2001). At this age, EGFR is exclusively localized in the VZ. The expression of EGFR increases from E16 and is most concentrated in VZ/SVZ, intermediate zone and inner layer of cortical plate in the developing forebrain. It is more intense in the ventral embryonic forebrain (Misumi & Kawano 1998; Caric et al. 2001; Sun et al. 2005). EGFR becomes highly expressed from late embryonic stages to the first postnatal weeks, and later is restricted to postnatal SEZ, rostral migratory stream (RMS), olfactory bulb (OB) in the adult rodent brain. EGFR is also expressed in other brain regions at various levels and with different timing, such as strong expression in external germinal layers of cerebellum, and weak expression in fiber tracts (Seroogy et al. 1995; Misumi & Kawano 1998; Anton et al. 2004; Aguirre et al. 2005). The temporal and spatial expression of EGFR in the brain is closely correlated to the onset and peak of gliogenesis, suggesting that EGFR may regulate the switch between neurogenesis and gliogenesis.

In addition to expression of EGFR in the brain, several lines of evidence have been demonstrated the important roles of EGFR in neurogenesis and gliogenesis during CNS development. Loss-of-function studies by constitutively knocking out EGFR indicated proliferation and differentiation defects in astrocytes and apoptosis of neurons, which then lead to severe necrosis in the forebrain after the first week of birth (Sibilia et al. 1998; Threadgill et al. 1995). In addition to cell proliferation and survival, EGFR positively regulates progenitor migration. Gain-of-function by viral transduction or transgenic mouse

models demonstrated that enhanced EGFR signaling increases progenitor cell migration from the VZ/SVZ to the cortex and OB (Caric et al. 2001; Aguirre et al. 2005). Previous studies have demonstrated that EGFR exerts a regulation of gliogenesis in a level-dependent manner (Burrows et al. 1997; Aguirre et al. 2007). A loss-of-function study utilized mice homozygous for hypomorphic EGFR waved2 alleles. In the waved2 allele, a glycine is substituted for a conserved valine residue near the amino terminus of EGFR tyrosine kinase domain, which results in more than 90% decrease in EGFR phosphorylation (Luetteke et al. 1994). The production of oligodendrocytes, especially Olig2+ progenitors decreases after demyelination in the brains of wave2 mice, when EGFR signaling is dramatically reduced (Aguirre et al. 2007). In contrast, overexpression of EGFR led to an increase of oligodendrogenesis using a transgenic mice model. The human EGFR transgene expression was driven by 2',3'-cyclic nucleotide 3'-phosphodiesterase (CNP) promoter, therefore EGFR is specifically overexpressed in the oligodendrocyte lineage. The numbers of Olig1/Olig2+ oligodendrocytes were significantly increased by enhanced EGFR expression. These studies suggest that both oligodendrocyte production and Olig1/Olig2 expression is associated to the level of EGFR expression. More importantly, EGFR may be involved in regulation of cell fate choice in NSCs. EGFR signaling pathway interacts with Notch to maintain the appropriate number of NSCs and progenitors in SEZ stem cell niche. Increased level of EGFR reduces the number of NSCs and its proliferation, while it increases the population of progenitor cells (Aguirre et al. 2010). These progenitor cells with enhanced EGFR expression are then most likely to give rise to glial cells. Previous studies illustrated that enhanced level of EGFR in progenitor cells differentiate into astrocytes in response to

cytokine signaling pathway. This regulation of EGFR signaling is through the increased expression of transcription factor STAT3, which is critical for astrocyte differentiation (Burrows et al. 1997; Viti et al. 2003). All these studies point out the importance of EGFR during neural development and its potential role in regulation of neurogenesis and gliogenesis.

Introduction to dissertation

Temporal generation of neurons and glial cells is precisely controlled by the interaction of intrinsic mechanisms and environmental cues during CNS development. EGFR signaling has been suggested that is sufficient to promote gliogenic competence in NSCs for glial cell generation. However, the necessity for EGFR in regulating the neurogenic/gliogenic fate specification in NSC is still arguable. Inactivation of EGFR signaling by inhibitors in NSCs showed that glial cell fate acquisition during development is independent of EGFR expression (Zhu et al. 2000), while another study suggested that EGFR is essential for developmental change in responsiveness to other signaling to induce gliogenesis (Viti et al. 2003). Although previous studies of EGFR-null mice have illustrated that EGFR plays an important role in cell survival, apoptosis and astrocyte differentiation (Sibilia et al. 1998), the lethality and necrosis of germline EGFR-null mutants impedes the detailed analyses of EGFR in NSC fate specification. Therefore, a genetic approach that is able to conditionally disrupt EGFR expression is needed. We utilized EGFR condition knockout model (Lee & Threadgill 2009)to delete its expression during perinatal transition from neurogenesis to gliogenesis. More importantly, conditional deletion of EGFR in the mosaic analysis with double markers (MADM) system allowed me to unveil an unexpected and potentially significant mechanism through which NSC fate specification is regulated by EGFR cell autonomously and through clonal cell-cell interactions.

MATERIALS AND METHODS

Animals

Mice were housed in a 12-hour light:dark cycle with ad libitum access to food and water. All procedures were performed under the regulations and approval from Institutional Animal Care and Use Committee and at North Carolina State University. We used cWT (*EGFR*$^{F/+,}$ *EGFR*$^{+/+}$ or *Nestin-Cre:EGFR*$^{+/+}$) and EGFR-cKO (*Nestin-Cre:EGFR*$^{F/F}$) mice for immunohistochemistry. For western blotting, we used cWT, Het (*Nestin-Cre:EGFR*$^{F/+}$) and EGFR- cKO mice.

For mosaic analyses, *Nestin-cre:MADM11*$^{TG/GT}$*:EGFR*$^{F/+}$ mice were generated using breeding schemes previously described (Liang et al. 2013). Briefly, Nestin-cre mice were crossed to *MADM11*$^{GT/GT}$ line to generate *Nestin-cre:MADM11*$^{GT/+}$, which were then crossed to *MADM11*$^{GT/GT}$ line again to generate *Nestin-cre:MADM11*$^{GT/GT}$. Mice with EGFR floxed alleles were crossed to the *MADM11*$^{TG/TG}$ line to generate *MADM11*$^{TG/+}$*:EGFR*$^{F/+}$, which were then crossed to *MADM11*$^{TG/TG}$ to generate *MADM11*$^{TG/TG}$*:EGFR*$^{F/+}$ mice. The resulting *Nestin-cre:MADM11*$^{GT/GT}$ mice were crossed to the *MADM11*$^{TG/TG}$*:EGFR* $^{F/+}$ mice to generate the *Nestin-cre:MADM11*$^{TG/GT}$*:EGFR* $^{F/+}$ (MADM-EGFR). *Nestin-cre:MADM11*$^{TG/GT}$ *EGFR*$^{+/+}$ mice were used as MADM control for immunohistochemistry. For fixed analyses of postnatal brains, mice were sacrificed at multiple developmental stages by Avertin overdose (7.5 mg/g body weight) followed by transcardial perfusion with 4% paraformaldehyde (PFA) in 0.1 M phosphate buffered saline (PBS).

BrdU administration

10 mg/ml 5'-Bromo-2'-deoxyuridine (BrdU) (Sigma) was dissolved in 0.9% saline. Mice at various developmental stages were administered BrdU at 100 μg/g body weight via intraperitoneal injections. Mice were sacrificed 1 hour after BrdU injections.

Perfusion and Immunohistochemistry

Mice were perfused with 4% paraformaldehyde (PFA) in 1x PBS, debrained, and brains were post-fixed in 4% PFA overnight (ON) at 4°C. Brains were embedded in 3% low melting agarose (Fisher Sci.) in 1X PBS and sliced into 50 μm sagittal sections with a vibrating blade microtome (Leica VT1000s). For immunohistochemistry, floating brain sections were blocked with 10% goat or donkey serum and 1% Triton-X 100 in 1X PBS for 1 hour at room temperature (RT). Rabbit anti-EGFR (1:1000, abcam), rabbit anti-Cleaved caspase3 (1:1000, cell signaling), rabbit anti-Olig1(1:500; generous gift from Dr. Charles Stiles Harvard University), rabbit anti-Olig2 (1:1000, Millipore), rabbit anti-GFAP (1:1000, Dako), mouse anti-CC1(1:1000, Millipore), rabbit anti-S100(1:1000, Dako), or rabbit-Pax6 (1:1000, cell signaling), mouse anti-PH3 (1:1500, abcam), or mouse anti-BrdU antibody (10:1000, BD biosciences) in 1XPBS containing 1% goat or donkey serum and 0.3% Triton-X 100 (Sigma) for ON at 4°C. Sections were washed with 1x PBS 3 times, 5 minutes for each wash, and then incubated with species-specific conjugated fluorescence secondary antibodies directed against the species of the primary antibody for 1 hour at RT. After secondary antibody incubation, the sections were washed with 1X PBS as indicated above,

mounted on glass slides, and coverslipped. Sections were then imaged using a Nikon Eclipse EZ- C1 confocal microscope.

Western blotting

Rostral forebrains from cWT and EGFR-cKO mice were rapidly dissected in lysis buffer (50mM Tris HCl PH8.3, 1% TritonX, 500mM EDTA PH8.0, 100mM NaCl, 50mM NaF with 1 protease inhibitor cocktail (Roche) and homogenized for 3 minutes with a bullet blender. Lysates were then centrifuged for 20 minutes at 13,000 rpm at 4°C. BCA assay was performed to determine protein concentration of supernatants following manufacture's protocol (Pierce BCA kit). Samples were boiled for 5 minutes with 2X SDS loading dye at 1:1 ratio.

40 µg protein samples were loaded and separated by size in a 10% polyacrylamide gel and transferred onto a nitrocellulose membrane using Tris-Glycine transfer buffer with 20% methanol. Membranes were then washed briefly with TBS-T (1x Tris Buffered Saline containing, 0.1% Tween-20) and transferred to blocking buffer (5% dry milk in TBS-T) for 1 hour at RT. Blots were incubated with EGFR antibody (1:5000, abcam) in blocking solution ON at 4°C. Blots were then washed with TBS-T 3 times, 5 minutes each, at RT, followed by incubation with species-species HRP-conjugated secondary antibody (1:10000, Millipore) for 1 hour at RT. Membranes were then washed three times in TBS-T and incubated for 1 min with ECL (Bio-Rad). Autoradiography films (Kodak) were used to capture the signal from each blot and then developed in an automated film developer. Actin was used as loading control.

Neurosphere culture

Rostral forebrains were collected rapidly from the cWT and EGFR-cKO at P0 in Hanks' balanced salt solution. Subependymal zone (SEZ) whole mounts (Mirzadeh et al. 2010) were then microdissected, cut into small pieces, and incubated in enzyme solution [20ml dissociation solution (20.44 ml 1M Na2SO4, 15 ml 0.5M K2SO4, 1.45ml 1M MgCl2, 0.63 ml 0.1M CaCl2, 0.25ml 1MHepes, 5ml 1M D-glucose, 0.5ml 0.5% phenol red, add nucleus free water to 250ml total volume) containing 6.4mg cysteine and 0.2ml papain (Roche)] for 40 minutes at 37 °C to mediate enzymatic dissociation. Following incubation, enzyme solution was removed carefully without disturbing the digested tissue and 2ml NEP basal (47.5ml Neurobasal (Gibco), 1ml B2(Gibco), 0.5ml N2(Gibco), 0.5ml 200mM L-glutamine, 0.5 ml 1x penicillin/ streptomycin) with 10% Fetal bovine serum (FBS) was added to deactivate enzymatic dissociation for 2 minutes at 37°C. Solution was then removed without disturbing the tissue pieces to initiate dissociation. 2ml NEP basal was added and tissues were triturated up and down slowly using 10 ml pipette 8 to 10 times. As soon as tissue pieces settled down, supernatant containing dissociated cells was transferred to a new 15ml conical tube and trituration was repeated 2 more times to collect adequate dissociated cells. Supernatant was centrifuged at 800 rpm at 4°C for 5 minutes and the dissociated cell pellet was re-suspended in 1ml NEP basal for cell counting using hemocytometer (Fisher Sci.). 20 cells per µl were plated in NEP basal supplemented with growth factors 20ng/ml hEGF (Invitrogen) and 10ng/ml bFGF (Invitrogen). Cells were cultured at 37°C/ 5% CO2 and growth factors were added every 2 days. Neurospheres were passaged every 4-5 days by mechanical dissociation, as previously described (Jacquet et al.

2009). Neurospheres were imaged by Nikon EZ-C1or Olympus FV-1000 confocal microscope once a day throughout all passage and the number of neurosphere was counted in 10 random areas in 20x magnification in each culture.

Confocal imaging and quantification

All sections were captured by Olympus FV1000 or Nikon EZ-C1 confocal microscope at 20X or 60X magnifications. For quantifying densities of BrdU+, cleaved-caspase3+, or Olig2+ cells, 3-5 areas of the dorsal subependymal zone and corpus callosum in each section were randomly selected and imaged at 60X magnification with 5 steps of 2μm step size interval in the Z dimension. A minimum of 9 sections from a minimum of 3 mice were analyzed for each marker. Three sampling grids with an area of 1000 μm^2 were randomly assigned for cell counting in each image. For quantifying densities of MADM neurons and MADM glial cells, 5 random spots of the cortex in each section were imaged at 20X magnification with 5 steps of 2μm step size interval in the Z dimension. All MADM-color labeled cells, with neuron or glial cell morphology, were counted in each section and at least 21 sections (n=3) were analyzed. The number of cells per mm^3 was determined by dividing total number of cells by estimated volume analyzed for each region. For quantifying cell percentages of double labeled cells, total number of double-marker labeled cells was divided by one of those cell specific markers to determine the proportion. Cells were considered co-labeled when markers were co-localized in the same Z-plane.

For regional quantification of GFAP immunoreactivity, rostral forebrains were acquired at 20X and then stitched using an Olympus FV1000 confocal microscope. The

average fluorescence intensities in the SEZ, CC, frontal cortex, and OB were measured by the Fiji software by subtracting background pixel density from measured pixel density in fluorescently labeled tissues. Comparisons of intensities were conducted between cWT and EGFR-cKO, and between MADM-Ctr and MADM-EGFR brains. Average values across all sections were calculated for each animal.

Cell transplantation

For cell transplantation assays, whole SEZs were rapidly dissected from P0 MADM-Ctr or MADM-EGFR brains, cut into small pieces, and then incubated in enzyme solution at 37°C for 40 minutes. After incubation, enzyme solution was removed and 2ml NEP basal with 10% FBS was added to deactivate enzymatic dissociation for 2 minutes at 37°C. The digested tissues were triturated to yield single-cell suspension with a Pasteur pipette. The suspensions were then centrifuged at 800 rpm at 4°C for 5 minutes and re-suspended in 1ml NEP basal for cell counting using hemocytometer (Fisher Sci.). The single-cell suspensions were centrifuge again and re-suspended in PBS with a density of 500,000 cells/µl.

P0 WT mice, used as host, were anesthetized by placing on ice for 3 minutes and maintaining hypothermia during cell injection using a stereotaxic instrument. 2µl of Single-cell suspensions were stereotaxically injected into lateral ventricle using Hamilton syringe (#80308), which was attached to the stereotaxic operation stage. The injection site was located 1mm caudal to the midpoint of a virtual line connecting the right eye with lambda. The needle was pierced through skull surface perpendicularly to a depth of approximately 2.5mm. Once the needle was hold in place, 2µl of single-cell suspension (500,000cells/µl)

was manually injected into the right lateral ventricle. After injection, mice were placed on a heat-pad until resumed movement and then return to the home cage with foster mother.

Data analysis

Tissue analyses were carried out using an Olympus FV1000 or Nikon EZ-C1 confocal microscope, and data were quantified using standard stereological estimation. Significance was determined using Student's t-tests and all values were expressed as mean± standard error of the mean (s.e.m).

CHAPTER 1

EGFR IS REQUIRED FOR OLIGODENDROCYTE SPECIFICATION DURING PERINATAL DEVELOPMENT

RESULTS

1.1 EGFR is expressed by embryonic and postnatal neural progenitors

EGFR has been demonstrated to be expressed in the postnatal subependymal zone SEZ stem cell niche of rodents (Seroogy et al. 1995; Misumi & Kawano 1998; Anton et al. 2004). Using in-situ hybridization panels provided by the Allen Brain Atlas (http://developingmouse.brain-map.org/), we confirmed developmental expression pattern of EGFR. The level of the signal varied at different ages in these regions. Low levels of EGFR can be detected in the lateral ganglionic eminence (LGE) in the early embryonic brain (E14.5-E15.5). However, increase in EGFR expression was observed around birth (E18.5-P4) in the SEZ, corpus callosum (CC), striatum, rostral migratory stream (RMS) and olfactory bulbs (OB). After P4, EGFR expression became concentrated in the SEZ (Figure 9a). Immunohistochemistry was also performed by using a commercially available EGFR antibody (Abcam #ab52894) to further confirm the expression pattern of EGFR protein. EGFR+ cells were detected primarily in the SEZ, CC, RMS and OB (Figure 9b). Similar to the in-situ hybridization pattern, the levels of immunoreactivity for EGFR varied at different ages in these regions. Stronger levels were detected between ages P4 and P21. These data suggest that EGFR is primarily expressed in SEZ, CC, RMS and OB during early postnatal development in mice.

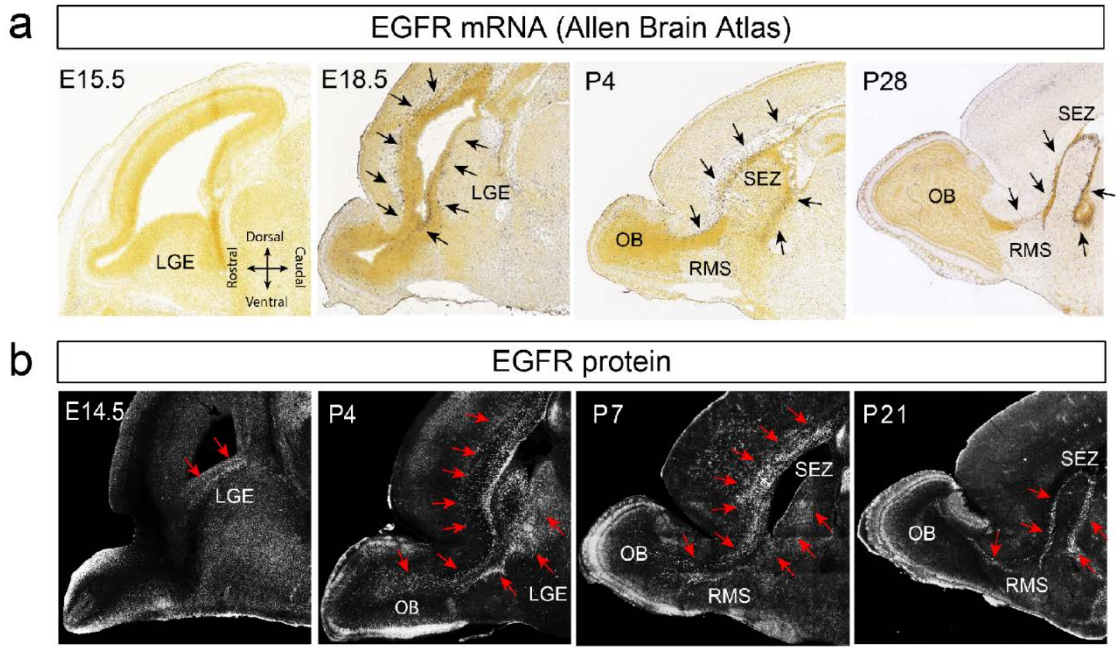

Figure 9. Developmental expression pattern of EGFR in the forebrain. (a). In-situ hybridization panels from the Allen Brain Atlas illustrating localization of EGFR mRNA in the embryonic and postnatal forebrain. **(b**). Confocal images of forebrain tissue immunostained for EGFR in the embryonic and postnatal forebrain. Arrows point to regions with high levels of EGFR mRNA and protein. SEZ: subependymal zone; RMS: rostral migratory stream; OB: olfactory bulb; LGE: lateral ganglionic eminence. Ages of mice are indicated on the top left corner of each panel. All images are sagittal views.

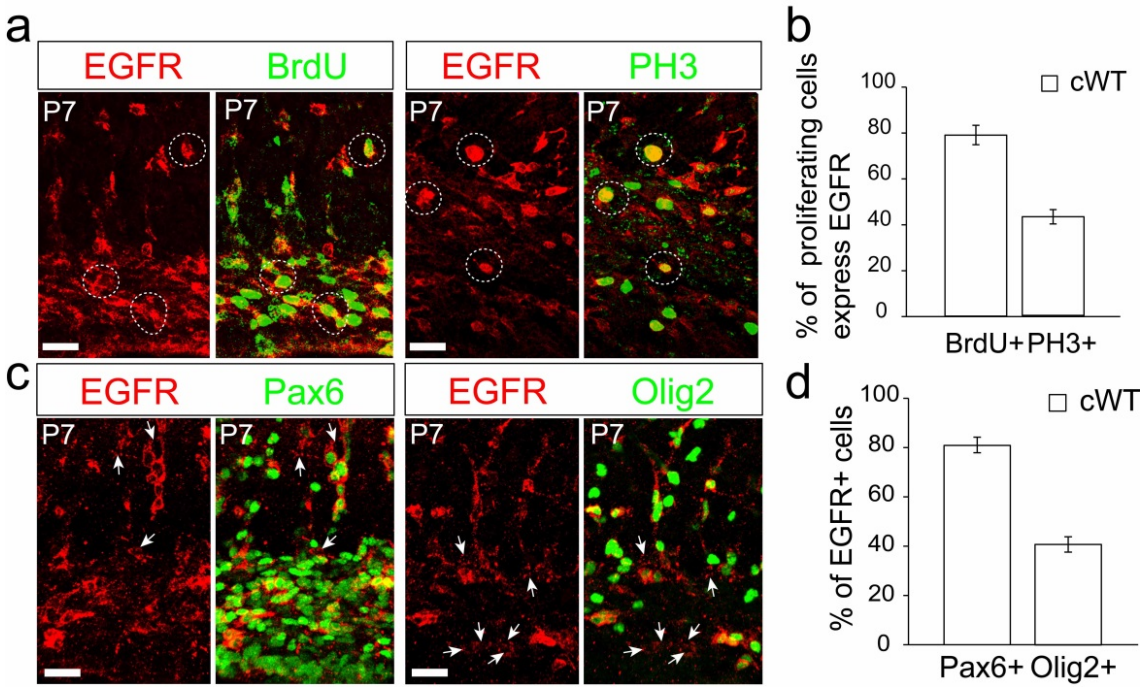

Figure 10. Identity of EGFR+ cells in SEZ. (a). Confocal images of EGFR+ (red) cells in cWT SEZ with antibodies (green) against BrdU and PH3. White circle indicate co-localization of EGFR with BrdU or PH3. Scale bar: 20µm. **(b).** Percentages of BrdU+ and PH3+ cells express EGFR. **(c).** Confocal images of EGFR+ (red) cells in cWT SEZ with antibodies (green) against Pax6 and Olig2. Arrows indicate EGFR+ cells that **DO NOT** overlap with Pax6 and Olig2. Scale bar: 20µm. **(d).** Percentage of EGFR+ cells that express Pax6 or Olig2. Data are mean ± s.e.m of percentages, n=3/age group; Student's t-test was used to test significance, *$p<0.05$.

To identify the cell specificity of EGFR+ cells, we conducted immunohistochemistry for EGFR in combination with various proliferation markers and cell lineage markers (Figure 9). First, we labeled proliferating progenitors with the S phase cell cycle marker Bromodeoxyuridine (BrdU) and M phase marker phospho-histone H3 (PH3). BrdU is a thymidine analog, which integrates into newly synthesized DNA in dividing progenitors upon administration *in vivo* and *in vitro*. Under a single pulse of BrdU administration *in vivo* followed by a one hour survival period, BrdU incorporation in SEZ largely labels S phase actively dividing progenitor cells. We found about 79% (±1%) of BrdU+ cells expressed EGFR and about 43% (±3.0%) of PH3+ cells expressed EGFR in the SEZ at P7 (Figure 10a-b), indicating that a substantial portion of proliferating cells are EGFR+ progenitors.

Based on the increasing evidence for the critical function of EGFR in oligodendrocyte production (Aguirre et al. 2005; Ivkovic et al. 2008), we next investigated the identity of EGFR+ progenitors by using the RG/IPC marker Pax6 and oligodendrocyte progenitor cell markers Olig2 and Olig1. More than 79% (±1.6%) of EGFR+ progenitors expressed Pax6 in the SEZ at P7 (Figure 10c), suggesting that EGFR is highly expressed in NSCs and IPCs. In addition, 39% (±1.7%) of Olig2+ cells express EGFR at P7 (Figure 10d), indicating that a substantial proportion of neural and glial progenitors express EGFR at any given time.

1.2 Conditional deletion of EGFR in late embryonic and early postnatal NSCs/ progenitors

According to the expression of EGFR in both embryonic and postnatal NSCs/IPCs, we decided to examine the role of EGFR in regulating the switch between neurogenesis and gliogenesis of NSCs. We adopted a loss-of-function approach via the conditional deletion of EGFR in NSCs during perinatal development. Mice were previously developed in which the EGFR exon 3 is flanked by two loxP sites (flox) (Lee & Threadgill 2009). Mice carrying the EGFR "floxed" alleles were crossed to a Nestin-cre transgenic line to generate EGFR conditional knockout mice (EGFR-cKO) (Figure 11a). In the specific transgenic line used here, Cre recombinase is expressed under the Nestin promoter, which we previously showed is active in NSCs during perinatal development (Liang et al. 2012). Upon recombination, exon 3 of EGFR is deleted resulting in a frame shift that generates two stop codons terminating EGFR expression in perinatal NSCs and their progenitor cells.

Mice with genotypes *Nestin-cre:EGFR*$^{+/+}$, *EGFR* $^{F/+}$, or *EGFR* $^{F/F}$ served as conditional control mice (cWT), while *Nestin-cre:EGFR* $^{F/+}$ were conditional heterozygous (cHET,) and *Nestin-cre:EGFR*$^{F/F}$ were conditional homozygous EGFR "knock-out" (EGFR-cKO) mice. To confirm successful deletion of EGFR in the brain, immunohistochemistry with EGFR antibody and western blotting were performed. EGFR+ cells were detected in SEZ, RMS and OB at P7 cWT animals. In contrast, the EGFR+ cells could not be observed in EGFR-cKO brains (Figure 11b). Western blotting further confirmed that EGFR was robustly deleted in the forebrains of EGFR-cKO mice at P7 age (Figure 11c).

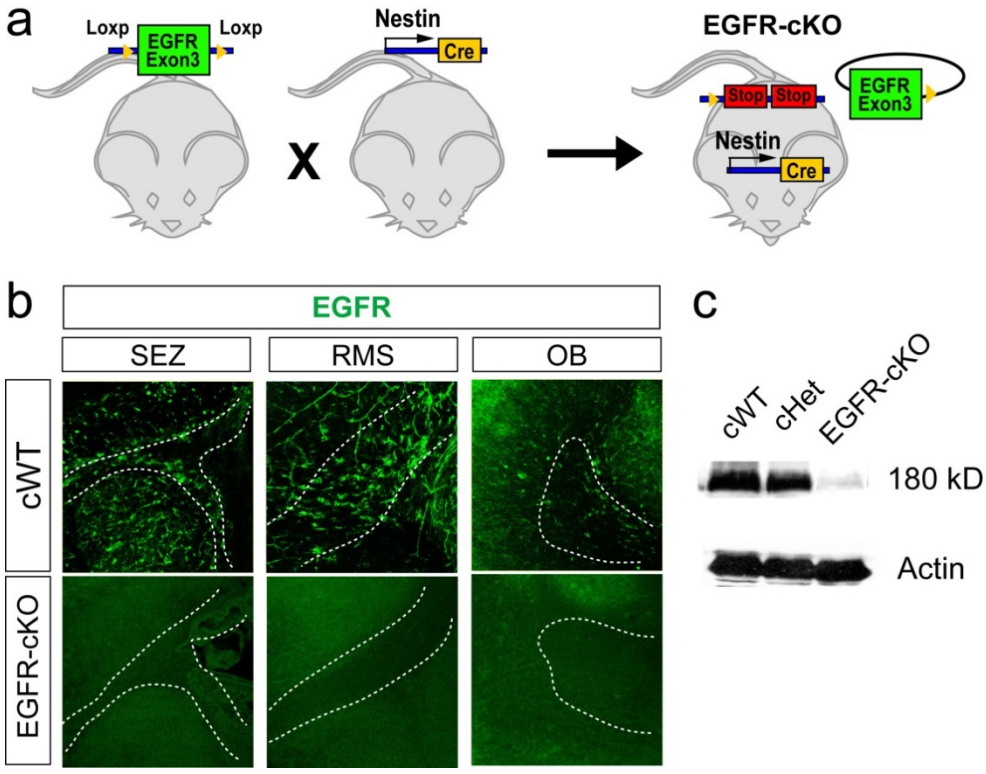

Figure 11. Deletion of EGFR with Cre/loxP system. (a). Scheme of crossing to generate EGFR-cKO mice. Conditional alleles for EGFR (exon 3 flanked by loxp sites) were crossed to Nestin-cre transgenic mice to generate EGFR-cKO animals. **(b).** Confocal images of EGFR antibody-stained tissue in the cWT and EGFR-cKO forebrain at P7. Note the near complete absence of EGFR protein in the SEZ, RMS, and OB in EGFR-cKO forebrains at this stage. Dotted lines delineate the boundaries of each structure. **(c).** Western blotting against EGFR in lysates obtained from cWT, EGFR-cHET, and EGFR-cKO forebrains at P0. Actin was used as loading control. SEZ: subependymal zone; RMS: rostral migratory stream; OB: olfactory bulb.

1.3 Deletion of EGFR causes growth retardation and histological anomalies in the brain

The first phenotype that became immediately obvious was significant growth retardation in EGFR-cKO mice. Despite being apparently normal at birth, EGFR-cKO mice grew more slowly during postnatal stages when compared to control cWT littermates. They were smaller in size and lighter in body weight after P7 (Figure 12a-b). Most of the EGFR-cKO mice (6 out of 7) were unable to survive more than three weeks when there were more than eight siblings in one litter. However, after separating from their littermates, EGFR-cKO mice were able to survive up to two years (n=10).

Specific defects within the CNS became apparent after the first week of postnatal life. A profound phenotype was spotty hemorrhages scattered within the forebrain. Spots of blood were observed in the OB in all EGFR-cKO mice analyzed and in the frontal cortex of 30% of the mice (n=10) (Figure 12c). Necrosis was detected in the EGFR-cKO forebrains (Figure 13). The upper layers of the frontal cortex were damaged in those EGFR-cKO brains with hemorrhage between P7 and P21. The observed necrosis was even more severe in the EGFR-cKO OB, including damage and absence of the granule and mitral cell layers at P7. However, unlike the frontal cortex, the defect in EGFR-cKO OB dissolved by P21 and was no longer visible (Figure 13). These data demonstrate that EGFR is important for cell survival in the OB at specific stages of early postnatal development.

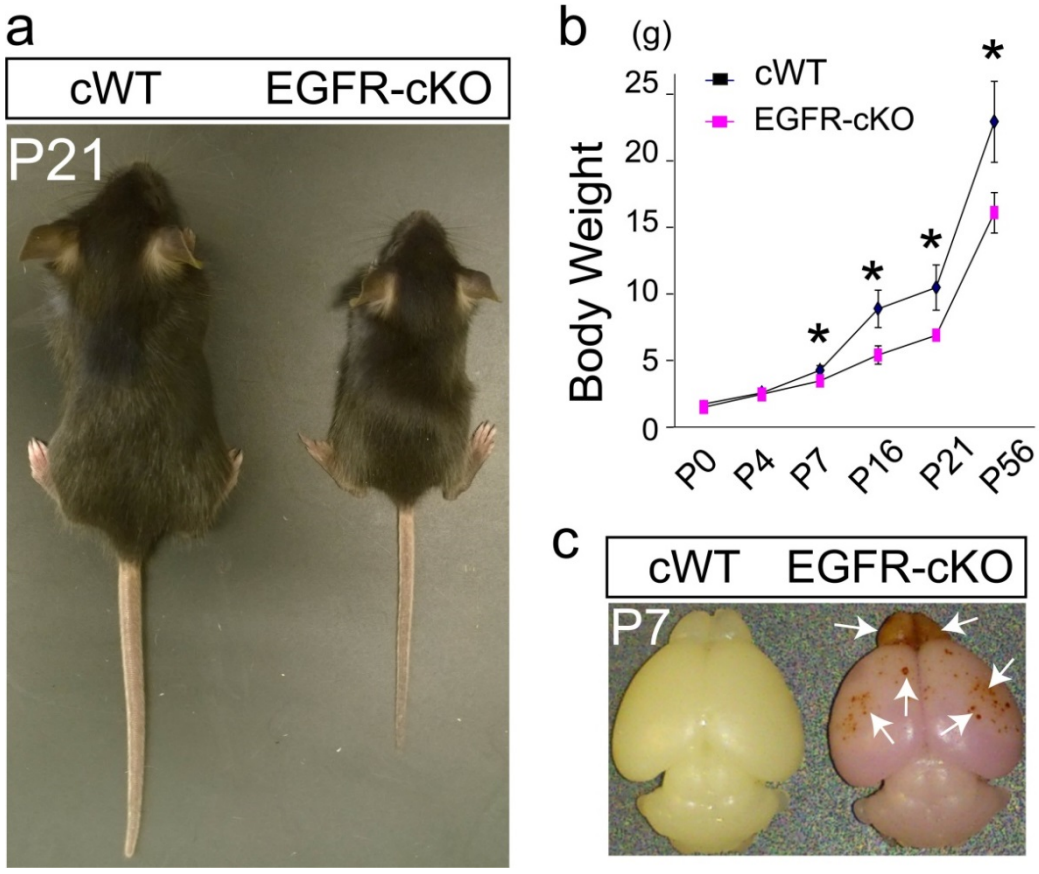

Figure 12. Growth retardation and forebrain hemorrhage in EGFR-cKO mice. **(a).** The body size of EGFR-cKO mouse is smaller than cWT littermate at P21. **(b).** Body weight of EGFR-cKO mouse is lighter after P7. Data are mean ± s.e.m of body weight, n≥3/age group; Student's t-test was used to test significance, $p<0.05$. **(c).** Hemorrhage is observed at P7 EGFR-cKO forebrain. Arrow indicates area of hemorrhage. Pink tint in EGFR-cKO brain is due to presence of reporter recombination throughout the brain.

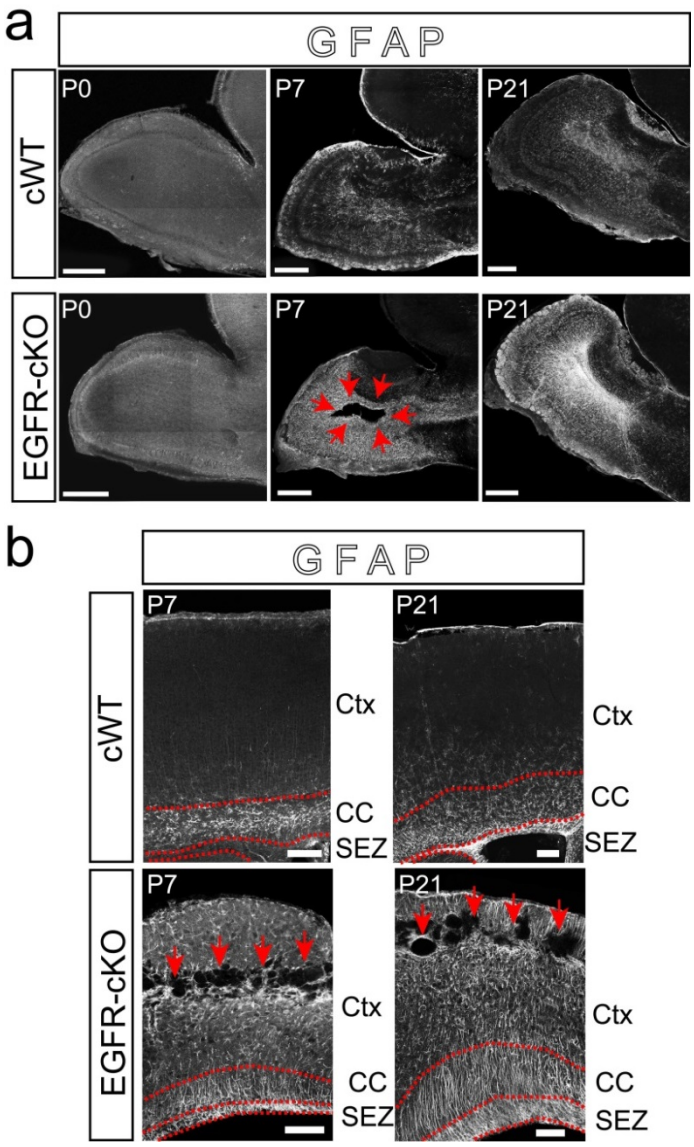

Figure 13. Neural degeneration in EGFR-cKO mice forebrain. (a). An olfactory bulb (OB) defect is observed at P7 age and disappeared after P21 in EGFR-cKO mouse. Red arrow indicates the necrosis area in OB. scale bar: 600µm. **(b).** Degeneration of frontal cortex was detected in EGFR-cKO between P7 and P21. Red arrow points to necrosis. Scale bar: 200µm

1.4 EGFR is required for proliferation in postnatal NSCs and progenitor cells

Since a significant fraction of the proliferating cells in the perinatal SEZ express EGFR (Figure 14a-b), we first conducted proliferation analysis with acute BrdU labeling to quantify overall density of cycling cells *in vivo*. BrdU was injected in animals 1 hour before fixation to label the proliferating cells. To our surprise, the density of BrdU labeled cells was only decreased at P7, but not at P0 or P21 (Figure 14a-b), suggesting that EGFR plays a role in progenitors proliferation at a specific stage of early postnatal development.

In the postnatal and adult brain, acute BrdU labeling primarily targets rapidly dividing IPCs. Because a subpopulation of postnatal NSCs are relatively quiescent with a long cell cycle interval up to 28 days (Morshead et al. 1994), while the active dividing NSCs have a much shorter S phase than IPCs (Ponti et al. 2013). In addition, NSCs are able to self-new to maintain the stem cell pool in the brain, while also possessing the capacity to expand in numbers rapidly. To examine whether the self-renewal and proliferation capacity of the dividing NSCs is affected by the loss of EGFR in SEZ, we performed the well-established *in vitro* neurosphere assay (Reynolds & Weiss 1992). Here, the size of individual neurospheres is an indicator of the expansion capacity of NSC clones, while the number of spheres helps gage their self-renewing ability. NSCs were harvested from SEZs of P0 cWT and EGFR-cKO brains and cultured to generate primary neurospheres, which were then dissociated into single cells to form secondary neurospheres. While the sizes of primary neurospheres and secondary neurospheres from EGFR-cKO NSCs were significantly smaller than cWT NSCs, their numbers were similar to cWT. This finding suggests that NSC self-renewal is not dependent on EGFR (Figure 14c-d). Taken together these results suggest that EGFR is an

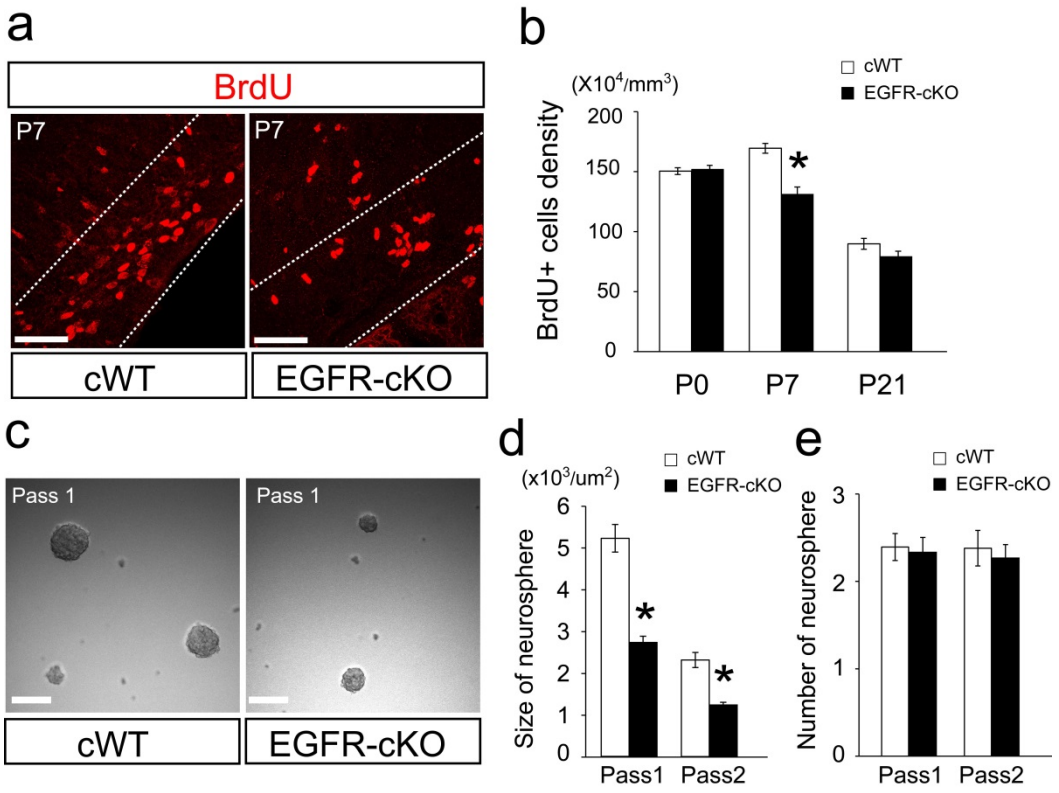

Figure 14. Decreased proliferation with loss of EGFR in the forebrain. (a). Confocal images of BrdU+ cells in cWT and EGFR-cKO SEZ at P7 age. Scale bar:50µm. **(b).** Quantification of BrdU+ cells in cWT and EGFR-cKO SEZ-CC. **(c).** Confocal images of cWT and EGFR-cKO neurospheres at passage 1 day 5. **(d).** Size of neurospheres between cWT and EGFR-cKO at passage 1 and passage 2. **(e).** Number of neurospheres between cWT and EGFR-cKO at passage 1 and passage 2. Data are mean ± s.e.m, n=3 animals; Student's t-test was used to test significance, *P<0.05. Pass1: primary neurosphere; Pass2: secondary neurosphere

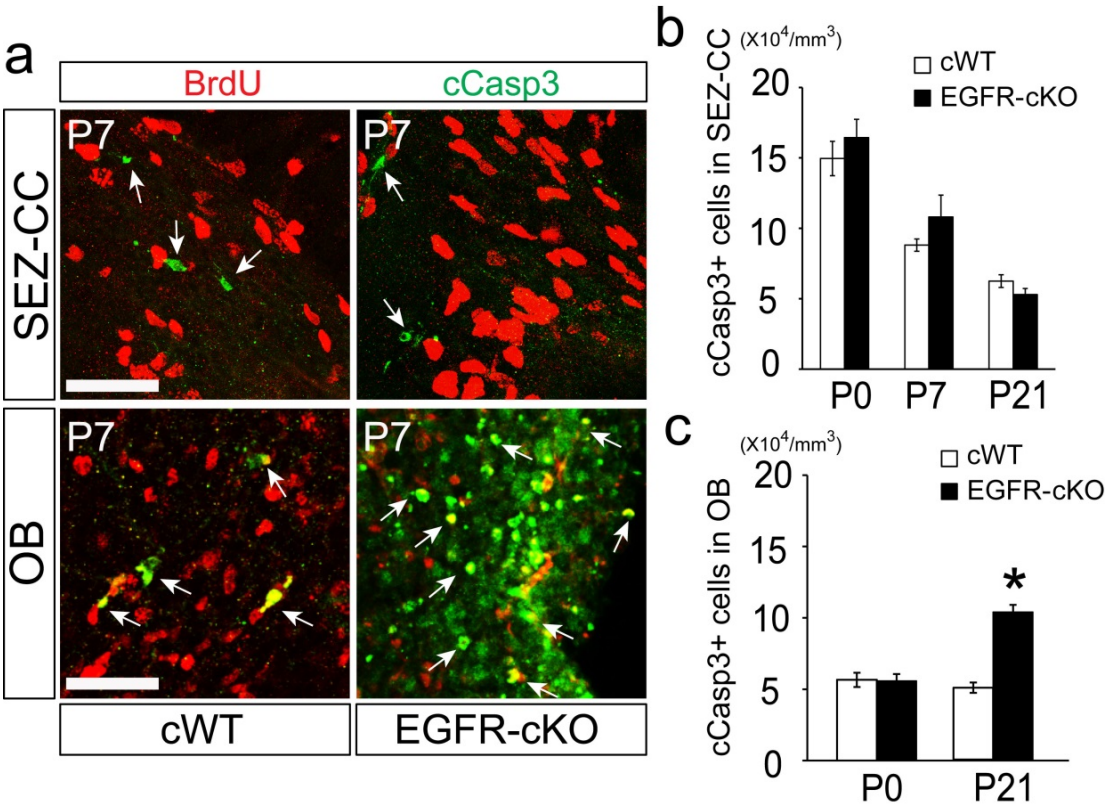

Figure 15. EGFR is not required for cell survival in SEZ-CC. (a). Confocal image of cCapse3+ (green) and BrdU+ (red) cells in cWT and EGFR-cKO SEZ-CC (upper panel) and OB (lower panel) at P7. Arrow indicates cCasp3+ cell. **(b).** Cell density of cCasp3+ cells in cWT and EGFR-cKO SEZ-CC. **(c).** Cell density of cCasp3+ cells in cWT and EGFR-cKO OB. Data are mean ± s.e.m of densities, n=3/age group; Student's t-test was used to test significance, $p<0.05$.

important regulator of proliferation in postnatal NSCs and IPCs at a specific stage of development.

In addition to proliferation, EGFR is also purported to be essential for cell survival. Therefore, we examined cell apoptosis in the SEZ and OB using the apoptosis marker cleaved caspase3 (cCasp3). Densities of cCasp3+ cells were not significantly different between cWT and EGFR-cKO in SEZ-CC from P0 to P21 (Figure 15a-b). The density of cCasp3+ cells was also identical between cWT and EGFR-cKO OBs at P0 (Figure 15a,c). Since the granule cell layer and mitral cell layer were degenerated in EGFR-cKO OBs at P7, we were unable to quantify the density of cCasp3+ cells. However, cCasp3+ cells and cell debris stained with cCasp3 were readily found throughout the degenerated OBs in EGFR-cKO brains at P7 (Figure 15a), indicating massive apoptosis in EGFR-cKO OBs. Even though the OBs appeared regenerated after P21, the density of cCasp3+ cells remained significantly higher in EGFR-cKO OB at this age (Figure 15c). Taken together, these data suggest that EGFR plays an important role in cell survival of differentiating cells in the OB, but not in progenitor cells of the SEZ.

1.5 EGFR is required for generation of specific set of glial cells in the SEZ and CC

Cell proliferation and survival were not affected by the loss of EGFR in SEZ progenitor cells at P0 (Figure 14b; Figure 15 b). These data indicate that EGFR may have a vital role in other cellular functions, such as cell fate specification. In support of this notion, past studies reported that overexpression of EGFR is sufficient in increasing glial precursors

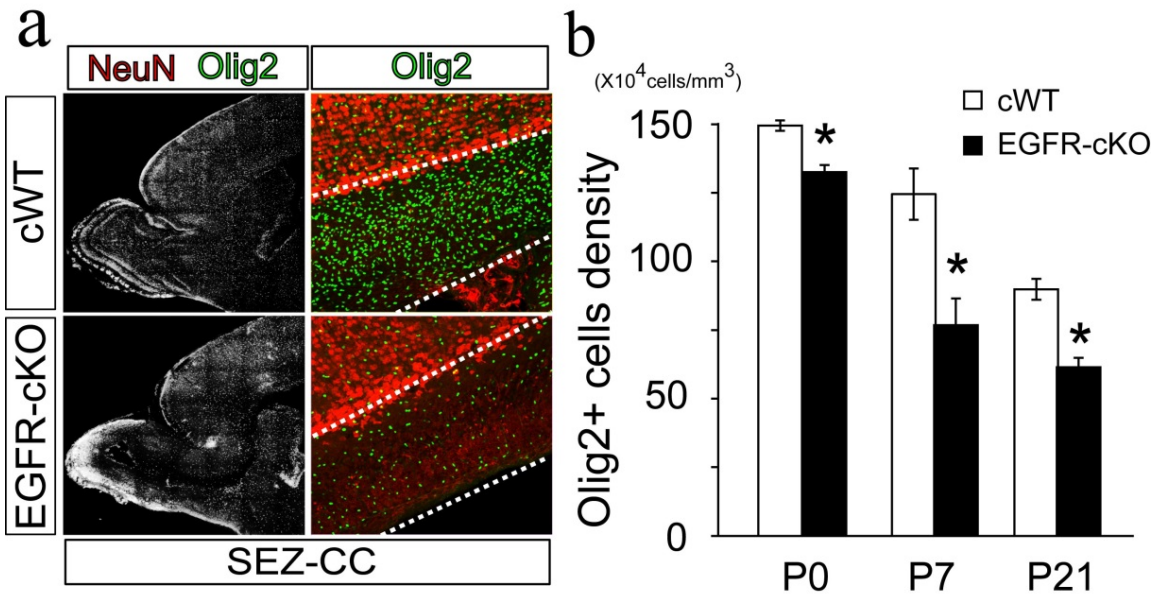

Figure 16. Decreased OPCs production with loss of EGFR in the forebrain. **(a).** confocal image of Olig2+ (green) cells in cWT and EGFR-cKO forebrains. Inserts are the high magnification images of indicated areas. Scale bar in left panel:600µm; right panel:100µm. **(b).** Cell density of Olig2+ cells in cWT and EGFR-cKO SEZ-CC at P0, P7 and P21. Data are mean ± s.e.m, n=3/age group; Student's t-test was used to test significance, *$p<0.05$.

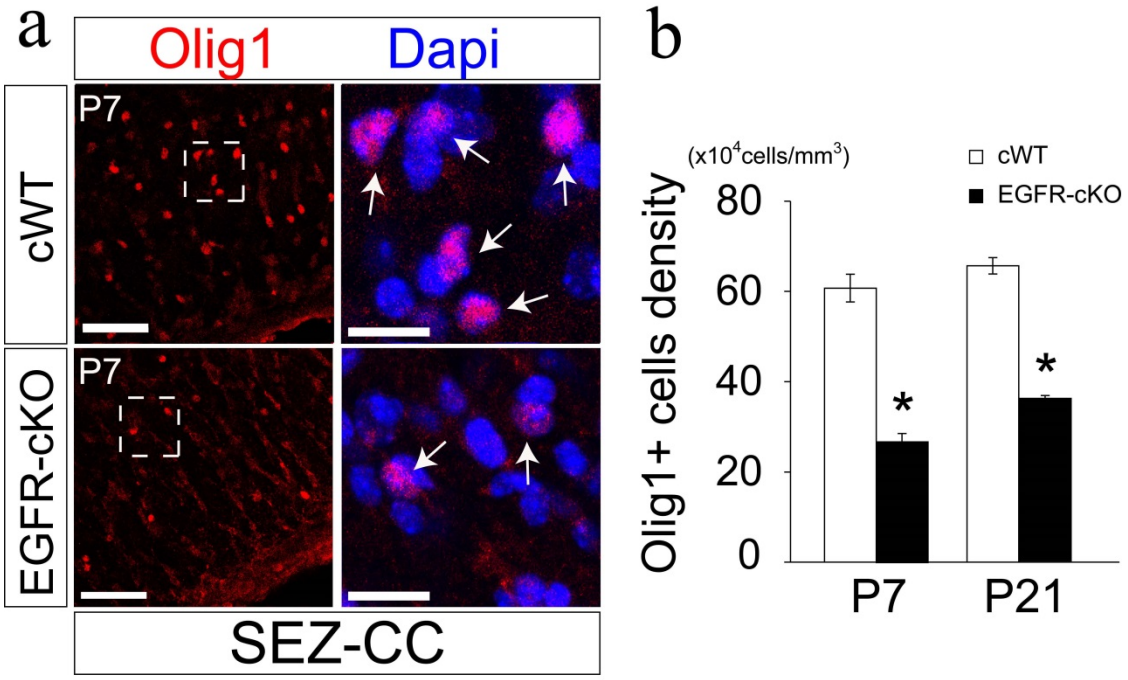

Figure 17. Decreased production of differentiating and mature oligodendrocyte in EGFR-cKO SEZ-CC. (a). confocal image of Olig1 (red) expression in cWT and EGFR-cKO SEZs at P7. Inserts are high magnification images in left panels. Arrow indicates co-localization of Olig1(red) with Dapi (blue). Scale bar in left panel: 50µm; right panel:10µm. **(b).** Quantification of Olig1+ cells in cWT and EGFR-cKO SEZ at P7 and P21. Data are mean ± s.e.m of densities, n=3/age group; Student's t-test was used to test significance, $p<0.05$.

in the mouse brain (Gonzalez-Perez et al. 2009). We therefore tested whether glial cell production is affected in the absence of EGFR. To address this question we first immunostained brain sections for the oligodendrocyte lineage marker Olig2. The densities of Olig2+ cells were significantly depleted in the EGFR-cKO SEZ and CC from P0 to P21 (Figure 16). Similarly, the densities of Olig1+ cells, the differentiating and mature Oligodendrocytes, were significantly reduced in EGFR-cKO SEZ and CC at P7 and P21 (Figure 17). Olig1+ cells were difficult to detect at P0 in both cWT and EGFR-cKO brains, likely due to the immature nature of OPCs at this stage. Since cell proliferation and apoptosis was not affected by the loss of EGFR at P0, the heavy depletion of Olig1/2+ cells in the EGFR-cKO SEZ and CC suggested that EGFR is a key regulator of oligodendrocyte fate acquisition.

Astrocytes are another important type of glial cells in the brain with multiple functions. To examine whether production of astrocytes was affected in the absence of EGFR, we used GFAP which largely marks reactive astrocytes. GFAP+ astrocytes in the CC exhibit a fibrous morphology (Figure 18a1), while GFAP+ cells situated in the SEZ resemble radial glia with one pole of them attached to the ependymal layer while their basal process contacting blood vessels (Figure 18a2). Surprisingly, there was no significant change in GFAP intensity in the SEZ, CC or the frontal cortex of EGFR-cKO mice compared to WT brains between P0 and P21 (Figure 19), unless there was necrosis present as in the few cases noted earlier (Figure 13). We also found a dramatic increase of GFAP intensity in EGFR-cKO OBs at P7 and P21. Since it is known that reactive astrocytes respond to brain damage, the increase of GFAP + astrocytes could constitute a secondary effect on OB

degeneration by the loss of EGFR. Taken together, these data suggest that EGFR plays a critical role in regulating a specific subtype of glial cell genesis during early postnatal development.

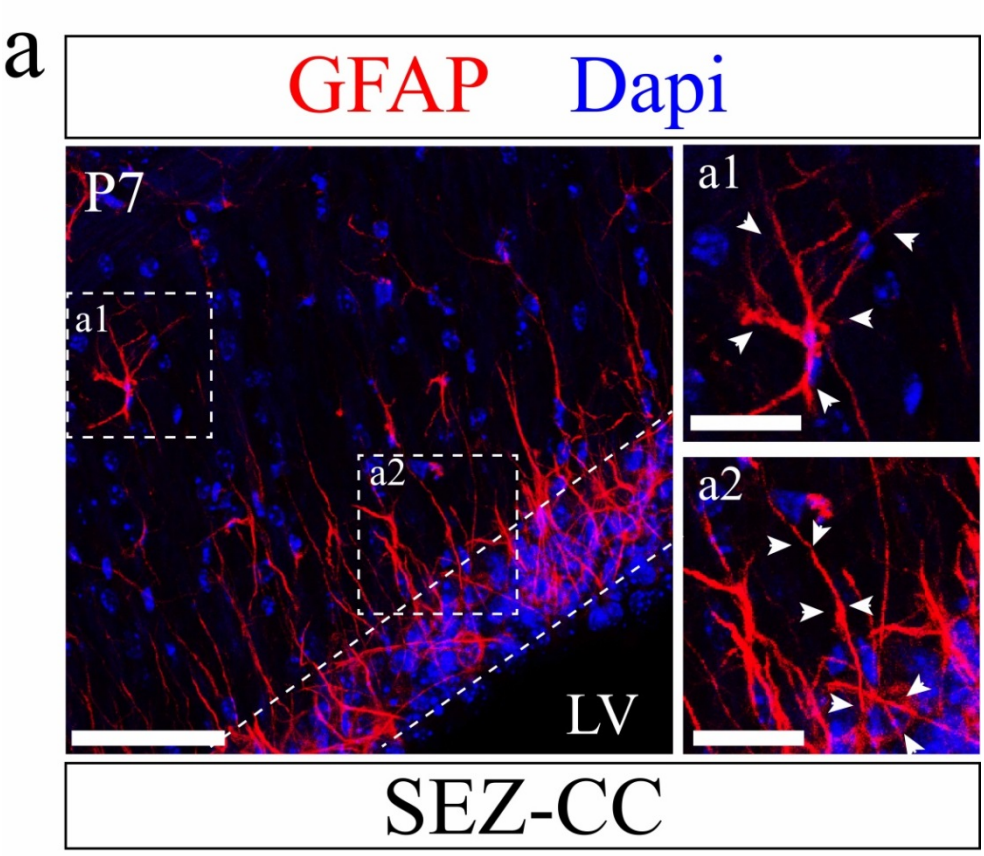

Figure 18. Distinct morphology of GFAP+ astrocyte in SEZ and CC. (a). Confocal image of GFAP+ astrocyte in P21 SEZ and CC. Inserts are high magnification of indicated areas. Dotted line outlines the SEZ. Scale bar:50μm. **(a1).** GFAP+ cell in CC display "star" shape morphology; **(a2).** GFAP+ cell in SEZ resemble radial glial cell morphology. Arrow head outlines the represented GFAP+ cell morphology in SEZ and CC. Scale bar: 20μm. LV: lateral ventricle

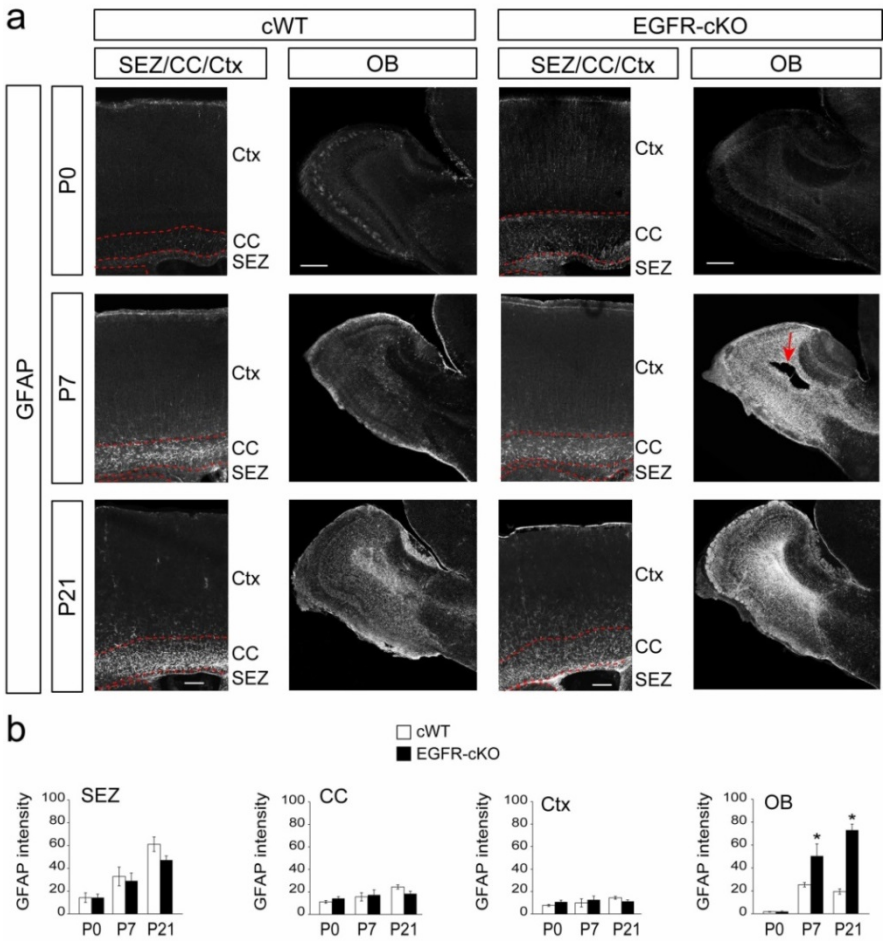

Figure 19. Characterization of reactive astrogliosis in the EGFR-cKO forebrain. (a). Confocal images of GFAP stained frontal cortices (Ctx), corpus callosum (CC), SEZ, and OB at P0, P7, and P21 in cWT and EGFR-cKO brains. Dotted lines demarcate boundaries between SEZ, CC, and Ctx; red arrow points to necrosis present in 100% of EGFR-cKO mice observed thus far at P7 (n=61). **(b).** Quantification of GFAP intensity in each region across the three ages in cWT and EGFR-cKO forebrains. Data are mean ± s.e.m, n=3 animals; Student's t-test was used to test significance, *$p < 0.05$.

DISCUSSION

The regulation of EGFR in cell survival during embryonic development

The expression of EGFR has been shown to be upregulated during perinatal development (Caric et al. 2001; Sun et al. 2005) and our data confirms this temporal pattern and we further identified the expression of EGFR in VZ and SEZ, which is highly expressed by proliferating progenitors, including dividing NSCs and oligodendrocyte progenitor cells. Additionally, previous loss-of-function studies have revealed that EGFR is critical for homeostasis during CNS development. For example, constitutive deletion of EGFR causes massive necrosis in the forebrain after the first week of birth (Sibilia et al. 1998). A similar phenotype was also observed in our study after conditional deletion of EGFR in perinatal NSCs and their progeny. However, no obvious abnormal brain damage was observed at birth by deleting EGFR either constitutively or conditionally at perinatal ages. This phenotype is more likely due to low expression of EGFR at early embryonic stage, which only dramatically increases around birth. In addition, the densities of apoptotic cells were identical at P0 between WT and EGFR-cKO mice in SEZ, CC and OB, suggesting that EGFR is less likely to be important for cell survival during embryonic brain development, opposing the prevailing views in the field.

The regulation of EGFR in NSCs glial fate specification

Past studies showed that overexpression of EGFR increases oligodendrocyte progenitors production (Ivkovic et al. 2008; Aguirre et al. 2007). Our data shows that conditional deletion of EGFR in NSCs during perinatal stages leads to decrease in

oligodendrocyte production, as a result of a decline in induction of well established oligodendrocyte specifiers, the Olig1 and Olig2 transcription factors. In addition, our data illustrated that proliferation and apoptosis of progenitors in SEZ are not affected by the loss of EGFR at birth. Taken together, these data indicate that EGFR plays an important role in oligodendrocyte fate specification in forebrain NSCs.

Previous studies illustrated that enhanced expression of EGFR in the embryonic VZ leads to early expression of astrocytes (Burrows et al. 1997), and constitutive deletion of EGFR causes defects in astrocyte differentiation after birth (Sibilia et al. 1998). Surprisingly, we did not find defects in GFAP+ astrocytes in the SEZ, CC or the cortex between cWT and EGFR-cKO mice, unless there was neuronal necrosis accompanying the damage. It is now known that astrocytes are heterogeneous both molecularly and functionally (Zhang & Barres 2010). For example, fibrous astrocytes are primarily located in the white matter, while protoplasmic astrocytes are detected in gray matter. GFAP primarily labels a subset of reactive astrocyte in the white matter. It is still unclear whether other subsets of GFAP negative astrocytes are affected by the loss of EGFR or not, such as the S100+ protoplasmic astrocyte. However, since GFAP+ reactive astrocyte significantly increased in the damaged OB we can conclude that the subset of astrocytes with the means to respond to injury, or the SEZ progenitors that migrate toward the degenerated OB, are not EGFR-dependent neither for their production nor for their other responses (e.g., migration toward injury).

Mechanisms of early postnatal forebrain necrosis in the absence of EGFR

In the developing cortex, early born neurons largely occupy the deeper layers, while the late born neurons are mostly located in the superficial layers. Perinatal progenitor cells in VZ and SEZ of the forebrain are able to give rise to neurons and glial cells which then migrate along radial fibers to reach the superficial cortical layers or along the RMS to the OB. The degenerated brain regions were primarily observed in the OB and in the superficial layers of the frontal cortex, which are locations mostly occupied by perinatally generated neurons. Therefore, the necrosis in the cortex and OB of EGFR-cKO brain is speculated to occur in response to death of neurons. However, it is still unclear the neuronal ablation in these regions is in response to programmed apoptosis or insufficient support by glial cells, such as astrocytes, after EGFR deletion. The necrosis was detected around P4 and magnified at P7 in both conditional in our data and constitutively EGFR knockout mutant (Sibilia et al. 1998). Interestingly, the peak of astrogliosis occurs during the first few postnatal weeks (Sauvageot 2002; Tien et al. 2012), which is correlated to appearance of forebrain degeneration in EGFR-cKO mice. As EGFR signaling can reduce cell death in neurons through the action of astrocytes in co-culture experiments *in vitro* (Casper et al. 1991), the observed forebrain necrosis may a combination of cell autonomous apoptosis of neurons and insufficient support by astrocytes. The specific subtype of astrocyte that is critical for neuron survival remain to be determine, as we found the GFAP+ reactive astrocyte do not significantly change in the absence of EGFR.

Another possibility of the massive forebrain necrosis could due to the dramatic reduction of oligodendrocytes. The primary function of oligodendrocytes is axon

myelination and remyelination. Loss of oligodendrocytes results in demyelination, which can lead to severe neuronal diseases such as multiple sclerosis (Compston & Coles 2008). In addition to their myelinating functions, oligodendrocytes have been shown to promote neuronal survival by releasing neurotrophic factors, such as insulin-like growth factor I (IGF-1) (Wilkins et al. 2001; Wilkins et al. 2003). Both oligodendrocyte progenitors and mature oligodendrocytes decrease in EGFR-cKO brains, which may then leads to insufficient secretion of neurotrophic factors to support the survival of neurons.

CHAPTER 2.

EGFR REGULATES NEURONAL/GLIAL FATE SWITCH THROUGH CELL AUTONOMOUS MECHANISM AND CLONAL CELL-CELL INTERACTION DURING PERINATAL DEVELOPMENT

The finding in chapter 1 demonstrated that EGFR is highly expressed by NSCs and progenitor cells in SEZ stem cell niche. Conditional deletion of EGFR mediated by perinatal specific driver Nestin-Cre illustrated that EGFR is required for cell proliferation at specific time period during early postnatal development. It is essential for cell survival in OB. Our date also indicate that EGFR may be required for a specific subtype of glial cell acquisition. To further investigate the mechanisms of EGFR in cell fate specification, we conditionally deleted EGFR in the mosaic analysis with double markers (MADM) mice (Zong et al. 2005).

RESULTS

2.1 Deletion of EGFR in MADM system does not cause forebrain necrosis

The findings in chapter 1 demonstrate that EGFR is expressed by a set of perinatal NSCs and IPCs in the forebrain. Conditional perinatal deletion of EGFR mediated by Nestin-Cre revealed that EGFR is required for cell proliferation during a specific period of perinatal development, and that its expression is essential for homeostasis in the OB. Our data also indicates that EGFR may be required for specification of a distinct subtype of glial cells that includes oligodendrocytes, but possibly also astrocytes. Specifically, the observed increase in astrogliosis in the EGFR-cKO OB may represent a secondary gliogenic response to repair mechanisms induced following hemorrhage and necrosis.

To further investigate this issue, we used a mouse genetic system called Mosaic Analysis with Double Markers (MADM) (Zong et al. 2005) in which genetic perturbation can be induced in low percentages of cells within tissues (Hippenmeyer et al. 2010). In this system, two reciprocal chimeric reporter genes were targeted in identical loci, in this case on the mouse chromosome 11 (MADM-11) where the EGFR gene also located. One allele contains N-terminus of the reporter gene GFP and C-terminus of another reporter gene, tdTomato (GT). The other allele contains the N-terminus of tdTomato and C-terminus of GFP (TG). An intron containing a loxp site was inserted between the coding sequences of the two reporter genes to allow for site directed interchromosomal cre-mediated recombination between the alleles. Moreover, since the EGFR locus is also located on chromosome 11, the combination of this system allowed us to analyze cell autonomous and non-autonomous effects of EGFR deletion in the same animal through generation of cWT (red), cHET (yellow) and cKO (green) cells (Figure 20). The animals that did not carry a floxed allele for EGFR were used as control (MADM-Ctr), in which all the color labeled cells are WT. Figure 21 illustrates sample confocal images of MADM mediated recombination in both these mice using the same *Nestin-cre* transgene used in Chapter 1.

To ensure the necrosis observed in EGFR-cKO mice did not occur in MADM-EGFR forebrains we conducted histological assessments and found no tissue damage in the frontal cortices or the OB from P0 to P30. Moreover, GFAP intensities were identical between MADM- Ctr and MADM-EGFR brains at P7 and P30, indicating that there was no potential brain damage or astrocytic response in MADM-EGFR animals (Figure 22).

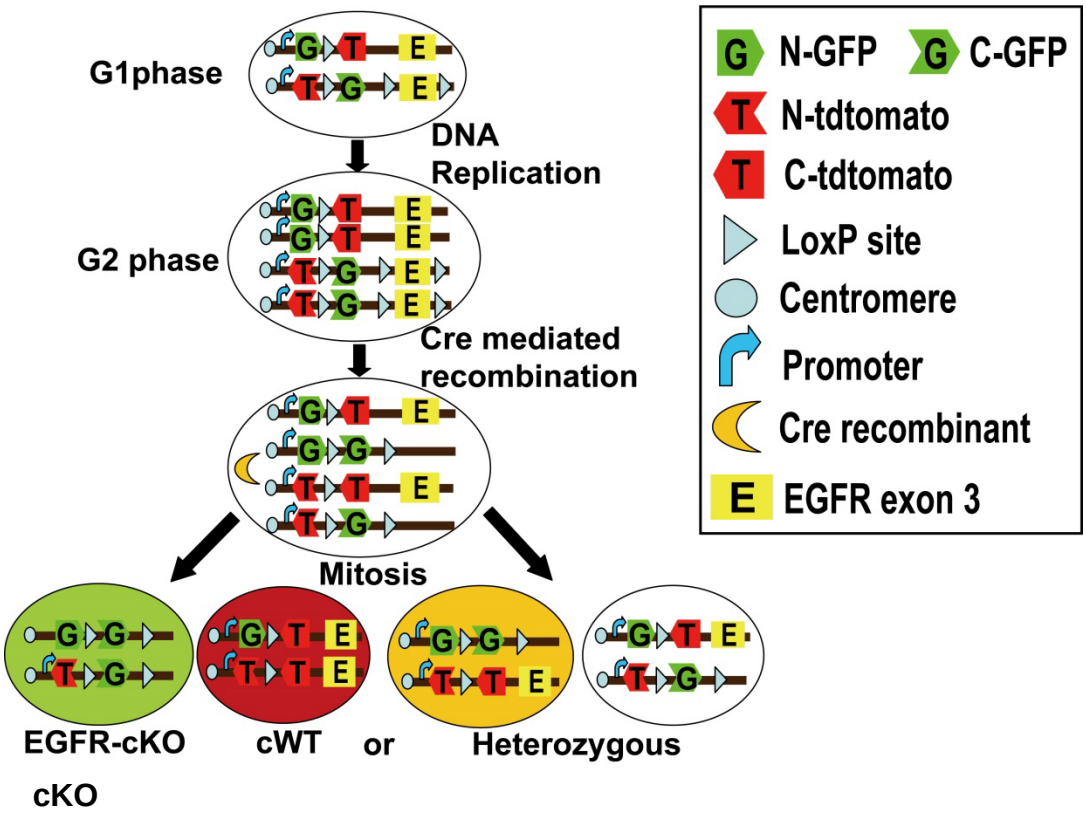

Figure 20. Utilization of Mosaic Analysis with Double Markers (MADM) with the EGFR floxed allele. EGFR floxed allele is introduced to MADM system, which follows c-terminal GFP. G2 phase cre- mediated mitotic interchromosomal recombination generate cWT (red; tdTomato+), cHet (yellow; GFP+ tdTomato+), and cKO (green; GFP+) cells from clones of NSCs that label distinctly with fluorescent reporters.

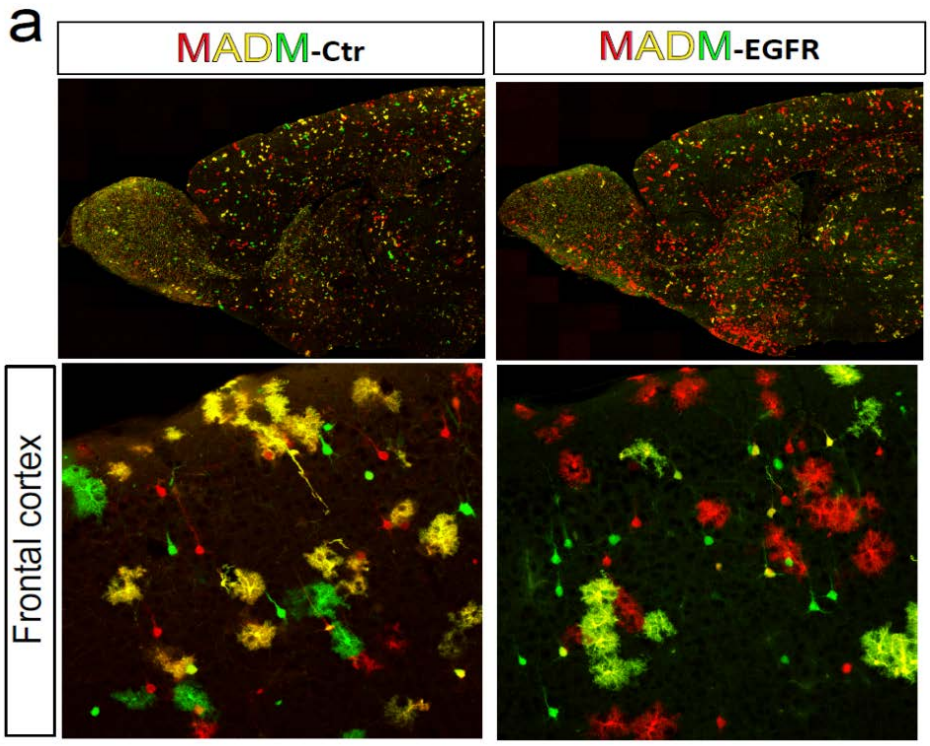

Figure 21. Sample confocal image of MADM11 with/without EGFR floxed allele. Confocal images of MADM-Ctr and MADM-EGFR forebrains at P30 (upper panels). Lower panels are high magnification images of MADM-Ctr and MADM-EGFR frontal cortex. All color cells in MADM-Ctr are WT. In MADM-EGFR mice, red cells are WT. Green cells are cKO. Yellow cells are heterozygous.

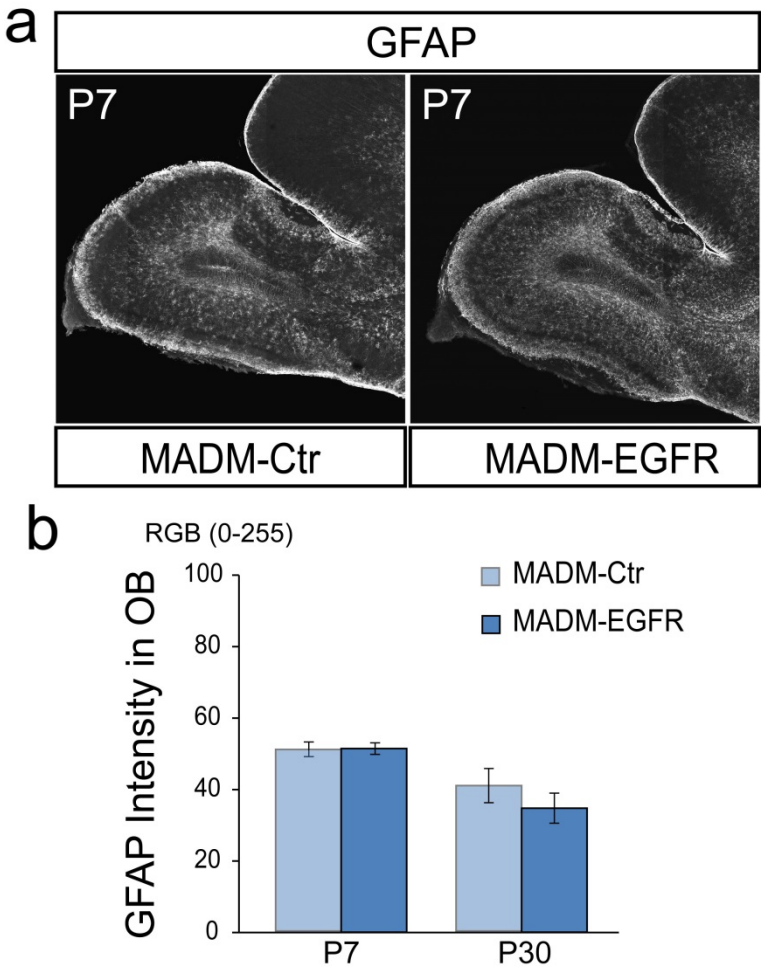

Figure 22. No potential OB damage in MADM-EGFR animal. (a). confocal image of MADM-Ctr and MADM-EGFR OBs stained for GFAP at P7. **(b).** Quantification of GFAP intensity in each MADM background reveals no increase of astrogliosis in MADM-EGFR OBs at P7 and P30. Data are mean ± s.e.m, n=3/age group; Student's t-test was used to test significance,* $p<0.05$.

2.2 EGFR is required for NSC neuronal/glial fate specification in a cell autonomous manner

To set a standard for analyzing proportions of neurons and glia in MADM cells with distinct genotypes, we first quantified the density and percentages of GFP+ and tdTomato+ MADM neurons and glia in the MADM-Ctr cortex. Glial cells can be distinguished by their characteristic "star" shape with numerous branches (Figure 23 a-f). Neurons are easily identifiable based on their dendritic arbors on one side of the cell opposed by a long axon (Figure 23 a-f). We found that the densities of both glial cells and neurons in the tdTomato+ cWT (red) population were not significantly different from GFP+ cWT (green) cells in MADM-Ctr cortex (Figure 23g). Similarly, the percentages of tdTomato+ glial cell (44±1.2%) and neuron (43±2.8%) as a fraction of the total tdTomato+ population were identical to GFP+ glial (46±1.3%) and neuronal (47±1.3%) populations (Figure 23h). In addition, both the density and percentage of glia were identical to neurons (Figure 23g-h), suggesting the NSCs generate glial cells and neurons in a 1:1 ratio in clones generated from MADM-11 recombination events.

Analysis of MADM-EGFR brains immediately revealed a visible and dramatic loss of cKO (green) cells in the forebrain (Figure 24). In addition, a dramatic increase in the cWT (red) cells with glial-like morphologies was noted. In contrast, most of the cKO cells exhibited neuronal features, such as long axons apposing thick dendrites on polarized sides of the cells (Figure 24a). It was difficult to detect cKO glial-like cells in MADM-EGFR forebrain (Figure 24a). The density of cKO (green) glial cells was only 662±104 cells/mm^3 in MADM-EGFR cortex at P30, which was a dramatic decline

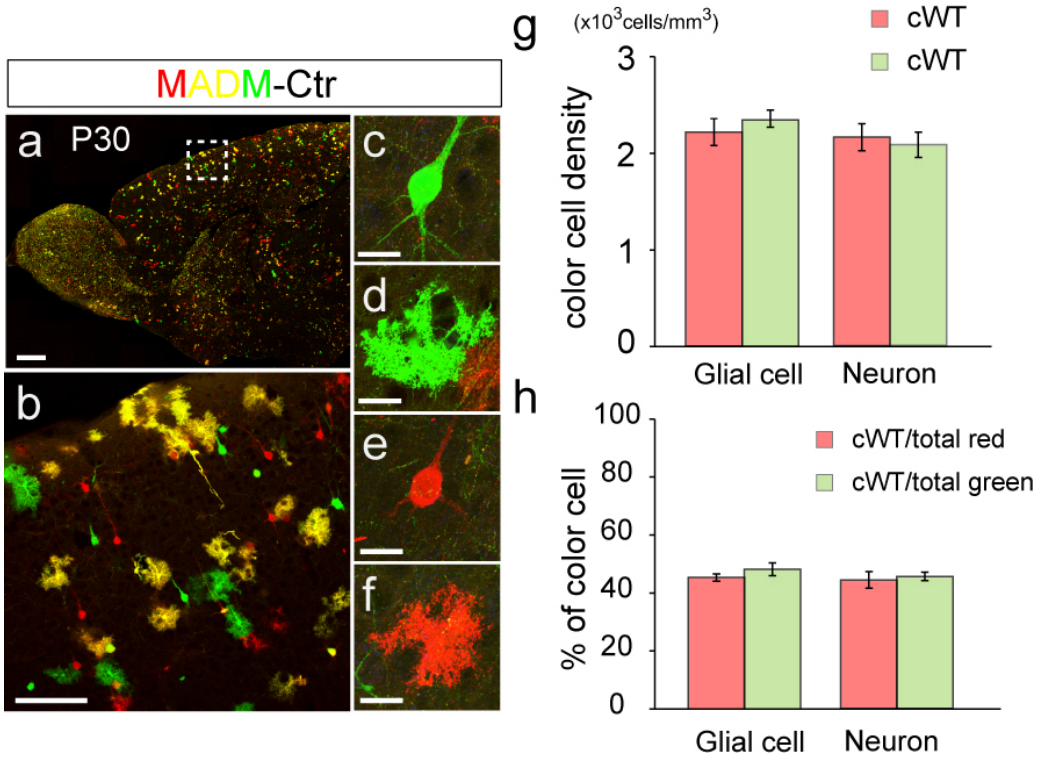

Figure 23. Equal number of MADM-labeled neuron and glial cell are generated in MADM-Ctr. (a-b). Confocal images of MADM-Ctr forebrain at P30. High magnification image of indicated area is shown in **(b).** Scale bar: **(a)** 600 µm; **(b)** 100 µm. **(c-f).** High magnification images of cWT neuron **(a,e)** and glial cells **(d,f)**. Scale bar: **(c-f)** 20 µm. **(g).** Cell densities of red/green neuron and glial cell in MADM-Ctr cortex. **(h).** Percentages of red/green neuron and glial cell in each color cells population; Data are mean ± s.e.m of densities and percentages, n=3/age group; Student's t-test was used to test significance, $p<0.05$.

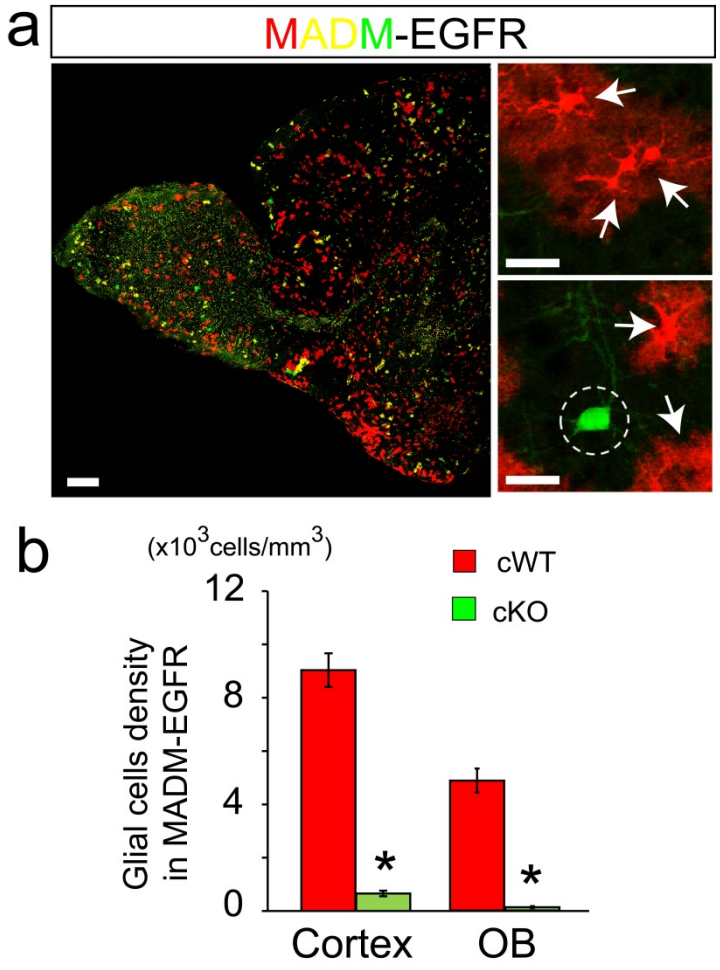

Figure 24. Decrease of cKO glial cells in MADM-EGFR forebrain. (a). Confocal image of MADM-EGFR forebrain (left panel). Right panel are representative images of MADM glial cells and neuron. Arrow indicates (cWT) glial cells and circle indicates (cKO) neuron. **(b).** Quantification of glial cells density in MADM-EGFR cortex and OB at P30. Data are mean ± s.e.m of densities, n=3/age group; Student's t-test was used to test significance, $p<0.05$.

compared to cWT (red) glial cells (9033±633 cells/mm^3). A similar phenotype was observed in the OB of MADM-EGFR mice (Figure 24b). The density of cKO glial cells (green) (124 ±36 cells/mm^3) was dramatically lower than the cWT glial cells (red) (4825±446 cells/mm^3) in MADM-EGFR OB at P30. To summarize, EGFR cell autonomously regulated the generation of glial cell.

Based on our findings and the known role for EGFR in oligodendrocyte fate specification, we next assessed the molecular fate of cKO and cWT type cells in MADM-Ctr and MADM-EGFR forebrains. To accomplish this, percentages of different cell types in MADM-EGFR SEZ, CC, and cortex labeled with various markers were calculated. We first we determined whether NSCs in the SEZ and CC are affected in the absence of EGFR by using Pax6. Pax6 is expressed in RGs and postnatal NSCs in SEZ, which is critical for neuron and glial cell specification (Englund et al. 2005; Jang & Goldman 2011). A significant decrease in density of Pax6+ nuclei was found in the cKO population compared to cWT cells in the SEZ at P0 which became more dramatic at P30 (Figure 25a-b). However, around 42% (±1.9%) of cWT and 45% (±2.4%) of cKO cells expressed Pax6 in the MADM-EGFR SEZ (Figure 25a-b) suggesting that EGFR is likely critical for expansion of distinct lineages but not their proportional maintenance.

Next, we analyzed the production of oligodendrocytes in the MADM-EGFR SEZ and CC using Olig2 immunoreactivity as a biomarker. 22% (±3.5%) of cWT cells expressed Olig2 at P0 and 36% (±5.2%) at P30. In contrast, only 5% of cKO cells expressed Olig2 at P0 and P30 which was significantly lower compared to the cWT population (Figure

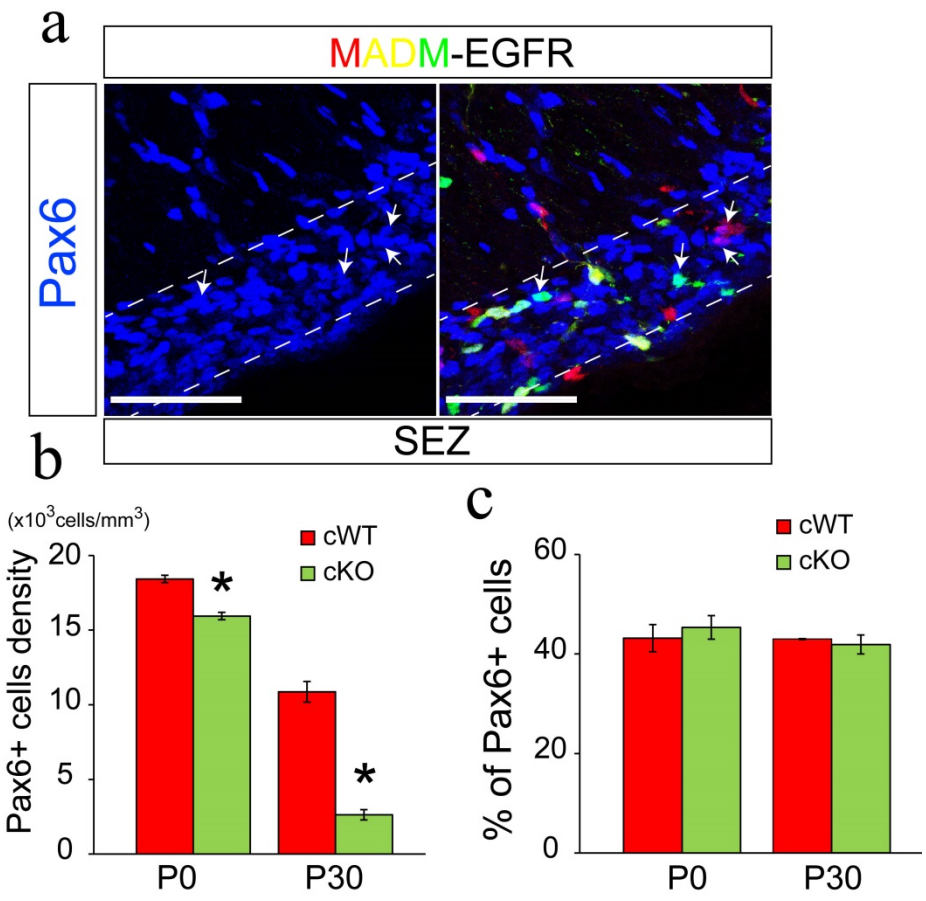

Figure 25. Maintenance of NSC/IPC proportion in SEZ stem niche is independent of EGFR expression. (a). Confocal images of Pax6+ cells in MADM-EGFR SEZ at P0. Arrows indicate co-localization of Pax6 with cWT and cKO cells. Scale bar:50µm. **(b).** Quantification of Pax6+ cWT and Pax6+ cKO cells densities in MADM-EGFR SEZ. **(c).** Percentage of cWT and cKO cells expressed Pax6 in MADM-EGFR SEZ. Data are mean ± s.e.m of densities and percentages, n=3/age group; Student's t-test was used to test significance, $p<0.05$.

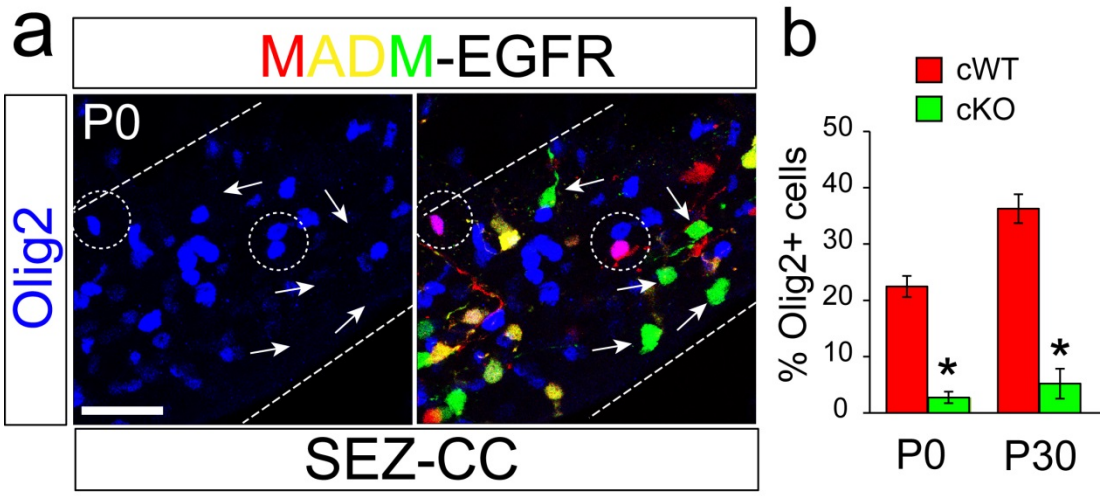

Figure 26. **A decreased percentage of cKO cells expressed Olig2 in MADM-EGFR SEZ. (a).** Confocal image of Olig2 expression (blue) in MADM-EGFR SEZ and CC at P0. Arrow represents MADM cell **DO NOT** co-localized with Olig2. Circle indicates co-localization of MADM cell with Olig2. Scale bar: 50µm **(b).** Percentage of Olig2+ cells expressed in MADM-cWT and MADM-cKO cells. Data are mean ± s.e.m of percentages, n=3/age group; Student's t-test was used to test significance, $p<0.05$.

26a-b). This was consistent with our previous data, suggesting that EGFR is required for oligodendrocyte fate specification in NSCs.

NSCs are able to give rise to both neuronal and glial progenitors, which migrate from the SEZ to their destined cortical layer where they differentiate into neurons or glial cells. To further investigate the role of EGFR in NSC fate decision, we next examined whether neuronal fate is also regulated by EGFR. We utilized the mature neuron marker NeuN for immunohistochemistry in MADM-EGFR forebrain. In contrast to Olig2, we found the percentage of cKO cells expressing NeuN at P0 was about 52% (±3.6%) in MADM-EGFR cortex, which was significantly higher than cWT cells (38±1.5%) (Figure 27). The difference was even more prominent at P30. About 58% (±7.3%) of cKO cells expressed NeuN at P30, while only 10% (±2%) of the cWT population were neurons. This data suggests that in the absence of EGFR, NSCs continue to be neurogenic instead of differentiating into, or giving rise to glial cells.

To further confirm our observation, we next compared the difference in NeuN expression between green cells in cortex of MADM-Ctr and MADM-EGFR mice. We found that the percentage of green (cWT) cells that expressed NeuN was about 40% in MADM-Ctr cortex at P30 (Figure 28a-b), which was significantly lower than green (cKO) cells (58±7.3%) in MADM-EGFR mice. Taken together, these data indicate that EGFR regulates NSC neuronal/glial fate specification in a cell autonomous manner.

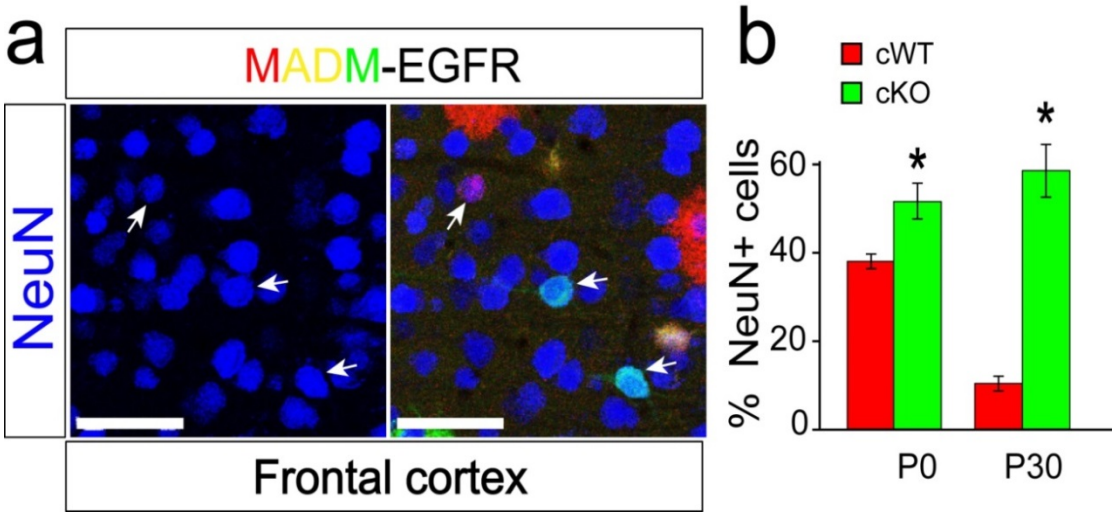

Figure 27. A higher percentage of neuron in cKO cells population in MADM-EGFR cortex. (a). Confocal image of NeuN+ cells in MADM-EGFR frontal cortex at P30. Arrow indicates co-localization of NeuN in MAMD cells. Scale bar: 50 µm **(b).** Percentage of cWT and cKO cells expressed NeuN in MADM-EGFR cortex at P0 and P30. Data are mean ± s.e.m of percentages, n=3/age group; Student's t-test was used to test significance, $p<0.05$.

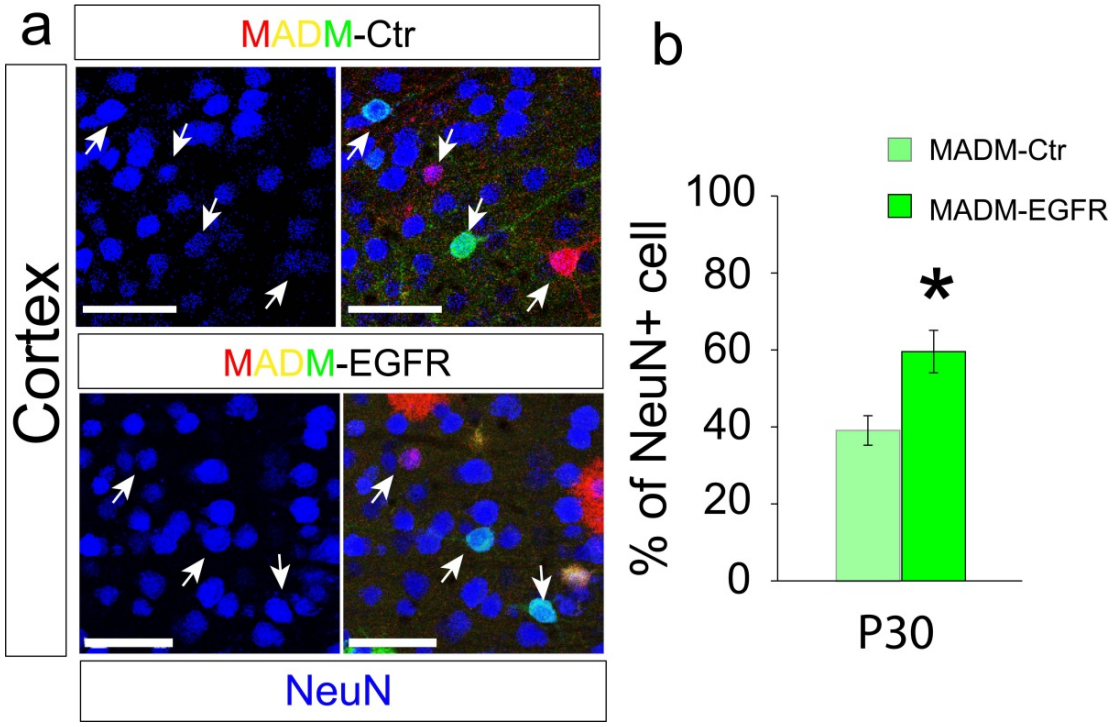

Figure 28. A higher percentage of neuron in cKO cell population in MADM-EGFR mice. (a). Confocal images of NeuN expression in MADM-Ctr and MADM-EGFR cortex at P30. Arrow indicates the co-localization of NeuN with reporter cells. Scale bar: 50μm. **(b).** Percentage of NeuN expression in cWT cells in MADM-Ctr and cKO cells in MADM-EGFR cortex at P30. Data are mean ± s.e.m of percentages, n=3/age group; Student's t-test was used to test significance, $p<0.05$.

Next, we set out to characterize the cWT glial cells using various glial cell markers such as pan-glial cell marker CC1, protoplasmic astrocyte marker S100, reactive/white matter astrocyte marker GFAP, Oligodendrocyte progenitor cell marker Olig2, and differentiating/mature oligodendrocyte marker Olig1. In MADM-EGFR cortex, we found that most of cWT (red) glial cells expressed CC1 (90±1%) and S100 (91±2.2%) (Figure 29a-b). In addition, 37% (±4%) of the cWT glial cells co-localized with GFAP, but only 4% (±1%) with Olig2. The cWT glial-like cells were rarely co-localized with Olig1, suggesting that they were mostly mature protoplasmic astrocytes, but not oligodendrocytes (Figure 29a-b). Taken together, these date suggest that EGFR cell autonomously regulate neuronal/glial cell fate specification, which is not only required for oligodendrocyte specification, but also astrocyte specification and differentiation during early postnatal development.

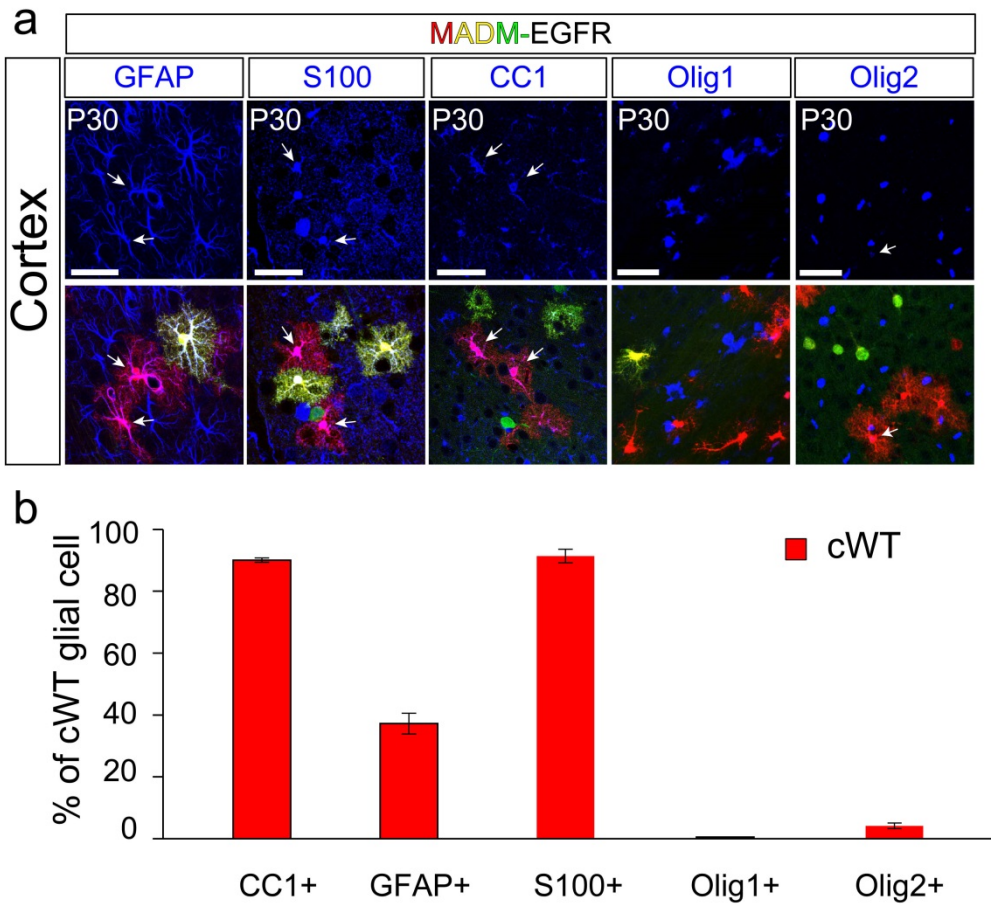

Figure 29. Identity of MADM glial cells. (a). Confocal images of MADM cells stained for GFAP, S100, CC1, Olig1 and Olig2 in MADM-EGFR cortex at P30. Scale bar: 50μm. **(b).** Percentages of MADM cWT glial cells co-labeled with various glial cell markers. Data are mean ± s.e.m of percentages, n=3/age group; Student's t-test was used to test significance, $p<0.05$.

2.3 The regulation of EGFR in NSC fate specification is background independent and through cell-cell interaction

An unexpected phenotype was that the percentage of mature neurons in MADM-EGFR cWT (red) population (10±2%) was almost four-fold lower than in MADM-Ctr cortices (39±6.3%) (Figure 30). In addition, cWT (red) cells were largely distributed throughout the forebrain in MADM-EGFR mice (Figure 21). This data may suggest that proliferation increases in cWT (red) cells, which then predominately differentiate into glial cells leading a decrease percentage of neuron in MADM-EGFR mice. To test this possibility, we first analyzed the overall densities of cWT (red) cells in the MADM-Ctr and MADM-EGFR cortices. The density of cWT cells in MADM-EGFR cortex was three-fold higher than MADM-Ctr (Figure 31). Thus, neuron/glial cell fate of cWT progenitors may be affected by the loss of EGFR. This phenotype could be explained three ways: 1) Since both cWT (red) cells in MADM-Ctr and MADM-EGFR had two functional EGFR alleles, the dramatic increase of cWT (red) cells in MADM-EGFR cortex may be due to signals from the remaining cKO cells to cWT cells through cell-cell interaction; 2) Since cWT cells express EGFR, they may respond to the loss of cKO cells and attempt to replace the depleted population; 3) Since the background in MADM system is essentially heterozygous and theoretically carrying half the amount of EGFR, the levels of EGFR ligands such as EGF and TGF available for cWT cells maybe higher in MADM-EGFR mice due to the decreased amount of EGFR in surrounding heterozygous cells. In other words, the increased gliogenesis in WT red cells ($EGFR^{+/+}$) could result from a selective advantage over the

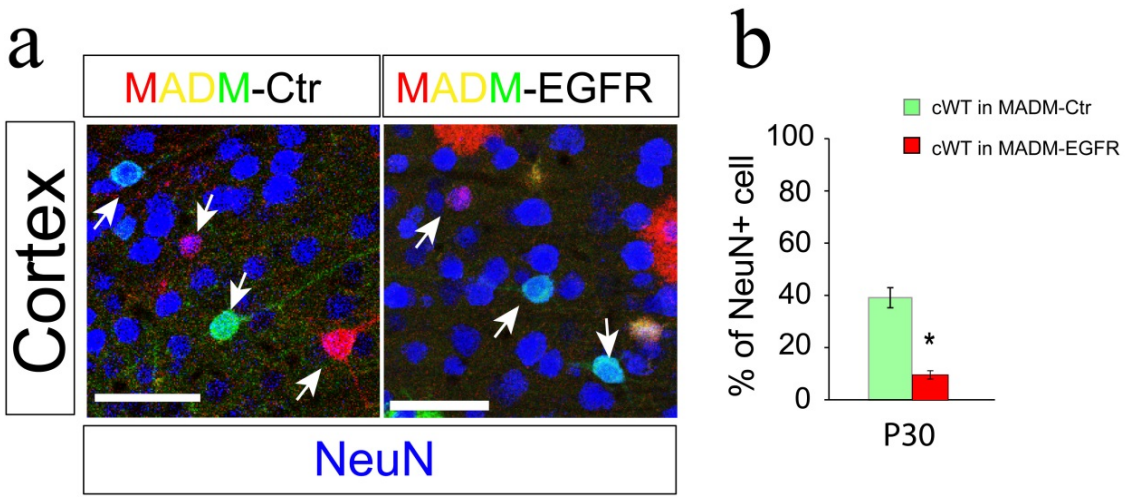

Figure 30. Decreased percentage of neuron in cWT population in MADM-EGFR mice. (a). Confocal image of NeuN+ cells in MADM-Ctr and MADM-EGFR frontal cortex at P30. Arrow indicates co-localization of NeuN in MAMD reporter cell. Scale bar: 50µm. **(b).** Percentage of cWT cells expressed NeuN in MADM-Ctr (green) and MADM-EGFR (red) cortex at P30. Data are mean ± s.e.m of percentages, n=3/age group; Student's t-test was used to test significance, $p<0.05$.

surrounding cells ($EGFR^{+/-}$) instead from a direct communication between the WT lineage and its sibling knockout green lineage ($EGFR^{-/-}$).

To test if the enhanced number of cWT (red) glia cells in the MADM-EGFR mice was due to the largely heterozygous background, we performed cell transplantation from MADM mice into WT animals. NSCs from MADM-Ctr and MADM-EGFR SEZs were isolated and transplanted into P0 WT mice through intraventricular injections. The identities of reporters labeled cWT and cKO cells were analyzed at P21 (Figure 32). Reporter-labeled cells were primarily detected in the forebrain, including the SEZ, RMS, OB, and the frontal cortex (Figure 32a). cWT (red) cells in the transplanted host brains appeared larger in density and with glial-like morphologies, similar to the phenotype observed in MADM-EGFR brains. Likewise, the transplanted cKO (green) cells were low in number and rarely labeled with S100 (5%) in the host WT brains (Figure 32b-c). Instead, there was a higher percentage of cKO cells labeled with NeuN (44±3%) than cWT (red) cells (4±1.3%) in the WT host forebrain (Figure 32b-c). These data confirmed that EGFR is a critical regulator of NSC glial fate specification both cell autonomously and non-autonomously. In addition, we found that the percentage of cWT (red) cells harvested from MADM-EGFR SEZs expressed S100 (49±5.3%), which was significantly higher than transplanted MADM-Ctr cells (29±3.8%) (Figure 32d-e). In contrast, the percentage of transplanted MADM-EGFR cWT (red) cells expressing NeuN (4±1.3%) was significantly lower than transplanted MADM-Ctr cells in wildtype host brains (27±2.3%) (Figure 32d-e). Taken together, these date suggest

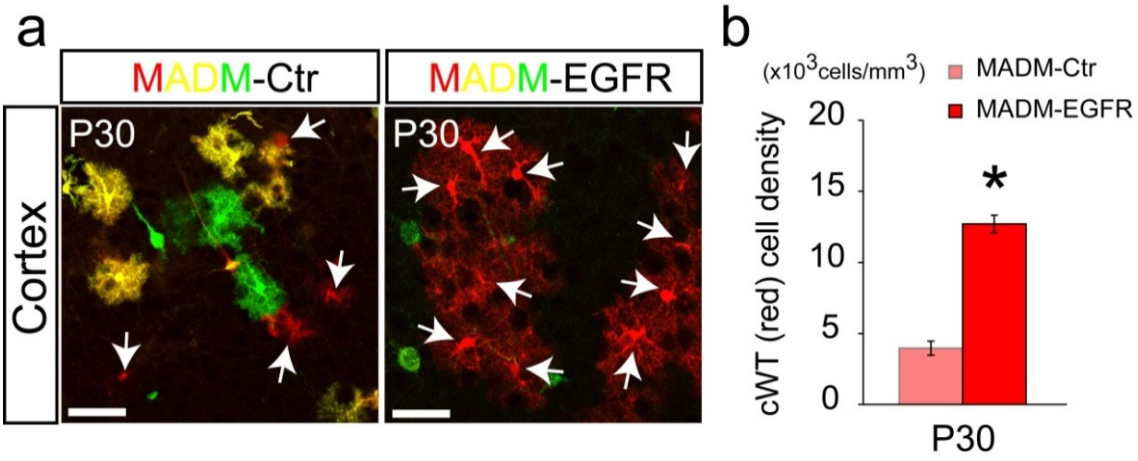

Figure 31. Increased cWT cells in MADM-EGFR forebrain. (a). Confocal image of cortex in MADM-Ctr and MADM-EGFR mice at P30. Arrows indicate cWT (red) cells. Scale bar: 50μm. **(b).** Cell densities of cWT (red) cells in MADM-Ctr and MADM-EGFR cortices at P30. Data are mean ± s.e.m of densities, n=3/age group; Student's t-test was used to test significance, $p<0.05$.

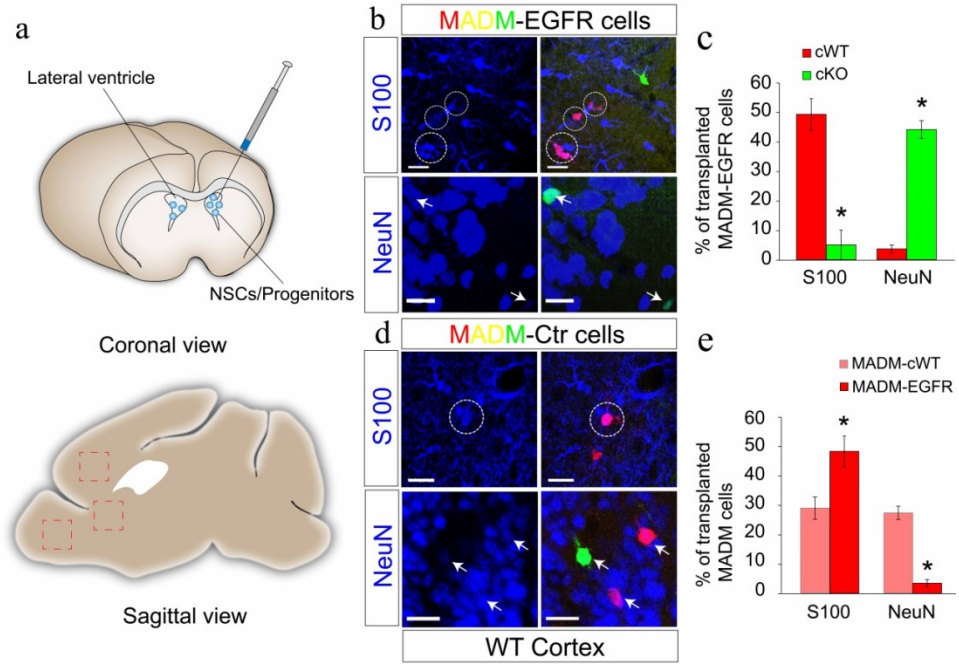

Figure 32. The regulation of EGFR in NSC fate specification is background independent. (a). Scheme of MADM cells transplantation. Red box indicates the quantification area of transplanted cells. **(b).** Confocal images of transplanted MADM-EGFR cells in WT cortex at P21. Circle indicates co-localization of MADM-EGFR cells with S100 (blue). Arrow indicates co-localization of MADM-EGFR cells with NeuN (blue). **(c).** Confocal images of transplanted MADM-Ctr cells in WT cortex at P21. Circle indicates co-localization of cWT (red) with S100 (blue). Arrow indicates co-localization of MADM-Ctr cells with NeuN (blue). **(d).** Percentage of MADM-EGFR cells expressed S100 or NeuN. **(e).** Percentage of MADM-EGFR and MADM-Ctr cWT (red) cells expressed S100 or NeuN. Scale bar:20μm. Data are mean ± s.e.m of percentages, n=3/age group; Student's t-test was used to test significance, $p<0.05$.

that the function of EGFR in NSC fate specification is likely through cell-cell interactions and independent of the heterozygous background in MADM-EGFR brains.

To better define the nature of the apparent cell-cell interaction that regulates the fate of sibling daughter cells in the presence and absence of EGFR, we used the power of clonal labeling inherent to the MADM system. Here, only 0.1% of cells are labeled with either GFP and tdTomato using the Nestin-cre line for recombination (Liang et al. 2012). In fact, the efficiency for generating cWT (red) and cKO (green) cells is even lower, because they depend on x-segregation during mitotic recombination and cannot be generated G1 or postmitotic recombinations unlike cHET cells. Moreover, since the red and green cells are generated from a single mother NSCs after cre-mediated mitotic recombination (Figure 20) their anatomical positioning, juxtapositioning, and numbers can be used as readouts of potential clonal cell-cell interactions between cWT and cKO cells (Figure 33). Thus, comparison of MADM-EGFR to MADM-Ctr brains should reveal whether or not clonal associations were altered in the absence of EGFR and what the effects of these interactions are on the fate of each sibling.

The difference in cWT (red) cell densities between MADM-Ctr and MADM-EGFR mice (Figure 31) suggested that their expansion was likely clonal. We analyzed the density and percentage of cWT (red) glial cells and neurons in MADM-Ctr and MADM-EGFR mice cortex. Similarly, glial cells and neuron were distinguished by their characteristic morphologies (glial cell: “star” shape and/or numerous branches; neurons: long axon and short dendrites) (Figure 34a-b). We found that most of the cWT (red) cell in MADM-EGFR

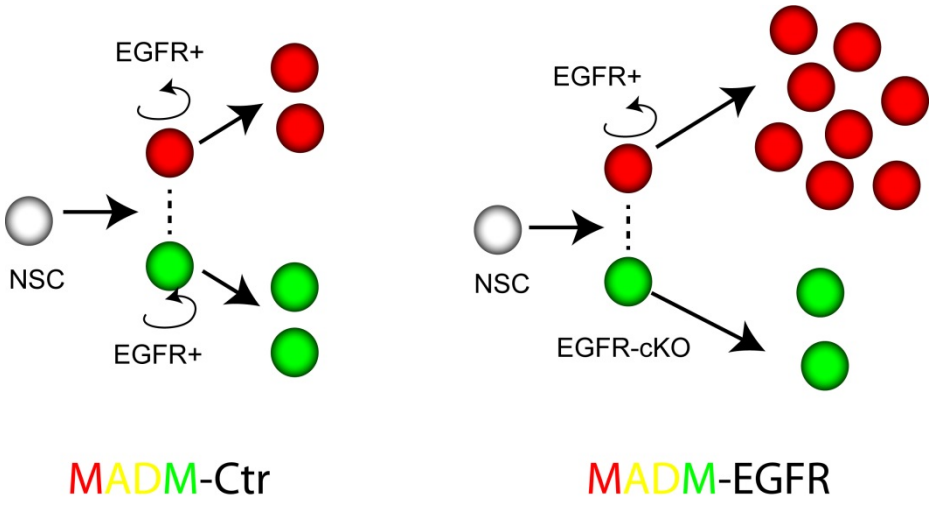

Figure 33. Cell-cell interaction between cWT and cKO sibling cells in MADM. Red and green labeled sibling progenitors are generated from a single NSC in MADM mice. When EGFR expression is deleted in MADM-EGFR, the clonal cell-cell interaction between two sibling progenitors increases the proliferation of red cWT cells resulting in a large number of red cWT cells than MADM-Ctr mice. Dotted line indicates the clonal cell-cell interaction.

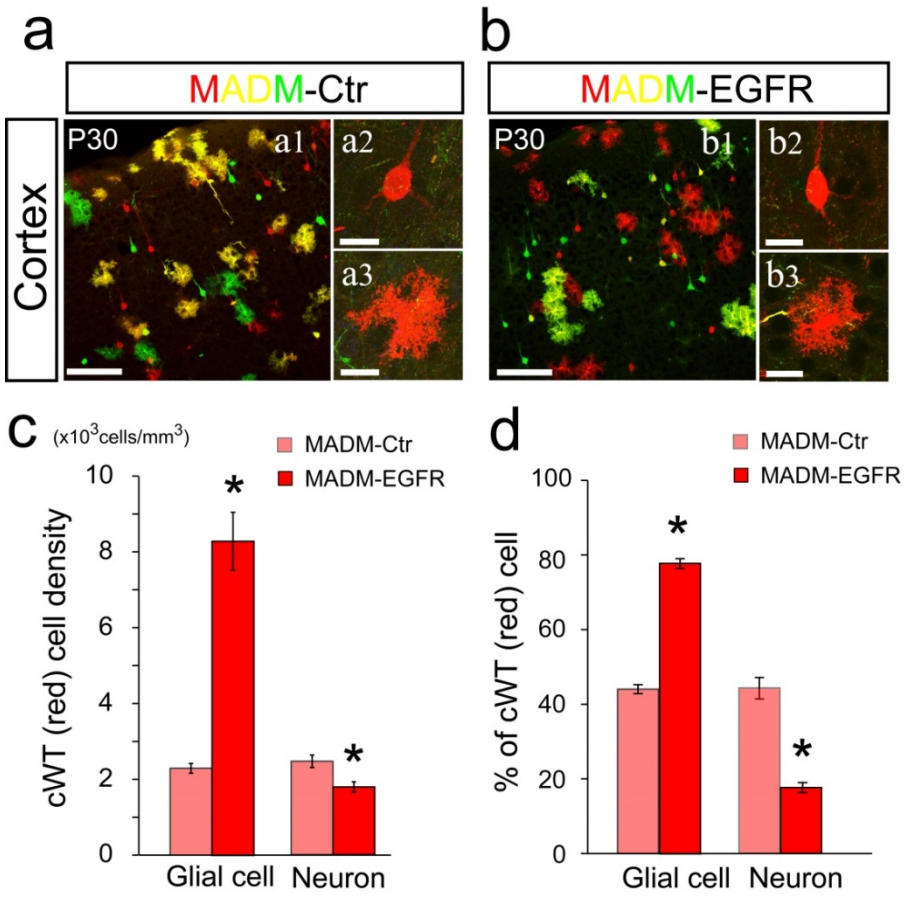

Figure 34. cWT NSCs favor glial cell fate in MADM-EGFR (a-b). Confocal images of MADM-Ctr and MADM-EGFR cortex at P30. **(a2-3)** and **(b2-3)** are represented high magnification images of cWT neuron and glial cell. Scale bar: **(a1)** and **(b1)**:100 µm; **(a2-3)** and **(b2-3)**:20 µm; **(c).** Cell densities of red neuron and glial cell in MADM-Ctr and MADM-EGFR cortex at P30. **(d).** Percentages of red neuron and glial cell in total red cells at P30. Data are mean ± s.e.m of densities and percentages, n=3/age group; Student's t-test was used to test significance, $p<0.05$.

cortex possessed glial cell features. The cell density of these glial cells was dramatically elevated (nearly four-fold higher) in MADM-EGFR cortex compared to MADM-Ctr (Figure 34c). The percentage of cWT (red) glial cell over the total cWT (red) population was 78% (±2.4%) in the MADM-EGFR cortex, which was significantly higher than MADM-Ctr (44±1.2%) (Figure 34d). Thus, cell-cell interaction with cKO cells promotes enhanced gliogenesis in the cWT population.

In contrast to glial cells, we found that the percentage of the cWT (red) neurons in total cWT (red) cells was less than 17% (±1.5%) in MADM-EGFR cortex, which was significantly lower than MADM-Ctr (43 ±2.8%) (Figure 34d). The decreased percentage of cWT (red) neuron in MADM-EGFR mice was primarily due to the dramatic increase of gliogenesis in the cWT population (Figure 34c). However, even though the decrease in cWT (red) neuron production was not as prominent as the increase in expansion of glia, we did find that the density of cWT (red) neurons was significantly lower in MADM-EGFR cortices than in MADM-Ctr (Figure 34c). This data suggests that cWT NSCs/IPCs favor a glial cell fate rather than neuronal fate in MADM-EGFR mice. Taken together, clonally derived cWT cells acquire a glial fate and extensively expand as siblings of cells lacking EGFR in NSCs and IPCs through clonal cell-cell interactions. In other words, the cWT population somehow senses the loss of EGFR in the cKO population and responds accordingly by increasing gliogenesis. The next question was whether or not this response constitutes a compensatory response to loss of oligodendrocytes, or alternate responses the nature of which remains to be determined.

Since the production of both oligodendrocyte and astrocytes decreased in the absence of EGFR, we next examined whether cWT (red) cells in MADM-EGFR mice differentiate into both glial cell types or favor specific subtype of glial cells. To address this question, various glial cell markers were utilized to reveal the composition of glial cell subtypes in MADM-Ctr and MADM-EGFR forebrains. In SEZ and CC, we found about 90% (±3.5%) of cWT (red) cells were CC1+ cells in MADM-EGFR SEZ and CC at P30, which was dramatically increased than in MADM-Ctr mice (54±0.5%), suggesting that cWT cells in MADM-EGFR SEZ and CC predominantly give rise to glial cell lineage (Figure 35a-b). In addition, the percentage of GFAP+ cells was also elevated in MADM-EGFR SEZ and CC (67±3%) than MADM-Ctr mice (27±2.2%) (Figure 35a-b). The percentages of cWT (red) S100+ ependymal cell and astrocyte, Olig1+ differentiating and mature oligodendrocyte, and Olig2+ oligodendrocyte progenitor were not statistically different between in SEZ and CC of MAMD-EGFR and MADM-Ctr mice (Figure 35a-b).

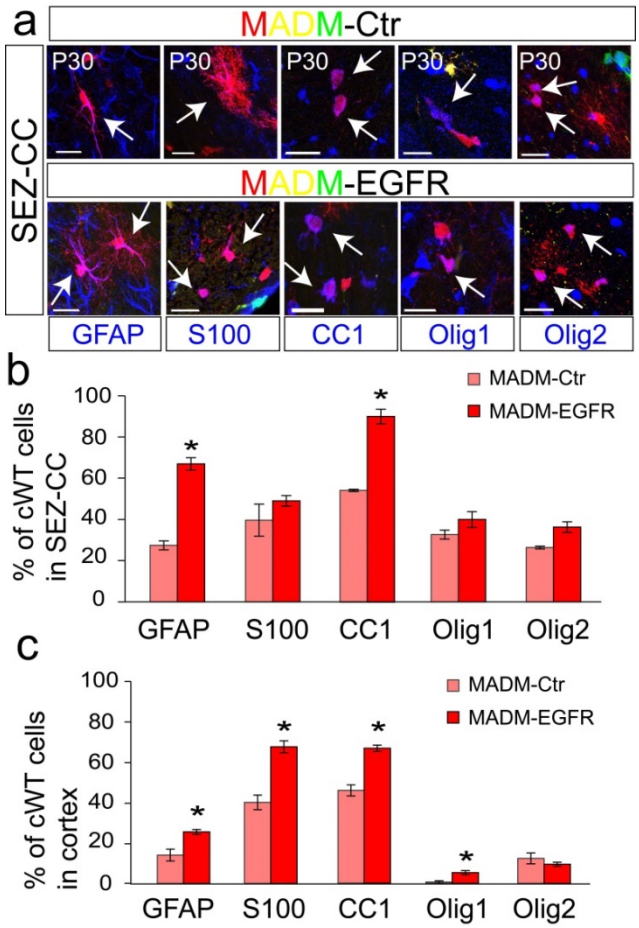

Figure 35. The increased cWT cells predominantly differentiate into astrocyte in MADM-EGFR brain. (a). Expression of glial cell markers in MADM-Ctr and MADM-EGFR SEZ and CC at P30. Arrow indicates co-localization of markers and cWT glial cells. Scale bar: 20μm. **(b).** Percentages of (marker +) glial cell subtypes in total cWT (red) cells in MADM-Ctr and MADM-EGFR SEZ and CC at P30. **(c).** Percentages of (marker +) glial cell subtypes in total cWT (red) cells in MADM-Ctr and MADM-EGFR cortex at P30. Data are mean ± s.e.m of percentages, n=3/age group; Student's t-test was used to test significance, *p<0.05.

Similarly, the percentage of CC+ and GFAP+ cWT cell was significantly higher in MADM-EGFR cortex (66±1.6%; 25±1.2% respectively) than MADM-Ctr (46±2.7%; 14±2.9% respectively) at P30 (Figure 35c). In the cortex, astrocytes primarily label with S100. We found more than 60% of cWT cells in MADM-EGFR cortex expressed S100, which was significantly increased compared to the same percentages calculated in MADM-Ctr mice (40±3.6%) (Figure 35c). Although the percentages of Olig2+ cWT cells were identical (9-12%), a higher percentage of cWT cells label with Olig1 in MADM-EGFR cortex compared to MADM-Ctr (Figure 35c), suggesting a slight increase of oligodendrogenesis occurs in MADM-EGFR cWT cells. Taken together, these data suggest the increased cWT cells in MADM-EGFR brain give rise to both astrocytic and oligodendrocyte lineages, but predominantly differentiate and expand an astrocyte population in response to loss of EGFR. This response to the loss of EGFR is most likely at the level of clonal interactions, which reveals a novel concept not only in developmental neurobiology, but possibly in stem cell biology in general.

The dramatic increase of gliogenesis in cWT (red) cells in MADM-EGFR forebrains led us to investigate the mechanistic correlates of EGFR expression in NSC fate specification through cell-cell interactions among clonal siblings. We have shown that EGFR is important for NSCs and IPC proliferation during early brain development (Figure 14). We hypothesized that the clonal cell-cell interaction between cWT and cKO cells leads to enhanced expression of EGFR in cWT cells. To test our hypothesis, we compared the expression of EGFR in cWT cells in MADM-EGFR and MADM-Ctr mice SEZs. We found that the percentages of EGFR expression were identical in cWT cells at P0 in both MADM-

Ctr and MADM-EGFR SEZs (Figure 36b). However, there was a significantly increased percentage of EGFR expression in cWT (red) cells in MADM-EGFR SEZ (32±2.9%) at P7 compared to MADM-Ctr mice (16±1.8%) (Figure 36a-b). We previously showed that EGFR is required for progenitor proliferation at P7 age (Figure 11a-b). Taken together, these data indicate the cell-cell interactions in the forebrain increase the expression of EGFR in cWT cells, which promote progenitor cells proliferation and differentiation into glial cells (Figure 37).

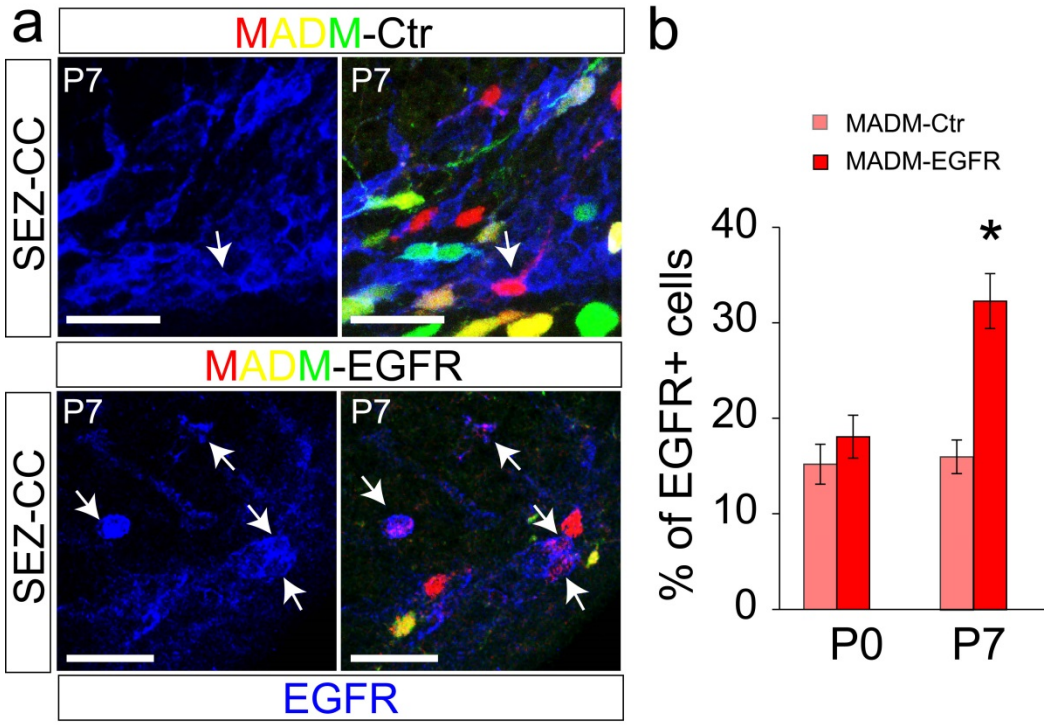

Figure 36. The expression of EGFR increased in cWT cells of MADM-EGFR SEZ (a). Confocal image of EGFR expression in MADM-EGFR and MADM-Ctr at P7. Arrow indicates the co-localization of EGFR (blue) with cWT cells (red). Scale bar:20μm. **(b).** Percentages of EGFR expression in MADM-EGFR and MADM-Ctr SEZs at P0 and P7. Data are mean ± s.e.m of percentages, n=3/age group; Student's t-test was used to test significance, $p<0.05$.

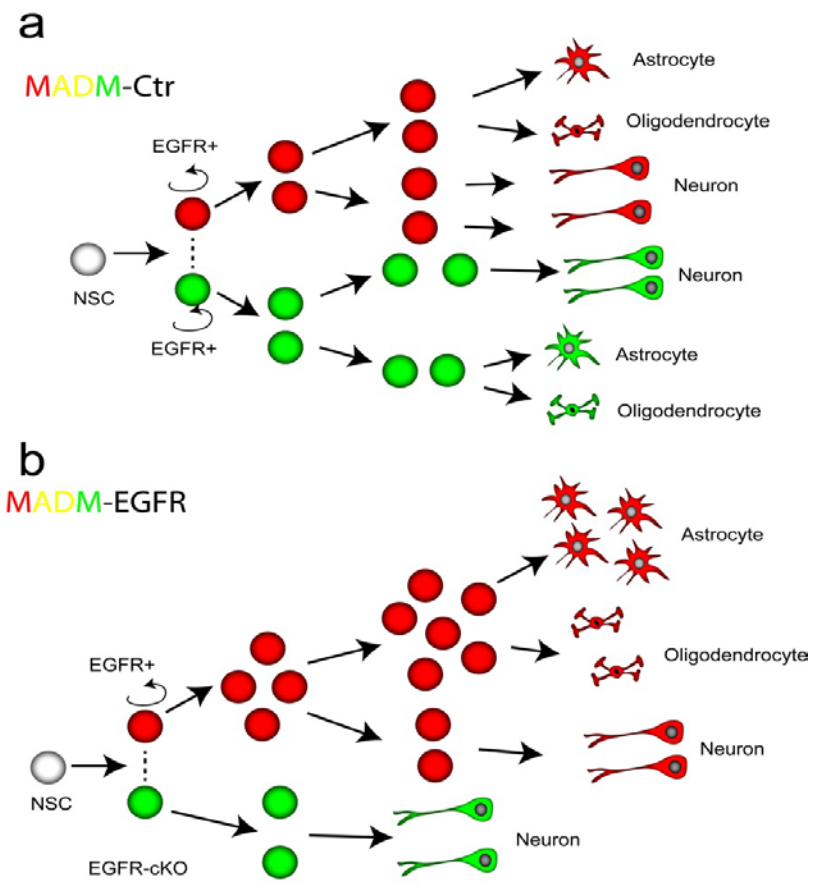

Figure 37. Regulation of EGFR in NSC fate specification. (a). Perinatal NSC is able to give rise to both neuronal and glial cell lineage and generate equal number neurons and glial cells. **(b).** When EGFR is deleted in one of the daughter progenitor from a single NSC, a clonal cell-cell interaction (indicated by dash line) occurs between two daughter progenitors. The clonal cell-cell interaction affects the proliferation and cell fate of the sibling progenitor, which expresses EGFR. The sibling WT progenitor then differentiates into glial cells, especially astrocytes, while the cKO cells give rise to neurons.

DISCUSSION

EGFR determines neuronal/glial cell fate of NSCs through cell-cell interaction

It is known that asymmetric distribution of EGFR generates distinct cell fates in siblings after individual mitoses in NSCs (Sun et al. 2005). When one daughter cell has EGFR expression and the sibling cell does not, the EGFR+ siblings are more likely to differentiate into astrocytes (Sun et al. 2005). However, it is still not clear how EGFR expression determines the cell fate of two sibling daughter cells during mitosis. In the MADM system, the cWT (red) cells and cKO (green) cells are generated from the same mother cells during mitosis, which is similar to the situation in asymmetric distribution of one cell expressing EGFR. In the progeny of the sibling with EGFR expression (red cWT cells), a higher density and percentage of cells differentiate into astrocytes, but only when the other sibling is cKO (green cells). Similarly, the Olig1+ oligodendrocytes are higher in the MADM-EGFR cortex. However, when we compare the cWT (red) cells with control animals (which have both functional EGFR alleles), the density and percentage of cWT (red) cells are still higher in MADM-EGFR mice than controls. Since the cWT cells have both functional alleles, the level of EGFR expression should be similar. Therefore, ligands, such as EGF, should not be significantly different. The elevated density of cWT cells discovered in this study mostly demonstrate differentiation into glial cells, which is supportive of the possibility for clonal cell-cell communications between two sibling daughter cells with different levels of EGFR, which affect the fate of their progeny.

The regulation of EGFR in glial cell subtype specification

Based on location and morphology, astrocytes can be distinguished as protoplasmic astrocytes in the gray matter and fibrous astrocyte in the white matter (Zhang & Barres 2010). Protoplasmic astrocytes make contact and ensheathe synapses with their numerous thin processes to regulate the level of ions and neurotransmitters in the extracellular environment (Lovatt et al. 2007). Fibrous astrocytes contact axon myelinated membranes to promote oligodendrocyte myelination (Watkins et al. 2008). In addition, white matter astrocytes are more responsive to injury than gray matter astrocytes (Shannon et al. 2007). Our data demonstrates that loss of EGFR expression leads to decrease in glial cells, including oligodendrocyte and astrocytes in MADM-EGFR. However, the intensity of GFAP+ fibrous astrocytes is not significantly different within the CC (i.e., forebrain white matter) of cWT and EGFR-cKO mice (chapter 1). These findings suggest that EGFR cells autonomously regulate glial fate specification in perinatal NSCs, which is required for differentiation of oligodendrocytes and protoplasmic astrocytes.

In addition to cell autonomous induction of a glial fate, we found that EGFR also regulates the important perinatal neuronal-to-glial fate switch. The clonal cell-cell interactions between EGFR+ and non-EGFR- sibling progenitors enhance the expression of EGFR in EGFR+ progenitors. Both Oligodendrocyte and astrocyte in cWT cell population increase in MADM-EGFR forebrain, while the production of cWT neurons decreases. Since the increase of glial cells is largely from astrocyte lineage in the forebrain, it is more likely that the clonal cell-cell interaction of EGFR favors astrocyte lineage, although there is also an increase in oligodendrocytes.

Regulation of EGFR on neuron survival

In chapter 1, we showed a severe necrosis occurs in EGFR-cKO forebrain, including the OB and superficial layer of frontal cortex, where protoplasmic astrocytes are mostly located. Since the production of protoplasmic astrocytes and oligodendrocytes are reduced in the absence of EGFR, the cell death of neurons is likely due to insufficient support from the protoplasmic astrocytes and oligodendrocytes. Interestingly, we found the cWT (red) protoplasmic astrocytes and Olig1+ oligodendrocytes are dramatically elevated in MADM-EGFR cortex through the clonal cell-cell interaction of EGFR expression between sibling cells. More importantly, we found that the density of cKO (green) neuron is higher than the cWT (red) neurons in MADM-EGFR cortex, suggesting the cell death of neurons may not cell intrinsically regulated by EGFR.

SUMMARY OF DISSERTATION

In summary, this study reveals that EGFR is a critical regulator for neuronal-to-glial cell fate specification during perinatal forebrain development. The expression of EGFR is required for glial cell fate acquisition of NSCs cell autonomously. Importantly, NSCs differentiate into neuronal lineage in the absence of EGFR. Additionally, for the first time it was demonstrated that EGFR regulates NSC fate specification through clonal cell-cell interactions, in which the non-EGFR expressing cells promote sibling EGFR expressing progenitors to proliferate and differentiate into astrocytes. How EGFR perfoms these important functions is the subject of future studies. In addition to its canonical tyrosine kinase receptor signaling mechanisms, EGFR has been shown to have DNA binding capacity and the ability to regulate gene transcription directly (Lin et al. 2001; Huo et al. 2010). The transcription factor Olig2 is not only critical for oligodendrocyte generation, it is also important for astrocyte differentiation (Marshall et al. 2005). We showed that Olig2+ progenitor cells were dramatically decreased in the absence of EGFR. It is possible that EGFR translocates to the nucleus and turns on Olig2 expression directly in the oligodendrocyte or astrocytic progenitors and their siblings. Conditional deletion of EGFR utilizing the MADM system provides a suitable model to study the regulation of EGFR in Olig2 expression *in vivo* and *in vitro*. In addition, another important future direction is to generate an EGFR knock-in cre mouse line for more direct lineage tracing studies. This mouse could conclusively determine the cell lineage of EGFR expressing NSCs during neural and glial development throughout the CNS.

REFERENCES

Abremski, K. & Hoess, R., 1984. Bacteriophage P1 site-specific recombination. Purification and properties of the Cre recombinase protein. *Journal of Biological Chemistry*, 259(3), pp.1509–1514. Available at: http://www.jbc.org/content/259/3/1509.short [Accessed July 18, 2014].

Aguirre, A. et al., 2007. A functional role for EGFR signaling in myelination and remyelination. *Nature neuroscience*, 10(8), pp.990–1002. Available at: http://www.ncbi.nlm.nih.gov/pubmed/17618276 [Accessed July 2, 2013].

Aguirre, A. et al., 2005. Overexpression of the epidermal growth factor receptor confers migratory properties to nonmigratory postnatal neural progenitors. *The Journal of neuroscience : the official journal of the Society for Neuroscience*, 25(48), pp.11092–106. Available at: http://www.ncbi.nlm.nih.gov/pubmed/16319309 [Accessed June 5, 2013].

Aguirre, A., Rubio, M.E. & Gallo, V., 2010. Notch and EGFR pathway interaction regulates neural stem cell number and self-renewal. *Nature*, 467(7313), pp.323–7. Available at: http://www.pubmedcentral.nih.gov/articlerender.fcgi?artid=2941915&tool=pmcentrez&rendertype=abstract [Accessed May 30, 2013].

Altman, J. & Bayer, S.A., 1991. *Neocortical Development*, New York: Raven Press.

Angevine, J. & Sidman, R., 1961. Autoradiographic study of cell migration during histogenesis of cerebral cortex in the mouse. *Nature*, 192(11), pp.766–768.

Anthony, T.E. et al., 2004. Radial glia serve as neuronal progenitors in all regions of the central nervous system. *Neuron*, 41(6), pp.881–90. Available at: http://www.ncbi.nlm.nih.gov/pubmed/15046721.

Anton, E.S. et al., 2004. Receptor tyrosine kinase ErbB4 modulates neuroblast migration and placement in the adult forebrain. *Nature neuroscience*, 7(12), pp.1319–28. Available at: http://www.ncbi.nlm.nih.gov/pubmed/15543145 [Accessed October 7, 2013].

Ayuso-Sacido, A. et al., 2010. Activated EGFR signaling increases proliferation, survival, and migration and blocks neuronal differentiation in post-natal neural stem cells. *Journal of neuro-oncology*, 97(3), pp.323–37. Available at: http://www.ncbi.nlm.nih.gov/pubmed/19855928 [Accessed July 4, 2013].

Burrows, R.C. et al., 1997. Response diversity and the timing of progenitor cell maturation are regulated by developmental changes in EGFR expression in the cortex. *Neuron*, 19(2), pp.251–67. Available at: http://www.ncbi.nlm.nih.gov/pubmed/9292717.

Bushong, E. a, Martone, M.E. & Ellisman, M.H., 2004. Maturation of astrocyte morphology and the establishment of astrocyte domains during postnatal hippocampal development. *International journal of developmental neuroscience : the official journal of the International Society for Developmental Neuroscience*, 22(2), pp.73–86. Available at: http://www.ncbi.nlm.nih.gov/pubmed/15036382 [Accessed June 3, 2014].

Cai, L., Morrow, E.M. & Cepko, C.L., 2000. Misexpression of basic helix-loop-helix genes in the murine cerebral cortex affects cell fate choices and neuronal survival. *Development (Cambridge, England)*, 127(14), pp.3021–30. Available at: http://www.ncbi.nlm.nih.gov/pubmed/10862740.

Caric, D. et al., 2001. EGFRs mediate chemotactic migration in the developing telencephalon. *Development (Cambridge, England)*, 128(21), pp.4203–16. Available at: http://www.ncbi.nlm.nih.gov/pubmed/11684657.

Casarosa, S., Fode, C. & Guillemot, F., 1999. Mash1 regulates neurogenesis in the ventral telencephalon. *Development (Cambridge, England)*, 126(3), pp.525–34. Available at: http://www.ncbi.nlm.nih.gov/pubmed/9876181.

Casper, D., Mytilineou, C. & Blum, M., 1991. EGF enhances the survival of dopamine neurons in rat embryonic mesencephalon primary cell culture. *Journal of neuroscience research*, 30(2), pp.372–81. Available at: http://www.ncbi.nlm.nih.gov/pubmed/1839162.

Cesetti, T. et al., 2009. Analysis of stem cell lineage progression in the neonatal subventricular zone identifies EGFR+/NG2- cells as transit-amplifying precursors. *Stem cells (Dayton, Ohio)*, 27(6), pp.1443–54. Available at: http://www.ncbi.nlm.nih.gov/pubmed/19489104 [Accessed June 13, 2013].

Chandra, A. et al., 2013. Epidermal Growth Factor Receptor (EGFR) Signaling Promotes Proliferation and Survival in Osteoprogenitors by Increasing Early Growth Response 2 (EGR2) Expression. *The Journal of biological chemistry*, 288(28), pp.20488–98. Available at: http://www.ncbi.nlm.nih.gov/pubmed/23720781 [Accessed August 8, 2013].

Compston, A. & Coles, A., 2008. Multiple sclerosis. *Lancet*, 372(9648), pp.1502–17. Available at: http://www.ncbi.nlm.nih.gov/pubmed/23122652.

Doetsch, F., 2003. A niche for adult neural stem cells. *Current Opinion in Genetics & Development*, 13(5), pp.543–550. Available at: http://linkinghub.elsevier.com/retrieve/pii/S0959437X03001230 [Accessed May 21, 2013].

Doetsch, F. et al., 2002. EGF converts transit-amplifying neurogenic precursors in the adult brain into multipotent stem cells. *Neuron*, 36(6), pp.1021–34. Available at: http://www.ncbi.nlm.nih.gov/pubmed/12495619.

Doetsch, F. et al., 1999. Subventricular zone astrocytes are neural stem cells in the adult mammalian brain. *Cell*, 97(6), pp.703–16. Available at: http://www.ncbi.nlm.nih.gov/pubmed/10380923.

Eiraku, M. et al., 2008. Self-organized formation of polarized cortical tissues from ESCs and its active manipulation by extrinsic signals. *Cell stem cell*, 3(5), pp.519–32. Available at: http://www.ncbi.nlm.nih.gov/pubmed/18983967 [Accessed May 27, 2014].

Englund, C. et al., 2005. Pax6, Tbr2, and Tbr1 are expressed sequentially by radial glia, intermediate progenitor cells, and postmitotic neurons in developing neocortex. *The Journal of neuroscience : the official journal of the Society for Neuroscience*, 25(1), pp.247–51. Available at: http://www.ncbi.nlm.nih.gov/pubmed/15634788 [Accessed May 24, 2014].

Feng, L., Hatten, M.E. & Heintz, N., 1994. Brain lipid-binding protein (BLBP): a novel signaling system in the developing mammalian CNS. *Neuron*, 12(4), pp.895–908. Available at: http://www.ncbi.nlm.nih.gov/pubmed/8161459.

Fode, C. et al., 2000. A role for neural determination genes in specifying the dorsoventral identity of telencephalic neurons. *Genes & …*, 14(1), pp.67–80. Available at: http://genesdev.cshlp.org/content/14/1/67.short [Accessed June 13, 2014].

Frantz, G.D. & McConnell, S.K., 1996. Restriction of late cerebral cortical progenitors to an upper-layer fate. *Neuron*, 17(1), pp.55–61. Available at: http://www.ncbi.nlm.nih.gov/pubmed/8755478.

Gaspard, N. et al., 2008. An intrinsic mechanism of corticogenesis from embryonic stem cells. *Nature*, 455(7211), pp.351–7. Available at: http://dx.doi.org/10.1038/nature07287 [Accessed June 3, 2014].

Ge, W. et al., 2002. Notch signaling promotes astrogliogenesis via direct CSL-mediated glial gene activation. *Journal of neuroscience research*, 69(6), pp.848–60. Available at: http://www.ncbi.nlm.nih.gov/pubmed/12205678 [Accessed May 29, 2014].

Ginhoux, F. et al., 2013. Origin and differentiation of microglia. *Frontiers in cellular neuroscience*, 7(April), p.45. Available at: http://www.pubmedcentral.nih.gov/articlerender.fcgi?artid=3627983&tool=pmcentrez&rendertype=abstract [Accessed May 23, 2014].

Gonzalez-Perez, O. et al., 2009. Epidermal growth factor induces the progeny of subventricular zone type B cells to migrate and differentiate into oligodendrocytes. *Stem cells (Dayton, Ohio)*, 27(8), pp.2032–43. Available at: http://www.pubmedcentral.nih.gov/articlerender.fcgi?artid=3346259&tool=pmcentrez&rendertype=abstract [Accessed June 13, 2013].

Götz, M. & Huttner, W.B., 2005. The cell biology of neurogenesis. *Nature reviews. Molecular cell biology*, 6(10), pp.777–88. Available at: http://www.ncbi.nlm.nih.gov/pubmed/16314867 [Accessed February 24, 2014].

Guillemot, F. & Joyner, a L., 1993. Dynamic expression of the murine Achaete-Scute homologue Mash-1 in the developing nervous system. *Mechanisms of development*, 42(3), pp.171–85. Available at: http://www.ncbi.nlm.nih.gov/pubmed/8217843.

Harris, R., 2003. EGF receptor ligands. *Experimental Cell Research*, 284(1), pp.2–13. Available at: http://linkinghub.elsevier.com/retrieve/pii/S0014482702001052 [Accessed June 3, 2014].

Hartfuss, E. et al., 2001. Characterization of CNS precursor subtypes and radial glia. *Developmental biology*, 229(1), pp.15–30. Available at: http://www.ncbi.nlm.nih.gov/pubmed/11133151 [Accessed June 7, 2014].

Haubensak, W. et al., 2004. Neurons arise in the basal neuroepithelium of the early mammalian telencephalon: a major site of neurogenesis. *Proceedings of the National Academy of Sciences of the United States of America*, 101(9), pp.3196–201. Available at: http://www.pubmedcentral.nih.gov/articlerender.fcgi?artid=365766&tool=pmcentrez&rendertype=abstract.

Hippenmeyer, S. et al., 2010. Genetic mosaic dissection of Lis1 and Ndel1 in neuronal migration. *Neuron*, 68(4), pp.695–709. Available at: http://www.pubmedcentral.nih.gov/articlerender.fcgi?artid=3044607&tool=pmcentrez&rendertype=abstract [Accessed February 6, 2014].

Huo, L. et al., 2010. RNA helicase A is a DNA-binding partner for EGFR-mediated transcriptional activation in the nucleus. *Proceedings of the National Academy of Sciences of the United States of America*, 107(37), pp.16125–30. Available at: http://www.pubmedcentral.nih.gov/articlerender.fcgi?artid=2941329&tool=pmcentrez&rendertype=abstract [Accessed June 13, 2013].

Ivkovic, S., Canoll, P. & Goldman, J.E., 2008. Constitutive EGFR signaling in oligodendrocyte progenitors leads to diffuse hyperplasia in postnatal white matter. *The Journal of neuroscience : the official journal of the Society for Neuroscience*, 28(4), pp.914–22. Available at: http://www.pubmedcentral.nih.gov/articlerender.fcgi?artid=2711628&tool=pmcentrez&rendertype=abstract [Accessed July 4, 2013].

Jacquet, B. V et al., 2009. FoxJ1-dependent gene expression is required for differentiation of radial glia into ependymal cells and a subset of astrocytes in the postnatal brain. *Development (Cambridge, England)*, 136(23), pp.4021–31. Available at: http://www.pubmedcentral.nih.gov/articlerender.fcgi?artid=3118431&tool=pmcentrez&rendertype=abstract [Accessed October 7, 2013].

Jang, E.S. & Goldman, J.E., 2011. Pax6 expression is sufficient to induce a neurogenic fate in glial progenitors of the neonatal subventricular zone. *PloS one*, 6(6), p.e20894. Available at: http://www.pubmedcentral.nih.gov/articlerender.fcgi?artid=3117849&tool=pmcentrez&rendertype=abstract [Accessed June 11, 2013].

Jorissen, R., 2003. Epidermal growth factor receptor: mechanisms of activation and signalling. *Experimental Cell Research*, 284(1), pp.31–53. Available at: http://linkinghub.elsevier.com/retrieve/pii/S0014482702000988 [Accessed May 25, 2013].

Kessaris, N. et al., 2004. Cooperation between sonic hedgehog and fibroblast growth factor/MAPK signalling pathways in neocortical precursors. *Development (Cambridge, England)*, 131(6), pp.1289–98. Available at: http://www.ncbi.nlm.nih.gov/pubmed/14960493 [Accessed June 7, 2014].

Kettenmann, H. & Verkhratsky, A., 2008. Neuroglia: the 150 years after. *Trends in neurosciences*, 31(12), pp.653–9. Available at: http://www.ncbi.nlm.nih.gov/pubmed/18945498 [Accessed July 11, 2014].

Kowalczyk, T. et al., 2009. Intermediate neuronal progenitors (basal progenitors) produce pyramidal-projection neurons for all layers of cerebral cortex. *Cerebral cortex (New York, N.Y. : 1991)*, 19(10), pp.2439–50. Available at: http://www.pubmedcentral.nih.gov/articlerender.fcgi?artid=2742596&tool=pmcentrez&rendertype=abstract [Accessed May 23, 2014].

Kriegstein, A. & Alvarez-Buylla, A., 2009. The glial nature of embryonic and adult neural stem cells. *Annual review of neuroscience*, 32, pp.149–84. Available at: http://www.pubmedcentral.nih.gov/articlerender.fcgi?artid=3086722&tool=pmcentrez&rendertype=abstract [Accessed May 26, 2013].

Kriegstein, A., Noctor, S. & Martínez-cerdeño, V., 2006. Patterns of neral stem ad progenitor cell division may underlie evolutionary cortical expansion. *Nature neuroscience*, 7(November), pp.883–890.

Kriegstein, A.R. & Noctor, S.C., 2004. Patterns of neuronal migration in the embryonic cortex. *Trends in neurosciences*, 27(7), pp.392–9. Available at: http://www.ncbi.nlm.nih.gov/pubmed/15219738 [Accessed May 23, 2014].

Lee, T.-C. & Threadgill, D.W., 2009. Generation and validation of mice carrying a conditional allele of the epidermal growth factor receptor. *Genesis (New York, N.Y. : 2000)*, 47(2), pp.85–92. Available at: http://www.ncbi.nlm.nih.gov/pubmed/19115345 [Accessed July 4, 2013].

Lendahl, U., Zimmerman, L.B. & McKay, R.D., 1990. CNS stem cells express a new class of intermediate filament protein. *Cell*, 60(4), pp.585–95. Available at: http://www.ncbi.nlm.nih.gov/pubmed/1689217.

Liang, H. et al., 2013. Neural development is dependent on the function of specificity protein 2 in cell cycle progression. *Development (Cambridge, England)*, 140(3), pp.552–61. Available at: http://www.ncbi.nlm.nih.gov/pubmed/23293287 [Accessed August 12, 2013].

Liang, H., Hippenmeyer, S. & Ghashghaei, H.T., 2012. A Nestin-cre transgenic mouse is insufficient for recombination in early embryonic neural progenitors. *Biology open*, 1(12), pp.1200–3. Available at: http://www.pubmedcentral.nih.gov/articlerender.fcgi?artid=3522881&tool=pmcentrez&rendertype=abstract [Accessed August 16, 2013].

Ligon, K.L. et al., 2006. Olig gene function in CNS development and disease. *Glia*, 54(1), pp.1–10. Available at: http://www.ncbi.nlm.nih.gov/pubmed/16652341 [Accessed May 27, 2013].

Lin, S.Y. et al., 2001. Nuclear localization of EGF receptor and its potential new role as a transcription factor. *Nature cell biology*, 3(9), pp.802–8. Available at: http://www.ncbi.nlm.nih.gov/pubmed/11533659.

Lo, L.C. et al., 1991. Mammalian achaete-scute homolog 1 is transiently expressed by spatially restricted subsets of early neuroepithelial and neural crest cells. *Genes & Development*, 5(9), pp.1524–1537. Available at: http://www.genesdev.org/cgi/doi/10.1101/gad.5.9.1524 [Accessed June 13, 2014].

Lovatt, D. et al., 2007. The transcriptome and metabolic gene signature of protoplasmic astrocytes in the adult murine cortex. *The Journal of neuroscience : the official journal*

of the Society for Neuroscience, 27(45), pp.12255–66. Available at: http://www.ncbi.nlm.nih.gov/pubmed/17989291 [Accessed July 18, 2014].

Lu, Q. et al., 2002. Common Developmental Requirement for Olig Function Indicates a Motor Neuron/Oligodendrocyte Connection. *Cell*, 109(1), pp.75–86. Available at: http://www.sciencedirect.com/science/article/pii/S0092867402006785 [Accessed June 16, 2014].

Lu, Q.R. et al., 2001. Ectopic expression of Olig1 promotes oligodendrocyte formation and reduces neuronal survival in developing mouse cortex. *Nature neuroscience*, 4(10), pp.973–4. Available at: http://www.ncbi.nlm.nih.gov/pubmed/11574831 [Accessed June 16, 2014].

Lu, Q.R. et al., 2000. Sonic hedgehog--regulated oligodendrocyte lineage genes encoding bHLH proteins in the mammalian central nervous system. *Neuron*, 25(2), pp.317–29. Available at: http://www.ncbi.nlm.nih.gov/pubmed/10719888.

Luetteke, N.C. et al., 1994. The mouse waved-2 phenotype results from a point mutation in the EGF receptor tyrosine kinase. *Genes & Development*, 8(4), pp.399–413. Available at: http://www.genesdev.org/cgi/doi/10.1101/gad.8.4.399 [Accessed July 4, 2013].

Ma, Q. et al., 1997. Mash1 and neurogenin1 expression patterns define complementary domains of neuroepithelium in the developing CNS and are correlated with regions expressing notch ligands. *The Journal of neuroscience : the official journal of the Society for Neuroscience*, 17(10), pp.3644–52. Available at: http://www.ncbi.nlm.nih.gov/pubmed/9133387.

Malatesta, P., Hartfuss, E. & Götz, M., 2000. Isolation of radial glial cells by fluorescent-activated cell sorting reveals a neuronal lineage. *Development (Cambridge, England)*, 127(24), pp.5253–63. Available at: http://www.ncbi.nlm.nih.gov/pubmed/11076748.

Maldonado, P.P. & Angulo, M.C., 2014. Multiple Modes of Communication between Neurons and Oligodendrocyte Precursor Cells. *The Neuroscientist : a review journal bringing neurobiology, neurology and psychiatry*, (April 2014). Available at: http://www.ncbi.nlm.nih.gov/pubmed/24722526 [Accessed July 18, 2014].

Marshall, C. a G., Novitch, B.G. & Goldman, J.E., 2005. Olig2 directs astrocyte and oligodendrocyte formation in postnatal subventricular zone cells. *The Journal of neuroscience : the official journal of the Society for Neuroscience*, 25(32), pp.7289–98. Available at: http://www.ncbi.nlm.nih.gov/pubmed/16093378 [Accessed May 30, 2013].

Merkle, F.T. et al., 2004. Radial glia give rise to adult neural stem cells in the subventricular zone. *Proceedings of the National Academy of Sciences of the United States of America*,

101(50), pp.17528–32. Available at: http://www.pubmedcentral.nih.gov/articlerender.fcgi?artid=536036&tool=pmcentrez&rendertype=abstract.

Mirzadeh, Z. et al., 2010. The subventricular zone en-face: wholemount staining and ependymal flow. *Journal of visualized experiments : JoVE*, (39), pp.1–7. Available at: http://www.pubmedcentral.nih.gov/articlerender.fcgi?artid=3144601&tool=pmcentrez&rendertype=abstract [Accessed September 25, 2013].

Misumi, Y. & Kawano, H., 1998. The expressions of epidermal growth factor receptor mRNA and protein gene product 9.5 in developing rat brain. *Brain research. Developmental brain research*, 107(1), pp.1–9. Available at: http://www.ncbi.nlm.nih.gov/pubmed/9602022.

Miyata, T. et al., 2001. Asymmetric inheritance of radial glial fibers by cortical neurons. *Neuron*, 31(5), pp.727–41. Available at: http://www.ncbi.nlm.nih.gov/pubmed/11567613.

Miyata, T. et al., 2004. Asymmetric production of surface-dividing and non-surface-dividing cortical progenitor cells. *Development (Cambridge, England)*, 131(13), pp.3133–45. Available at: http://www.ncbi.nlm.nih.gov/pubmed/15175243 [Accessed May 31, 2014].

Morrow, T., Song, M.R. & Ghosh, a, 2001. Sequential specification of neurons and glia by developmentally regulated extracellular factors. *Development (Cambridge, England)*, 128(18), pp.3585–94. Available at: http://www.ncbi.nlm.nih.gov/pubmed/11566862.

Morshead, C.M. et al., 1994. Neural stem cells in the adult mammalian forebrain: a relatively quiescent subpopulation of subependymal cells. *Neuron*, 13(5), pp.1071–82. Available at: http://www.ncbi.nlm.nih.gov/pubmed/7946346.

Nadarajah, B. et al., 2003. Neuronal migration in the developing cerebral cortex: observations based on real-time imaging. *Cerebral cortex (New York, N.Y. : 1991)*, 13(6), pp.607–11. Available at: http://www.ncbi.nlm.nih.gov/pubmed/12764035.

Nagy, a, 2000. Cre recombinase: the universal reagent for genome tailoring. *Genesis (New York, N.Y. : 2000)*, 26(2), pp.99–109. Available at: http://www.ncbi.nlm.nih.gov/pubmed/10686599.

Nery, S., Wichterle, H. & Fishell, G., 2001. Sonic hedgehog contributes to oligodendrocyte specification in the mammalian forebrain. *Development (Cambridge, England)*, 128(4), pp.527–40. Available at: http://www.ncbi.nlm.nih.gov/pubmed/11171336.

Nieto, M. et al., 2001. Neural bHLH genes control the neuronal versus glial fate decision in cortical progenitors. *Neuron*, 29(2), pp.401–13. Available at: http://www.ncbi.nlm.nih.gov/pubmed/11239431.

Noctor, S.C. et al., 2004. Cortical neurons arise in symmetric and asymmetric division zones and migrate through specific phases. *Nature neuroscience*, 7(2), pp.136–44. Available at: http://www.ncbi.nlm.nih.gov/pubmed/14703572 [Accessed January 24, 2014].

Noctor, S.C., Martínez-Cerdeño, V. & Kriegstein, A.R., 2008. Distinct behaviors of neural stem and progenitor cells underlie cortical neurogenesis. *The Journal of comparative neurology*, 508(1), pp.28–44. Available at: http://www.pubmedcentral.nih.gov/articlerender.fcgi?artid=2635107&tool=pmcentrez&rendertype=abstract [Accessed May 30, 2014].

Parnavelas, J.G., 1999. Glial cell lineages in the rat cerebral cortex. *Experimental neurology*, 156(2), pp.418–29. Available at: http://www.ncbi.nlm.nih.gov/pubmed/10328946.

Ponti, G. et al., 2013. Cell cycle and lineage progression of neural progenitors in the ventricular-subventricular zones of adult mice. *Proceedings of the National Academy of Sciences of the United States of America*, 110(11), pp.E1045–54. Available at: http://www.pubmedcentral.nih.gov/articlerender.fcgi?artid=3600494&tool=pmcentrez&rendertype=abstract [Accessed July 15, 2014].

Qian, X. et al., 1997. FGF2 concentration regulates the generation of neurons and glia from multipotent cortical stem cells. *Neuron*, 18(1), pp.81–93. Available at: http://www.ncbi.nlm.nih.gov/pubmed/9010207.

Qian, X. et al., 2000. Timing of CNS cell generation: a programmed sequence of neuron and glial cell production from isolated murine cortical stem cells. *Neuron*, 28(1), pp.69–80. Available at: http://www.ncbi.nlm.nih.gov/pubmed/11086984.

Rakic, P., 1972. Mode of cell migration to the superficial layers of fetal monkey neocortex. *The Journal of comparative neurology*, 145(1), pp.61–83. Available at: http://www.ncbi.nlm.nih.gov/pubmed/4624784.

Rakic, P., 1971. Neuron-glia relationship during granule cell migration in developing cerebellar cortex. A Golgi and electronmicroscopic study in Macacus Rhesus. *The Journal of comparative neurology*, 141(3), pp.283–312. Available at: http://www.ncbi.nlm.nih.gov/pubmed/4101340.

Rakic, P., 1974. Neurons in rhesus monkey visual cortex: systematic relation between time of origin and eventual disposition. *Science (New York, N.Y.)*, 183(4123), pp.425–7. Available at: http://www.ncbi.nlm.nih.gov/pubmed/4203022.

Reynolds, B. a & Weiss, S., 1992. Generation of neurons and astrocytes from isolated cells of the adult mammalian central nervous system. *Science (New York, N.Y.)*, 255(5052), pp.1707–10. Available at: http://www.ncbi.nlm.nih.gov/pubmed/1553558.

Ritter, M.R. et al., 2006. Myeloid progenitors differentiate into microglia and promote vascular repair in a model of ischemic retinopathy. *The Journal of Clinical Investigation*, 116(12), pp.3266–3276.

Rowitch, D.H. & Kriegstein, A.R., 2010. Developmental genetics of vertebrate glial-cell specification. *Nature*, 468(7321), pp.214–22. Available at: http://www.ncbi.nlm.nih.gov/pubmed/21068830 [Accessed May 22, 2013].

Rudolf, V., 1854. Ueber eine im Gehirn und Riickenmark des Menschen aufgefumiene Substanz mit der chemischen Reaction der Cellulose. *Arch. pathol. Anat. Physiol. klin. Med*, 6, pp.135–138.

Sadler, T.W., 2005. Embryology of neural tube development. *American journal of medical genetics. Part C, Seminars in medical genetics*, 135C(1), pp.2–8. Available at: http://www.ncbi.nlm.nih.gov/pubmed/15806586 [Accessed March 6, 2014].

Sakamoto, M. et al., 2003. The basic helix-loop-helix genes Hesr1/Hey1 and Hesr2/Hey2 regulate maintenance of neural precursor cells in the brain. *The Journal of biological chemistry*, 278(45), pp.44808–15. Available at: http://www.ncbi.nlm.nih.gov/pubmed/12947105 [Accessed June 15, 2014].

Sauvageot, C., 2002. Molecular mechanisms controlling cortical gliogenesis. *Current Opinion in Neurobiology*, 12(3), pp.244–249. Available at: http://linkinghub.elsevier.com/retrieve/pii/S0959438802003227 [Accessed July 25, 2014].

Schuurmans, C. et al., 2004. Sequential phases of cortical specification involve Neurogenin-dependent and -independent pathways. *The EMBO journal*, 23(14), pp.2892–902. Available at: http://www.pubmedcentral.nih.gov/articlerender.fcgi?artid=514942&tool=pmcentrez&rendertype=abstract [Accessed July 28, 2014].

Seroogy, K.B. et al., 1995. Proliferative zones of postnatal rat brain express epidermal growth factor receptor mRNA. *Brain research*, 670(1), pp.157–64.

Shannon, C., Salter, M. & Fern, R., 2007. GFP imaging of live astrocytes: regional differences in the effects of ischaemia upon astrocytes. *Journal of anatomy*, 210(6), pp.684–92. Available at:

http://www.pubmedcentral.nih.gov/articlerender.fcgi?artid=2375753&tool=pmcentrez&rendertype=abstract [Accessed July 27, 2014].

Shen, Q. et al., 2006. The timing of cortical neurogenesis is encoded within lineages of individual progenitor cells. *Nature neuroscience*, 9(6), pp.743–51. Available at: http://www.nature.com.prox.lib.ncsu.edu/neuro/journal/v9/n6/full/nn1694.html [Accessed June 5, 2014].

Sibilia, M. et al., 1998. A strain-independent postnatal neurodegeneration in mice lacking the EGF receptor. *The EMBO journal*, 17(3), pp.719–31. Available at: http://www.pubmedcentral.nih.gov/articlerender.fcgi?artid=1170421&tool=pmcentrez&rendertype=abstract.

Smart, I.H.M., 1973. Proliferative characteristics of the ependymal layer during the early development of the mouse neocortex : a pilot study based on recording the number , location and plane of cleavage of mitotic figures. *Journal of anatomy*, 116(1), pp.67–91.

Sommer, L., Ma, Q. & Anderson, D., 1996. neurogenins, a Novel Family of atonal-Related bHLH Transcription Factors, Are Putative Mammalian Neuronal Determination Genes That Reveal Progenitor Cell Heterogeneity in the Developing CNS and PNS. *Molecular and Cellular Neuroscience*, 241(0060), pp.221–241. Available at: http://www.sciencedirect.com/science/article/pii/S1044743196900603 [Accessed June 13, 2014].

Sriuranpong, V. & Borges, M., 2002. Notch signaling induces rapid degradation of achaete-scute homolog 1. *Molecular and cellular biology*, 22(9), pp.3129–3139. Available at: http://mcb.asm.org/content/22/9/3129.short [Accessed June 15, 2014].

Sun, Y. et al., 2001. Neurogenin promotes neurogenesis and inhibits glial differentiation by independent mechanisms. *Cell*, 104(3), pp.365–76. Available at: http://www.ncbi.nlm.nih.gov/pubmed/11239394.

Sun, Y., Goderie, S.K. & Temple, S., 2005. Asymmetric distribution of EGFR receptor during mitosis generates diverse CNS progenitor cells. *Neuron*, 45(6), pp.873–86. Available at: http://www.ncbi.nlm.nih.gov/pubmed/15797549 [Accessed June 6, 2013].

Suzuki, S.O. & Goldman, J.E., 2003. Multiple cell populations in the early postnatal subventricular zone take distinct migratory pathways: a dynamic study of glial and neuronal progenitor migration. *The Journal of neuroscience : the official journal of the Society for Neuroscience*, 23(10), pp.4240–50. Available at: http://www.ncbi.nlm.nih.gov/pubmed/12764112.

Takebayashi, H. & Yoshida, S., 2000. Dynamic expression of basic helix-loop-helix Olig family members: implication of Olig2 in neuron and oligodendrocyte differentiation and identification of a. *Mechanisms of …*, 99(2000), pp.143–148. Available at: http://www.sciencedirect.com/science/article/pii/S0925477300004664 [Accessed June 16, 2014].

Tanigaki, K. et al., 2001. Notch1 and Notch3 instructively restrict bFGF-responsive multipotent neural progenitor cells to an astroglial fate. *Neuron*, 29(1), pp.45–55. Available at: http://www.ncbi.nlm.nih.gov/pubmed/11182080.

Tarabykin, V. et al., 2001. Cortical upper layer neurons derive from the subventricular zone as indicated by Svet1 gene expression. *Development (Cambridge, England)*, 128(11), pp.1983–93. Available at: http://www.ncbi.nlm.nih.gov/pubmed/11493521.

Tatsumi, K. et al., 2008. Genetic fate mapping of Olig2 progenitors in the injured adult cerebral cortex reveals preferential differentiation into astrocytes. *Journal of neuroscience research*, 86(16), pp.3494–502. Available at: http://www.ncbi.nlm.nih.gov/pubmed/18816798 [Accessed June 30, 2013].

Tekki-Kessaris, N. et al., 2001. Hedgehog-dependent oligodendrocyte lineage specification in the telencephalon. *Development (Cambridge, England)*, 128(13), pp.2545–54. Available at: http://www.ncbi.nlm.nih.gov/pubmed/11493571.

Temple, S., 1989. Division and differentiation of isolated CNS blast cells in microculture. *Nature*.

Threadgill, D.W. et al., 1995. Targeted disruption of mouse EGF receptor: effect of genetic background on mutant phenotype. *Science (New York, N.Y.)*, 269(5221), pp.230–4. Available at: http://www.ncbi.nlm.nih.gov/pubmed/7618084.

Tien, A.-C. et al., 2012. Regulated temporal-spatial astrocyte precursor cell proliferation involves BRAF signalling in mammalian spinal cord. *Development (Cambridge, England)*, 139(14), pp.2477–87. Available at: http://www.pubmedcentral.nih.gov/articlerender.fcgi?artid=3383225&tool=pmcentrez&rendertype=abstract [Accessed July 11, 2014].

Viti, J. et al., 2003. Epidermal growth factor receptors control competence to interpret leukemia inhibitory factor as an astrocyte inducer in developing cortex. *The Journal of neuroscience : the official journal of the Society for Neuroscience*, 23(8), pp.3385–93. Available at: http://www.ncbi.nlm.nih.gov/pubmed/12716946.

Wanaka, a, Milbrandt, J. & Johnson, E.M., 1991. Expression of FGF receptor gene in rat development. *Development (Cambridge, England)*, 111(2), pp.455–68. Available at: http://www.ncbi.nlm.nih.gov/pubmed/1654250.

Wang, D.D. & Bordey, A., 2008. The astrocyte odyssey. *Progress in neurobiology*, 86(4), pp.342–67. Available at: http://www.pubmedcentral.nih.gov/articlerender.fcgi?artid=2613184&tool=pmcentrez&rendertype=abstract [Accessed May 23, 2013].

Watkins, T. a et al., 2008. Distinct Stages of Myelination Regulated by g-Secretase and Astrocytes in a Rapidly Myelinating CNS Coculture System. *Neuron*, 60(4), pp.555–69. Available at: http://www.pubmedcentral.nih.gov/articlerender.fcgi?artid=2650711&tool=pmcentrez&rendertype=abstract [Accessed July 27, 2014].

Wegiel, J. et al., 2010. The neuropathology of autism: defects of neurogenesis and neuronal migration, and dysplastic changes. *Acta neuropathologica*, 119(6), pp.755–70.

Wilkins, A. et al., 2001. A Role for Oligodendrocyte-Derived IGF-1 in Trophic Support. , 57(February), pp.48–57.

Wilkins, A. et al., 2003. Oligodendrocytes promote neuronal survival and axonal length by distinct intracellular mechanisms: a novel role for oligodendrocyte-derived glial cell line-derived neurotrophic factor. *The Journal of neuroscience : the official journal of the Society for Neuroscience*, 23(12), pp.4967–74. Available at: http://www.ncbi.nlm.nih.gov/pubmed/12832519.

Wu, Y. et al., 2003. Hes1 but not Hes5 regulates an astrocyte versus oligodendrocyte fate choice in glial restricted precursors. *Developmental dynamics : an official publication of the American Association of Anatomists*, 226(4), pp.675–89. Available at: http://www.ncbi.nlm.nih.gov/pubmed/12666205 [Accessed June 15, 2014].

Yoon, K. & Gaiano, N., 2005. Notch signaling in the mammalian central nervous system: insights from mouse mutants. *Nature neuroscience*, 8(6), pp.709–15. Available at: http://www.ncbi.nlm.nih.gov/pubmed/15917835 [Accessed May 27, 2013].

Zhang, Y. & Barres, B. a, 2010. Astrocyte heterogeneity: an underappreciated topic in neurobiology. *Current opinion in neurobiology*, 20(5), pp.588–94. Available at: http://www.ncbi.nlm.nih.gov/pubmed/20655735 [Accessed May 24, 2013].

Zhou, Q. & Anderson, D.J., 2002. The bHLH transcription factors OLIG2 and OLIG1 couple neuronal and glial subtype specification. *Cell*, 109(1), pp.61–73. Available at: http://www.ncbi.nlm.nih.gov/pubmed/11955447.

Zhou, Q., Wang, S. & Anderson, D.J., 2000. Identification of a novel family of oligodendrocyte lineage-specific basic helix-loop-helix transcription factors. *Neuron*, 25(2), pp.331–43. Available at: http://www.ncbi.nlm.nih.gov/pubmed/10719889.

Zhu, G. et al., 2000. Developmental changes in neural progenitor cell lineage commitment do not depend on epidermal growth factor receptor signaling. *Journal of neuroscience research*, 59(3), pp.312–20. Available at: http://www.ncbi.nlm.nih.gov/pubmed/10679766.

Zimmer, C. et al., 2004. Dynamics of Cux2 expression suggests that an early pool of SVZ precursors is fated to become upper cortical layer neurons. *Cerebral cortex (New York, N.Y. : 1991)*, 14(12), pp.1408–20. Available at: http://www.ncbi.nlm.nih.gov/pubmed/15238450 [Accessed June 6, 2014].

Zong, H. et al., 2005. Mosaic analysis with double markers in mice. *Cell*, 121(3), pp.479–92. Available at: http://www.ncbi.nlm.nih.gov/pubmed/15882628 [Accessed May 21, 2013].